

An aerial photograph of a large, modern steel-arch bridge spanning a wide river. The bridge features a prominent white steel arch structure supported by several concrete piers. The water is a deep greenish-blue, and the surrounding landscape includes green banks and a small island in the middle of the river. The bridge is the central focus of the image.

Shear force in bolted connections for hybrid steel-FRP bridges

Due to traffic, temperature and fatigue loading

Koen Gribnau



Rijkswaterstaat

 **TU Delft**

The logo for TU Delft, featuring a stylized white flame or 'D' shape above the text 'TU Delft' in a bold, white sans-serif font.

Cover: Bridge Nieuw Vossemeer (Beeldbank Rijkswaterstaat)

Shear force in bolted connections for hybrid steel-FRP bridges

Due to traffic, temperature and fatigue loading

by

Koen Gribnau

Date: June 2021
Supervisors: Dr. ir. Marko Pavlovic, TU Delft
Ir. Johan de Boon, Rijkswaterstaat, daily supervisor
Dr. ir. Geert Ravenshorst, TU Delft
Ir. Angeliki Christoforidou TU Delft

(This page is intentionally left blank)

Preface

This thesis presents my research into the shear force in bolted connections for hybrid steel-FRP bridges. It is the last hurdle for obtaining my degree of Master of Science at the Delft University of Technology. For most people, the thesis is a big adventure, some like it, some do not. Also for me, my thesis was a big adventure with parts I liked and parts I did not like. It has been an informative and fruitful period, not only in the educational field, but also beyond.

A long time has passed since the start of my thesis. At the start, I set myself the goal of finishing my thesis before the Olympics games in Tokyo. But life is not always predictable, things do not go as planned, accidents happen and you have to deal with it. Sometimes easier said than done...

The more I learn, the less I know. Through every high, and every low. I'll grow

During a difficult period, the dream and desire to continue with my thesis was present, every day, but reality punched me in my face. While rest was the thing I needed, too many thoughts were bouncing through my head. It wrecked me. Getting back was a slow process. It was never going fast enough with a lot of ups and downs. Still afraid of the dark, I managed to slowly move on with the realisation that every cloud has a silver lining. Cycling, music and especially friends and family brought me the distraction I needed and gave me the motivation to move on. It is hard to describe how grateful I am for all the support I have received.

Without support of my committee, this thesis would not have been possible. Thank you all for your enthusiasm, feedback and patience. I need to thank Marko Pavlovic for all the advises he gave me and the guidance during my thesis. It defines you as a person that you were always there for me without asking, even when there was no progress in the thesis. Besides, I wanted to do my thesis in collaboration with a company to taste the atmosphere at an office. Marko brought me in contact with Rijkswaterstaat. I would like to thank Johan de Boon for giving me the opportunity to join Rijkswaterstaat and the tips he gave me during the entire process. If you ever need any advice for the departments football TOTO, you can always send me a message. Furthermore I need to thank Angeliki Christoforidou for all the help she offered me. Many thanks for all the questions you asked me. It really helped me to get back into my topic. It was pleasant to work with you at the university and thanks for the nice deep and honest conversations. Working at your office boosted my productivity. Last I would like to express my thanks to Geert Ravenshorst. I am glad you could join the committee and thankful for the recommendations you gave me to improve my thesis. There are many more people I have spoke to about my thesis, and I would like to thank them too.

At the end of the storm, there is a golden sky. And the sweet silver song of the lark

Writing your thesis is quite a lonely profession, especially during the corona pandemic. Thanks to my (old) roommates for making the period less lonely and for the daily (card) games we played. It would have been a much harder time without you. In addition I must thanks my friends and fellow students. Quite often you helped without knowing by just having fun. You have always supported me, no matter what. Last I would like to say a big thank you to my family. Especially to my mom and dad for there unconditional love. It was a turbulent time for you too, a lot happened in which you both had many things on your mind. It is admirable how you both handled everything.

And last, the Tokyo Olympic games have not yet started when I wrote this line as the very last line of my report.

Enjoy your reading!

Koen Gribnau

(This page is intentionally left blank)

Contents

Preface	iii
Abstract	xi
1 Introduction	1
1.1 Problem definition	1
1.2 Research objectives	2
1.3 Research scope	2
1.4 Thesis outline	3
2 FRP Bridge decks	5
2.1 FRP	5
2.1.1 Material properties	5
2.1.2 FRP panels	6
2.1.3 Connection methods.	7
2.2 Hybrid interaction	7
2.2.1 Type of connections	8
2.2.2 Connection layout	8
2.2.3 Modelling hybrid interaction.	9
2.3 Girder distribution	10
2.4 Loadings	11
3 Model definition	13
3.1 Definition of axis orientations.	13
3.2 Model.	15
3.3 Linear finite element analyses	18
3.4 Generic model	18
3.5 Connectors	19
3.6 Mesh sensitivity.	21

3.7	Limitations	22
3.8	Model verification.	22
4	Bridge layout	25
4.1	Bridge type	25
4.2	FRP deck layout.	28
4.2.1	FRP deck script	28
4.2.2	FRP deck results	32
5	Hybrid interaction	35
5.1	Effect hybrid interaction	35
5.2	Non-hybrid Model	36
5.3	Hybrid vs Non-hybrid.	38
6	Static shear force	43
6.1	Load definition	43
6.1.1	Traffic load.	43
6.1.2	Temperature load	45
6.2	Methodology for static analyses.	45
6.3	Static results on the generic bridge	47
6.3.1	Traffic load.	47
6.3.2	Temperature load	48
6.4	Static results on highway bridges in the Netherlands	50
6.4.1	Discussion of static shear force results	52
7	Fatigue shear force	53
7.1	Load definition	53
7.2	Process for evaluation.	56
7.3	Methodology for fatigue analyses	57
7.4	Evaluation of a heavy loaded static bridge.	61
7.5	Multiple lorries	65
7.6	Discussion of fatigue shear force results.	67

8	Conclusions & recommendations	69
8.1	Conclusions.	69
8.2	Recommendations	70
	Appendices	71
A	Benchmark study	73
B	Classical laminate theory	87
C	Verification model	91
D	Bridge layout	95

(This page is intentionally left blank)

Acronyms

Acronyms

LM1	load model 1
LM2	load model 2
FRP	fibre reinforced polymers
FLM	fatigue load model
FLM4	fatigue load model 4
FEM	finite element method
UD	unidirectional
S-N	cyclic stress (S) against cycles to failure (N)
iSRR	injected steel reinforced resin
PX	shear force in connectors in longitudinal direction
PY	shear force in connectors in transverse direction
CTE	coefficient of thermal expansion

(This page is intentionally left blank)

Abstract

Fibre reinforced polymers (FRP) can be a solution for future bridge renovation when only the deck of the bridge needs replacement. In these cases the deck is replaced with an FRP sandwich panel deck. The main advantages are a high strength-to-weight ratio which is beneficial for the ever heavier lorries and the fast installation which prevents hindrance. To connect the FRP deck with the steel superstructure, bolted connectors are used. One of the aspects that needs to be investigated before the bolted connectors can be applied are the relevant loads on the bolted connectors. The focus of this thesis will be to investigate the relevant static and fatigue forces on the connectors.

55 existing girder and arch bridges have been selected from a database of Rijkswaterstaat. For each bridge an appropriate FRP deck has been designed with an analytical method. The bridges are modelled in SOFiSTiK to investigate the shear forces in the connectors. The layout of the bolted connectors is kept constant for all bridges, as well as the transverse stiffness of the connector. The shear forces are calculated with a linear analysis. Before the static and fatigue analyses, first the hybrid interaction of the model is investigated. The hybrid interaction is the amount of horizontal forces transferred between the FRP deck and the steel superstructure. Hybrid interaction is beneficial as it increases the strength of the structure. Two models of a generic bridge have been investigated, the first is the standard model which is supposed to use hybrid interaction. The second model is an adjusted version to create a non-hybrid model. Three parameters are investigated: the deflection, the slip and the longitudinal stress over the height of the beam. The results show that hybrid interaction is created with the bolted connectors in the standard model.

In the static analyses two loads are investigated: traffic loads and temperature loads. The shear forces in the longitudinal direction are investigated as this is the governing direction. Before the loads are applied on the existing bridges, first a generic bridge has been investigated to gain knowledge over three bridge parameters. First the facing laminate of the FRP deck is changed. Second the direction of the webs of the FRP deck, and this also changes the connector layout due to feasibility. Third the expansion coefficient of the resin is changed. For traffic loads mainly the direction of the webs influences the shear forces in the connectors. For temperature loading the shear forces are largely depending on the expansion coefficient of the laminate, the closer the expansion coefficient to the expansion coefficient to the steel superstructure, the lower the shear forces. The existing bridges that have been investigated resulted in a large scatter in results. The layout of the superstructure of the bridge influences the facing laminate and the number of connectors, which influences the maximum shear forces in the connectors. For both traffic and temperature loads, the connectors close to the supports experience the highest shear forces.

Besides the static loading, also fatigue is investigated. The shear forces in the connectors are calculated for one bridge, namely the approach bridge Nieuw Vossemeer. This bridge is one of the heaviest loaded bridges in the static analyses and it is according to expert judgement facing deck problems. Two aspects are investigated in the fatigue analysis, first the magnitude and second the type of load cycles. The magnitude is important as this needs to be below the slip resistance of the bolted connectors. The type of load cycles is important as this is related to how damaging the load cycle is. Because there are no S-N curves for bolted connectors between an FRP deck with a steel superstructure, the damage cannot be calculated. The R-ratio is used to investigate the type of load cycles. To calculate the R-ratio of a load cycle, the minimum shear force is divided by the maximum shear force. The resulting number expresses the type of load cycle. For the results, distinction has been made between the connectors close to the supports and connectors in the lengthwise middle of the bridge span. Both the magnitude as the type of loading is different.

Finally, it is concluded that the shear forces in the connectors is one of the aspects to be considered when designing a bridge with hybrid interaction between the FRP deck and steel superstructure. A large scatter of shear forces can be expected, depending on the bridge layout. Incorrect deck design can result in unnecessary high shear forces. The connector layout can be optimised to make the design more cost efficient.

(This page is intentionally left blank)

Introduction

1.1. Problem definition

Highway bridges are vital for the economy of the Netherlands. Closing them would cause serious damage to the Dutch economy. Many bridges in the Netherlands are reaching the end of their lifespan. Figure 1.1 shows the number of bridges and viaducts that have been built in the last 100 years. An overall trendline is indicated in blue. Since most bridges in the Netherlands have a theoretical lifespan of 100 years, the identified trend can be imposed on the next century. From this it is clear to see that a large number of bridges and viaducts will need replacement or renovation in about 30 years. At this moment the bridges that need renovation or replacement are most of the time renovated because of lower costs, thereby extending their lifetime by 30 years. As a result, bridges that need replacement and renovation in 30 years is only growing. Rijkswaterstaat, being the practical executor of public works in the Netherlands, has a limited capacity to replace and renovate bridges. The growing number of bridges that need replacement or renovation, and the limited capacity of Rijkswaterstaat, poses the question how to prevent the closure of bridges that do not fulfil the requirements.

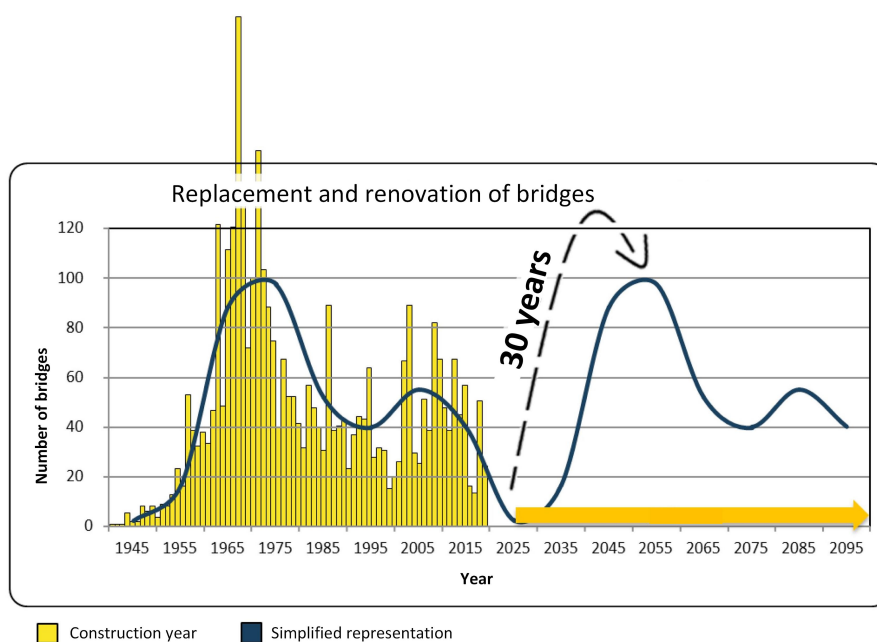


Figure 1.1: Overview of the replacement and renovations that Rijkswaterstaat will be facing (Rijkswaterstaat, 2019).

Fibre reinforced polymers (FRP) can be a solution to help solve this bridge renovation problem (Tromp, 2018). Conventional decks can be replaced by FRP decks to extend bridge lifetime. FRP is a widely used material in many applications. However, the material is not (yet) used as often in civil engineering, despite FRP's high strength-to-weight ratio. The high strength-to-weight ratio reduces the self-weight of the deck compared to conventional decks and thus reduces the load on the superstructure and foundation. Lighter decks prevent reinforcement of foundations and superstructures and allow for heavier traffic to be accommodated. Furthermore, FRP decks can be prefabricated in a controlled environment and transportation is simplified due to light weight decks. Prefabricated deck also reduces traffic hindrance. Additional benefits include better durability and corrosion resistance than steel and concrete (Davalos et al., 2010) (Reising et al., 2004).

Rijkswaterstaat investigates whether it is possible to renovate bridges in such a way that the lifespan increases with 60 years instead of the usual 30 years in order to tackle the problems regarding replacement of existing bridges they will be facing soon. Also for this FRP could be a solution.

Before FRP decks will be used in bridge renovation projects, knowledge is needed about the behaviour of the connections under the loading circumstances. A consortium which includes Rijkswaterstaat is investigating the behaviour of bolted connectors in continuous panels of FRP-steel hybrid structures with the purpose to find the possibilities for using FRP decks in bridges. Three aspects need to be investigated. First the behaviour of the bolted connectors. Second the relevant loads on the bolted connectors and third the feasibility of the bolted solution in existing bridges.

1.2. Research objectives

In this thesis a SOFiSTiK model is created to develop a better understanding of the shear forces in the connectors in hybrid steel-FRP bridges. Based on the research objective the following research question is formulated:

What are the relevant static and fatigue forces on bolted connectors in hybrid steel-FRP bridges?

Based on the objective the following sub-questions are formulated:

1. What is the effect of hybrid interaction on bolted connections in hybrid steel-FRP bridges
2. What are the maximum shear forces in bolted connections of hybrid steel-FRP bridges due to traffic loading.
3. What are the maximum shear forces in bolted connections of hybrid steel-FRP bridges due to temperature loading.
4. What is the maximum shear force ranges in bolted connections of hybrid steel-FRP bridges due to fatigue loading.
5. What type of load cycles are the most dominant in bolted connections of hybrid steel-FRP bridges due to fatigue loading

1.3. Research scope

- Only fixed girder and arch bridges owned and managed by Rijkswaterstaat are included in this thesis. Why only those two are included is explained in chapter 4.
- To determine the shear forces in the bolted connectors, local details are not modelled. A global scale is used for the models.
- Only linear finite element analysis is used. Non-linear finite element analysis is beyond the scope of this research as explained in section 3.3.

- This thesis focuses on determining the maximum shear forces in the connectors. Failure of bolts, laminate, steel superstructure or any other part of the bridges is not taken into account.
- It is supposed that non slip bolts are used to connect the FRP deck with the steel superstructure.

1.4. Thesis outline

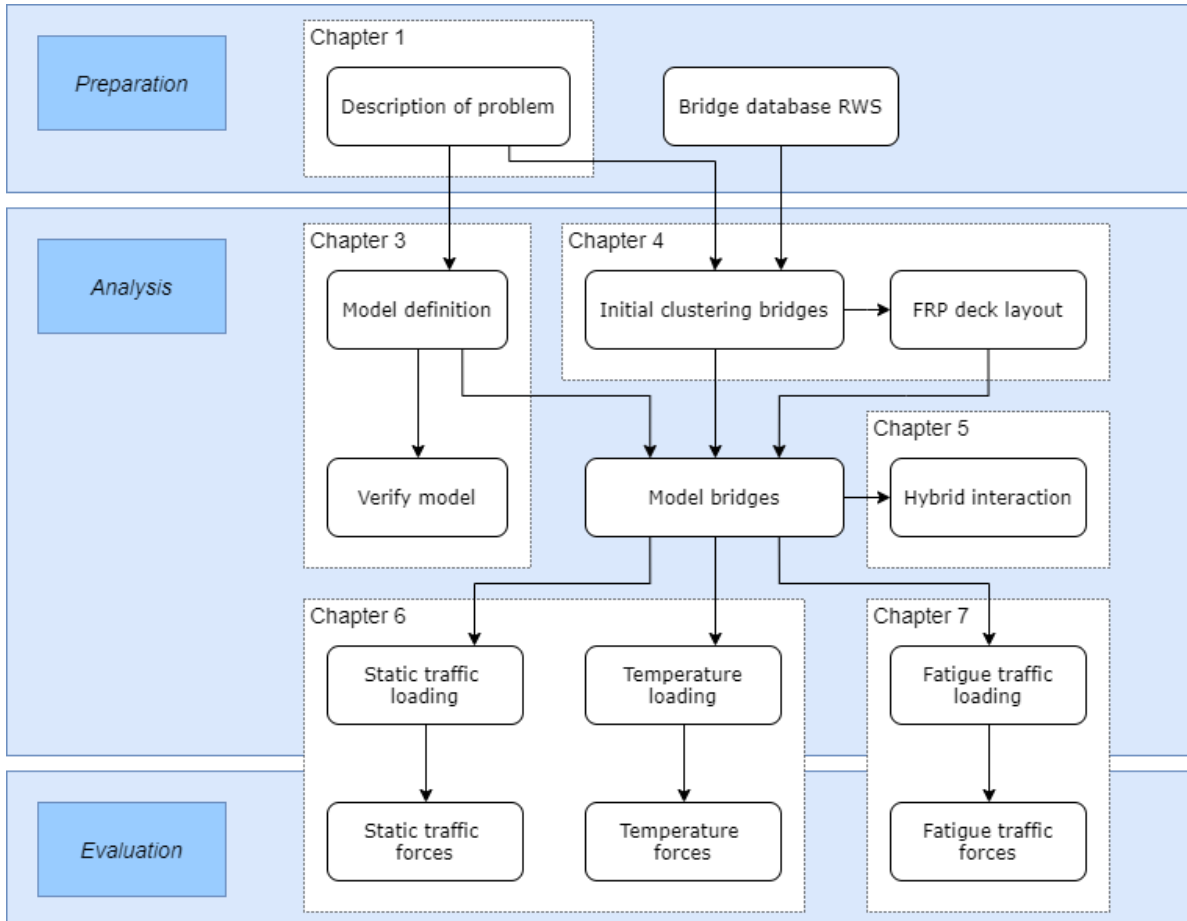


Figure 1.2: The flowchart indicates the outline of this thesis.

(This page is intentionally left blank)

2

FRP Bridge decks

Some basic background about fibre reinforced polymers (FRP) and FRP bridge decks is given in this chapter.

2.1. FRP

FRP are mixtures of two materials: fibres and resins. In this mixture fibres have a load-bearing function. The function of the resin, also called matrix, is to fix the fibres to their location. The matrix also transfers the forces to the fibres, prevents buckling of the fibres and protect the fibres from humidity.

2.1.1. Material properties

Fibres can be made from different materials. Glass fibres are the most commonly used material but also other materials like carbon fibres and aramid fibres can be used. Types of resins can be separated in two groups: thermosetting resins which cannot be softened or reformed by heating and thermoplastic resins which softens every time it is heated. Examples of the most used resins are unsaturated polyester, vinyl ester and epoxy.

The orientation of the fibres co-determine the properties of the FRP panel. When all fibres are orientated in the same direction in the matrix it is called unidirectional. FRP panels are build-up from different layers called plies. Often the fibres in a ply are in the same direction but the fibres in the adjacent plies are located in different orientations. The reason to apply fibres in multiple direction is to get strength and stiffness in multiple directions. Multiple plies together are called a laminate.

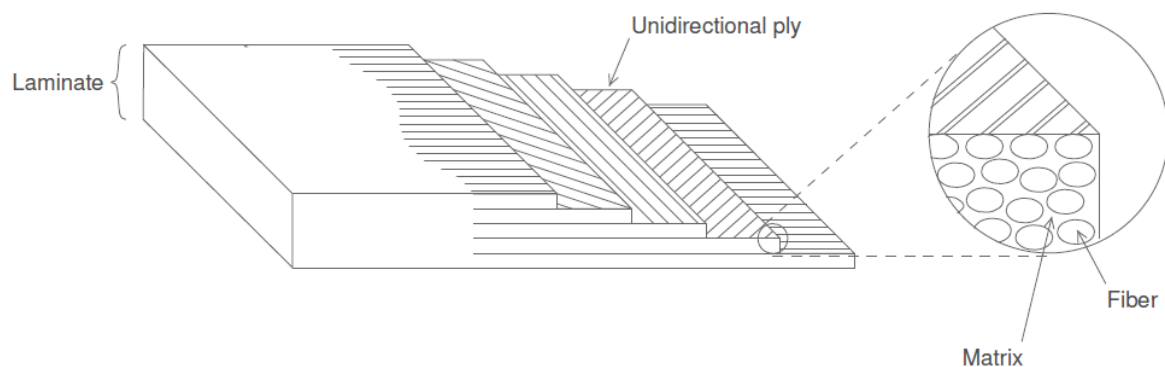


Figure 2.1: Overview of a laminate with 4 plies. The fibres in the plies are in different directions.

To denote the set up of a laminate a specific notation is used. The orientation of the plies is indicated in degrees ($^{\circ}$) with a number between $+90^{\circ}$ and -90° compared to reference axis. The orientation -90° is never used since this is the same as $+90^{\circ}$. For example laminate $[0/45/90/-45]$ consists out of four plies, which each have a different fibre orientation. Some extra notations are introduced to simplify things. When two adjacent plies have the same orientation it can be denoted only once with the addition of an extra subscript showing the number of plies. For example $[0_2/90_2]$ is a laminate consisting out of two 0° plies and two $+90^{\circ}$ plies. When the same laminate is used multiple times on top of each other it can also be written with a subscript, for example a $[45/-45/45/-45]$ is the same as $[45/-45]_2$. When a laminate is symmetric a subscript s can be introduced so $[0/90/90/0]$ is the same as $[0/90]_s$.

FRP deck are an alternative for conventional steel and reinforced concrete decks. Moreover FRP decks can also be used to extend the lifespan of existing bridges. Due to the high strength-to-weight ratio of FRP decks panel, the self-weight of the bridge deck is reduced. This provides the possibility to prefabricate complete decks in a controlled environment and transport the complete light weight decks to the site. It furthermore reduces the inconvenience that arises when a new deck must be installed. In case of renovation of an existing bridge the foundation does not need to be reinforced. Beside the low weight of FRP panels there are more advantages over steel and concrete. The durability of FRP is better, the material is corrosion resistant and FRP has a better fatigue resistance (Davalos et al., 2010) (Reising et al., 2004) (Chen & Davalos, 2014).

The potential of FRP bridge decks against fatigue damage is shown in a research by Chiewanichakorn. The fatigue life of a truss bridge was almost doubled when an FRP deck system was installed compared to a reinforced deck system. The FRP was connected to the steel girders by an adhesive (Chiewanichakorn et al., 2007).

Except from the positive points FRP has some downsides. The large strength and moderate E-modulus results in large deflections. Beside is the initial material cost of FRP relative high, FRP also has a low fire resistance and reduced ductility. In addition, FRP is vulnerable to humidity, alkaline and UV radiation.

FRP is an anisotropic material due to orientation of the fibres. Beside the orientation of the fibres the properties of a laminate also depend on the type of fibres and resin that is used. Compared with steel and concrete the strength is relative high while the stiffness is moderate.

2.1.2. FRP panels

Sandwich panel have a core which is covered by two FRP facings. The core can filled with a lightweight material like polyurethane foam. It is possible that the core is strengthened with FRP webs. The reason for using a sandwich panel is the structural efficiency. The stiffness of the panel is increased without adding extra FRP. Different core layout are available. Webs can be placed in a square or rectangular layout but it is also possible to create triangular or hexagonal layouts (also called honeycomb). The webs are placed perpendicular to the facings. It is also possible that (some) webs are placed under an different angle. A variation on the layout with webs perpendicular to the facings are the InfraCore panels from FibreCore Europe. This panel consists out of Z-shaped elements which overlap in the facings. When an impact hits a panel it is possible that the core is crushed and the facing debonds locally. A crack will propagate parallel in the facings. Because of the Z-shaped elements in the InfraCore panels the crack will not propagate over the full cross section. When the FRP panel is damaged, cracks will not grow. It is constricted by the fibres.

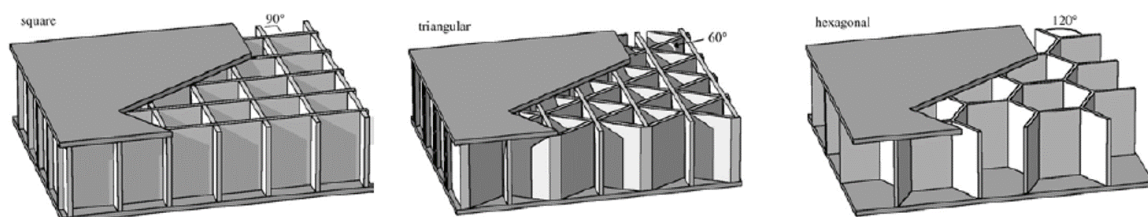


Figure 2.2: Different type of core layouts in FRP sandwich constructions.

Joints are needed to connect FRP panels to each other, when the panel becomes too large to produce or transport, or to connect the FRP panels to other structural parts. Different types of joints can be distinguished. Bonded joints connect the panels by using an adhesive. Mechanical joints use a fastener, for example a screw, rivet or bolt, to connect the different parts. Combinations of bonded and mechanical joints are also possible. Bonded joints have more tolerances for assembly and a lower cost compared to mechanical joints. Mechanical joints are on the other hand easier to prepare and dismantlable. Disadvantage of bonded joints is the sensitivity to environmental conditions and the brittle failure. The biggest drawback of mechanical joints are the high stress concentrations. Besides bonded and mechanical joints also shear studs are used. The shear stud is fixed to the girder and the other part is inside an FRP cell. This cell is filled with a material to fix the shear stud to the FRP. Another option is mechanical interlocking. The parts are clamped in position. In the past years many different connections variants have been developed.

2.1.3. Connection methods

To connect FRP decks to steel girders, different connection methods can be used. The most common techniques are bolted fasteners, adhesive bonding or shear studs. Different types of bolts, adhesives and shear studs are available in the market with each its own advantages and disadvantages. The injected steel reinforced resin (iSRR) connector is a type of shear stud. It consists of a mechanical shear stud which is located in the middle of a cylindrical cut-out in the bottom facing of the FRP deck. The cut-out is filled with steel-reinforced resin so there are no cavities in the FRP deck. The composition of the steel-reinforced resin is steel shot particles embedded in polymer resin. Besides promising static, fatigue and creep experiments, this type of connection can be easily assembled (Csillag, 2018) (Olivier & Csillag, 2020). Besides it can be disassembled which makes reuse of the FRP deck possible.

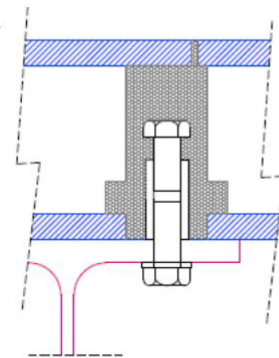


Figure 2.3: An iSRR connector connecting a steel girder with an FRP deck (Csillag, 2018).

2.2. Hybrid interaction

Composite beams consist of multiple materials, for example concrete and steel or FRP and steel. The interaction between those materials is called hybrid interaction. In case there are no horizontal forces transferred between the materials there is no hybrid interaction. Conversely, full hybrid interaction is achieved when 100% of the horizontal forces is transferred between the materials. No hybrid interaction and full hybrid interaction are the extreme and it is possible that a part of the horizontal forces is transferred, called partial hybrid interaction. The degree of hybrid interaction affects the behaviour of the beam. When a girder and deck are loaded with a vertical load and they have full hybrid interaction, the strain between at the top of the girder and the bottom of the deck is equal so there is no jump in the diagram. In case the girder and the deck have no hybrid interaction the strain at the top of the girder and the bottom of the deck is not equal to each other. The bottom of the deck is in tension and elongates while the top of the girder is in compression and shortens. This means that slip occurs between the two surfaces. In case of partial hybrid interaction some slip occurs but it is lower compared to no hybrid interaction. Figure 5.1 shows the strains for different types of hybrid interaction. To change the hybrid interaction the type and amount of shear connections must be changed because they are directly related to each other.

The neutral axis can be used to determine the degree of hybrid action. The theoretical neutral axis can be calculated using formula 2.1 where A is the area of the cross section parts and x is the vertical length towards the bottom of the cross section (Park et al., 2006). The lower limit, when there is no hybrid interaction, can be determined by only considering the steel girder in the calculation. The upper limit, when there is full hybrid interaction, can be determined by considering the girder and the deck. The theoretical neutral axis can be compared with experiments. To determine the neutral axis from test results strain measurements are needed. The neutral axis of the test specimen can be found by connecting the strain value from the upper flange of the FRP deck with the strain value from the lower flange of the girder. The neutral axis is the location where the strain is zero. The degree of composite action (DCA) of a specimen can be determined with formula 2.2 (Davalos et al., 2012). N_0 and N_{100} correspond to the neutral axis at no hybrid interaction and full hybrid interaction respectively. N_p is the neutral axis of the tested specimen.

$$N.A. = \frac{\sum A * x}{\sum A} * 100 \quad (2.1)$$

$$DCA(\%) = \frac{N_p - N_0}{N_{100} - N_0} * 100 \quad (2.2)$$

2.2.1. Type of connections

The degree of hybrid interaction for different connections have been investigated in literature. Park investigated the degree of composite action for bolted connections. Bolts were applied with an interval of 48 cm. On average the degree of composite action was 46.1 %. The neutral axis, and so the degree of composite action, is gradually increased with an increasing load (Park et al., 2006).

Shear connectors were used in the experiments performed by Davalos. They were welded on the steel girders. The FRP panels had a holes at the corresponding locations. They were connected by transverse tongue-and-groove connections which were joined together using polymer resin. The composite action that was achieved is equal to 25 % (Davalos et al., 2012).

The deck of a truss bridge was replaced by an FRP deck. The deck was connected with the superstructure with a locking nut. The drilled holes were then filled with a non-shrink grout. No composite action between the deck and superstructure was found (Alampalli & Kunin, 2003). Clamped connections cannot develop hybrid interaction but can be effective in preventing uplift (Alnahhal et al., 2008).

Keller did research to adhesive bonds between FRP decks and steel girders. They assumed full hybrid interaction and results showed that this assumption was correct. The FRP decks and girders were stiff and resistant enough to provide full hybrid interaction (Keller & Gürtler, 2005b). Other research about adhesive bonds again showed that the connection was sufficiently stiff to guarantee full composite action but the deck was flexible in its plane and therefore did not fully activate the upper facing (Keller & Gürtler, 2005a).

2.2.2. Connection layout

Changing the bolt spacing influences the degree of hybrid interaction. Christopher performed tests with changing interval between the bolts. With an interval of 0.3 m the degree of hybrid interaction was about 23 %. Increasing the bolt spacing results in a lower degree of hybrid interaction. From 1.8 m the degree of hybrid interaction is no longer lowered and stays constant at about 7 % (Waldron, 2001). Other research shows that the spacing only has a marginal effect on the degree of hybrid interaction. Tests with bolt spacing of 0.6 and 1.2 m resulted in very similar neutral axis as can be seen in figure 2.4. The degree of composite action is approximately 25 % (Davalos et al., 2010).

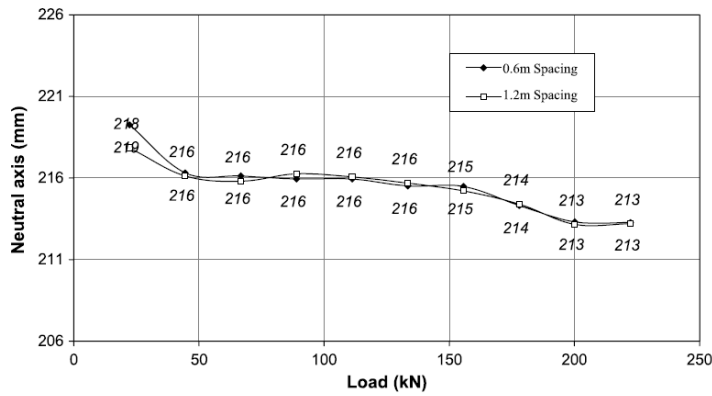


Figure 2.4: Neutral axis for different bolt spacing (Davalos et al., 2010).

Ascione did a research about the shear distribution on multi-row bolted connections between FRP plates. Nine bolts were installed with a center-to-center distance of 60 mm. Also the distance to the edge of the plate was 60 mm. The diameter of the bolts was 14 mm. Although the experiment consisted only out of 1 set-up it can be seen that the minimum bolt transferred 8.2 % of the shear forces and the maximum bolt transferred 12.9 %. This result was measured with experiments and confirmed with a numerical model (Ascione, 2010).

2.2.3. Modelling hybrid interaction

To model full hybrid interaction elements of the deck must be connected with elements of the girders top flange. How it should be done depends on the type of elements that is used but all degrees of freedom of the deck and girder must be connected with each other.

Data from a field test has been used to check if it is possible to properly model partial hybrid interaction (Zhang & Cai, 2007). The field bridge has 14 steel girders and an FRP deck. The girder and deck are connected by clips every 2.439 m and on every third girder. Due to these connections there is partial hybrid interaction. The bridge was loaded by a truck which passed the bridge ten times, every time the axles were shifted a bit along the width of the bridge. The same bridge was modelled with partial hybrid interaction (connector every 2.439 m along the girder) and full hybrid interaction (connectors all along the girders). For numerical stability reasons the connections were placed every girder. The results are shown as distribution factor, which is the percentage of load carried by each girder. The field measurements matched the partial hybrid interaction model better than the full hybrid interaction model. Figure 2.5 showed the results for load position 5, which is nearly halfway the width of the bridge, and load position 10 at the side of the bridge.

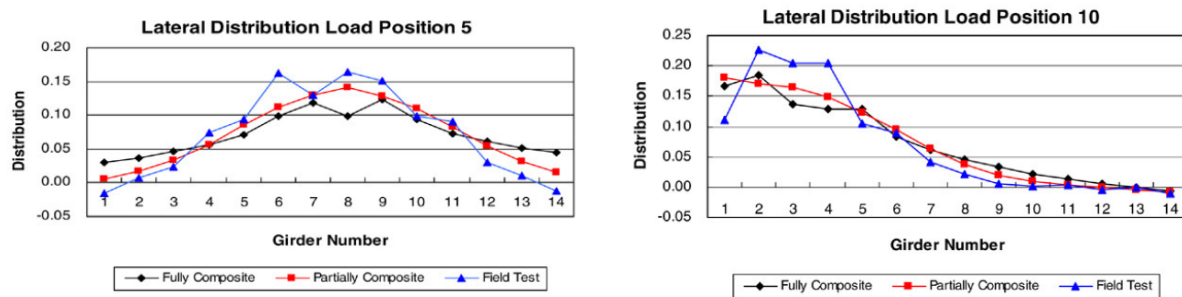


Figure 2.5: Partial and full hybrid interaction are modelled and compared with field tests. Load position 1 is at the edge of the bridge and load position 5 is in the middle of the bridge.

2.3. Girder distribution

The load distribution throughout bridges is important in the design of bridges. The distribution factor (DF) compares the stress (σ) on a girder with the total stress in the structure, as can be seen in formula 2.3. In other words the distribution factor shows the contribution of each girder in carrying the load. DF of the same magnitude means that the load is evenly distributed over the girders. Contrariwise, major differences in the DF means the load is not distributed over all the girders. The position of the load is of great importance on the load distribution among the girders. In case a truck is driving at the side of the bridge, the DF will be larger compared to a truck driving in the middle of the bridge. This can be seen in figure 2.5.

Beside the DF also the load distribution factor (LDF) is used when designing bridges. The LDF in case all girder have the same section modulus can be calculated with formula 2.4. The formula includes multiple presence factors that is intended to account for coincident loading.

$$DF_i = \frac{\sigma_i}{\sum \sigma_j} \tag{2.3}$$

$$LDF_i = \frac{n\sigma_i}{\sum \sigma_j} \tag{2.4}$$

A steel girder bridge and prestressed concrete girder bridge has been modelled by Zhang to investigate the influence of the type of girder on the LDF (Zhang & Cai, 2007). The bridges have the same dimensions and they are designed for the same loading. In addition to the concrete deck that is used, which has been modelled with full hybrid interaction, also FRP decks are used. An FRP deck with full hybrid interaction is used and an FRP deck with partial hybrid interaction.

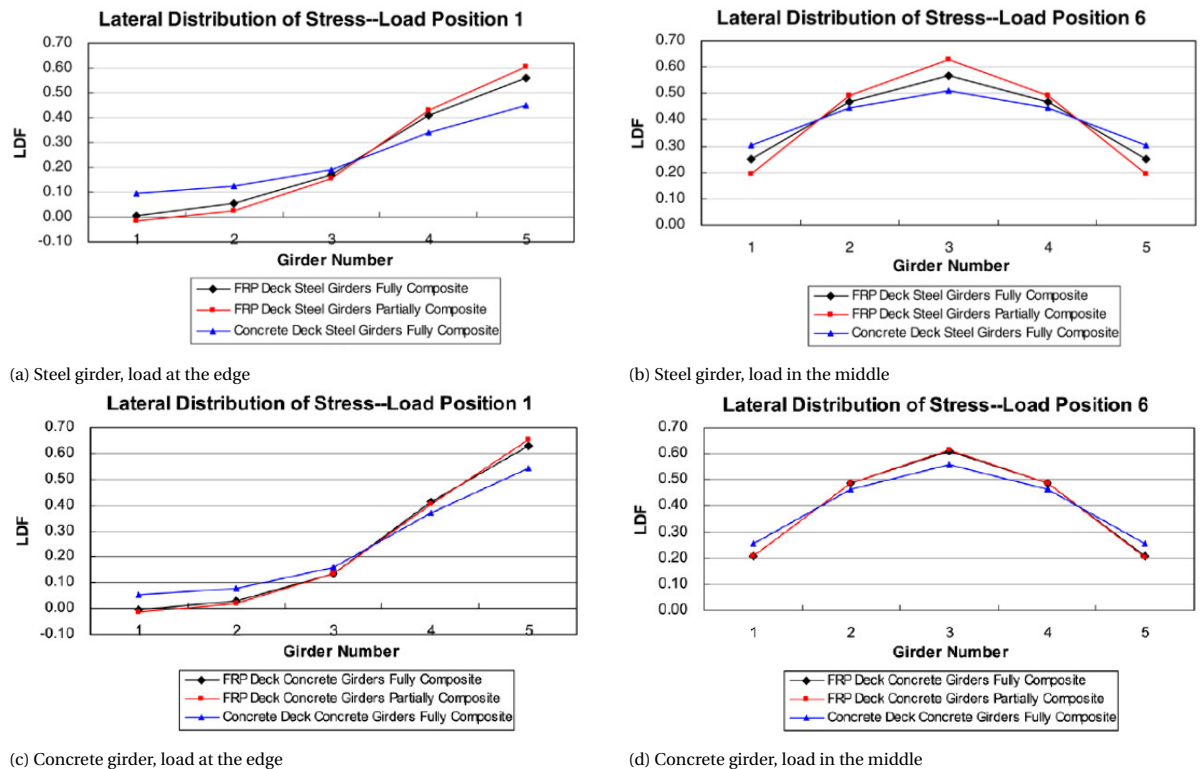


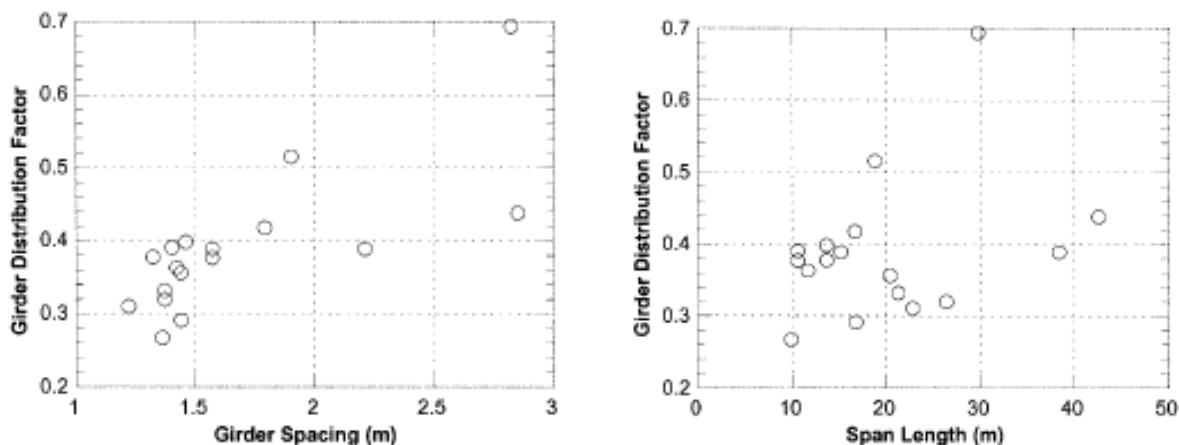
Figure 2.6: LDF for a bridge with different type of decks and girders. Load position 1 is at the edge of the bridge and load position 6 is in the middle of the bridge (Zhang & Cai, 2007).

The LDF is influenced by the type of deck that is used as can be seen in figure 2.6. Comparing the concrete and FRP full hybrid interaction decks it can be observed that the LDF of the concrete variant is lower. This is due to higher stiffness of the concrete deck. When the two FRP decks are compared it can be seen that the LDF is higher in case of partial hybrid interaction. Deck and girders with partial hybrid interaction cannot distribute loads as uniform as bridges with full hybrid interaction. The highest LDF are obtained by using FRP deck with partial hybrid interaction.

The bridge which was modelled by Zhang was an actual bridge in Kansas. The bridge deck has been replaced by an FRP bridge deck and the DF of the measured with the original and the FRP deck. The FRP deck was connected with special clips and there was only little change in the DF visible (Schreiner & Barker, 2005).

Due to the larger stiffness of concrete girders compared with steel girders the LDF of concrete girders are more equal than for the steel girders. The larger stiffness of the concrete girders also results in less sensitivity to the stiffness of the deck. This can be seen well when comparing load position 6.

The effect of the girder spacing, span and support condition on the LDF for slab-on-girder bridges have been investigated in different studies. The girder spacing has a significant influence on the LDF. An increasing girder spacing increases the LDF but the relationship is non linear (Tarhini & Frederick, 1992). This can also be seen in figure 2.7a where field test were done with 17 bridges. The researches about the effect of the span on the LDF results in contradictory results. Some results show an decrease in the LDF with an increasing span (Zou et al., 2010) (Mabsout et al., 1999) (Zokaie, 2000) but other researches show that the effect on the LDF is minor (Tabsh & Tabatabai, 2001) (Bishara et al., 1993). Figure 2.7b shows the distribution factor for 17 bridges plotted against the span length based on field tests. Although the bridges are not only different in span it can be seen that there is no correlation between the bridges. The effect of different support conditions has been investigated (Eom & Nowak, 2001). FEM analysis showed that roller-hinge support results in most uniform LDF



(a) Steel girder, load in the middle

(b) Steel girder, load at the edge

Figure 2.7: LDF for different bridge spans and different girder spacings (Eom & Nowak, 2001).

2.4. Loadings

Cyclic stress (S) against cycles to failure (N) (S-N) curves for FRP connected with steel are different than steel connected with steel. 10 tests are done to determine the S-N curve for shear connectors connecting honey comb FRP with steel (Davalos et al., 2010). The results can be seen in figure 2.8. The control parameter was the stress range on the shear stud. There is no cut-off limit visible.

A dynamic analysis on a truss bridge with an FRP deck was done to find the number of stress cycles per truck passage which is needed for computing fatigue life (Chiewanichakorn et al., 2007). It is found that the number of cycles depends on the stress range. For low stress ranges the number of cycles can be greater

than 100 cycles but for higher stress ranges the numbers are comparable with the number of cycles per truck provided in the American code.

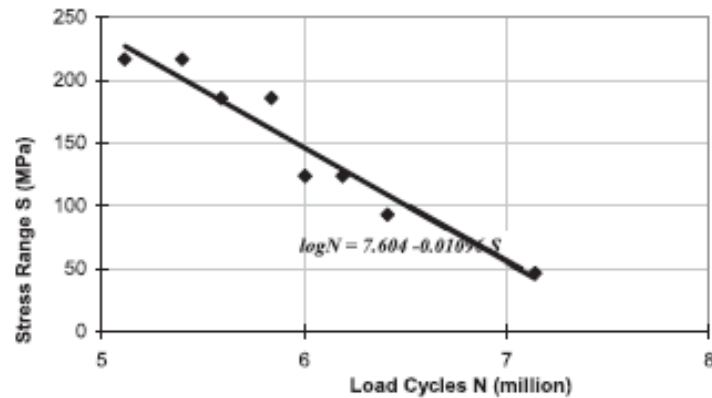


Figure 2.8: S-N curve for shear stud connecting honeycomb FRP with steel (Chen & Davalos, 2014).

Bridges must withstand fatigue loads in every weather condition. Five different type of decks were tested to see what the influence is of temperatures of $-30\text{ }^{\circ}\text{C}$ and $50\text{ }^{\circ}\text{C}$ (Kwon et al., 2003). The first deck was a conventional reinforced-concrete deck and the second deck was a hybrid FRP-concrete deck. The other three decks are all FRP decks but manufactured with different procedures. Deck three used Vacuum-assisted resin transfer molding, deck four is a pultruded deck and deck five fabricated by the contact molding hand lay-up process. All decks were loaded with ten million cycles of fatigue loading. The three FRP decks did not show damage but the FRP decks showed more reduction in stiffness due to the extreme temperature compared to the decks with concrete.

Keller tested the creep behaviour for a sandwich panel due to tensile top chord stresses (Keller & Schollmayer, 2006). For creep load corresponding to 50 % of the serviceability limit state there is no creep deformation measured. For creep loads corresponding to 100 % of the serviceability limit state the creep deformation is substantial. The permanent weight on the bridge is much smaller than the service load. Therefore it is concluded that, due to the lightweight character of bridges with FRP decks, especially when steel girders are used, the in-plane creep deformation is not determinant for the design. Also other research of Keller about creep due to traffic loads, where an FRP deck was connected with the girders by adhesive bonding, suggested that this is not a concern in the design (Keller & Gürtler, 2005a).

3

Model definition

To investigate the shear force in the connectors, a finite element method (FEM) model is used. First the definition of the axis orientation is given. Afterwards it is explained how the model is created and what type of analyses is applied. Furthermore the layout of the generic model is explained. This generic case will be used in several parts of the report to investigate the influence of specific deck parameters. Finally the limitations of the model are explained and the verification of the model is discussed.

3.1. Definition of axis orientations

The entire report uses the same definitions for axis orientations. A three dimensional Cartesian coordinate system is used to define the dimensions of the bridges in which each axis is always pointed in the same direction. The x-axis is pointed in the longitudinal direction of the bridge, this direction is also the driving direction. The y-axis is pointed in the the width of the bridge, also known as the transverse direction. The z-axis is always pointed downward. These directions can also be seen in figure 3.1.

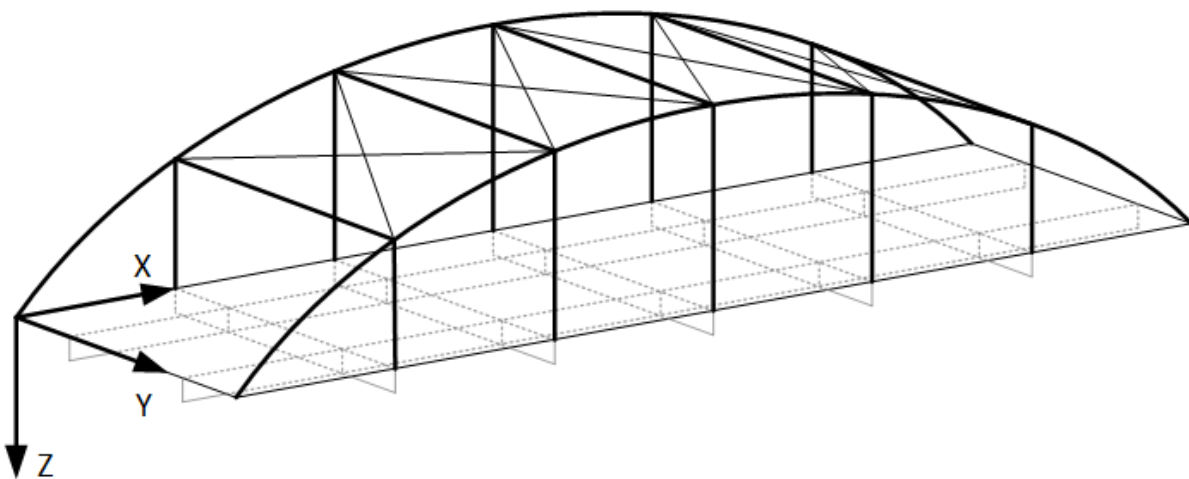


Figure 3.1: The coordinate system used for the bridges.

The bridge deck is built with fibre reinforced polymers (FRP) sandwich panels. The sandwich panels consist of two facings connected with webs. The facings are plates always located in the XY-plane. The webs are

plates located in the YZ-plane or XZ-plane depending on the direction of the webs. They are denoted with Web_0 or Web_{90} as can be seen in figure 3.2.

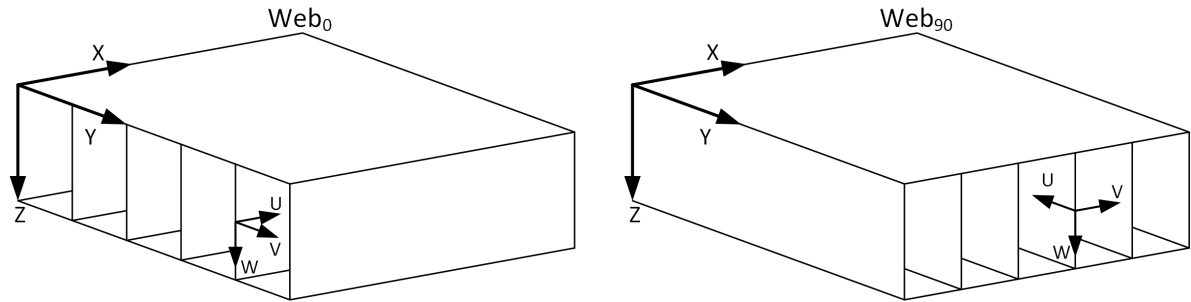


Figure 3.2: The definition of the directions of the webs including their local coordinate system.

The facings and webs are laminates built up from different unidirectional FRP layers. The fibres in each layer, called ply, can be directed in four directions. They are notated with degrees in the XY-plane in which the 0° fibres are always direction parallel to the global X-direction. The four fibre direction in the facings can be seen in figure 3.3.

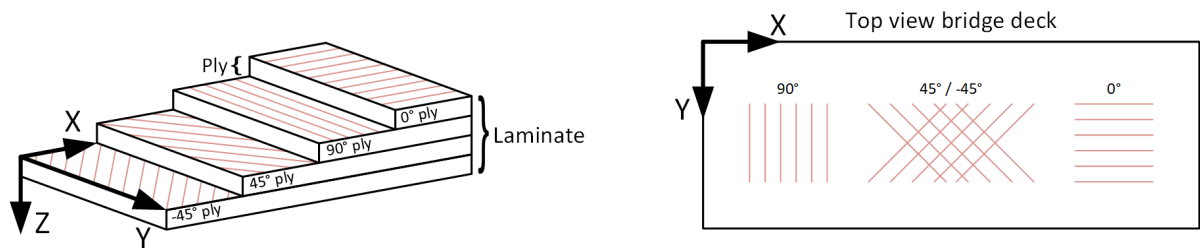


Figure 3.3: The definition of the fibre directions for the laminates in the facings.

To define the composition of the webs, a local UVW-coordinate system is used because webs can be placed in different planes. The local coordinate system is only used for defining the fibre directions in the webs. The W-direction is always parallel to the Z-direction. The U-direction is the other in plane direction of the web panels. The V-direction is the out of plane direction of the web panels. The local coordinate systems for the webs can also be seen in figure 3.2. Just like with the facings, the fibres in the webs can be directed in four direction and use a degree system to define their direction. The definition of the fibre direction in the webs can be seen in figure 3.4.

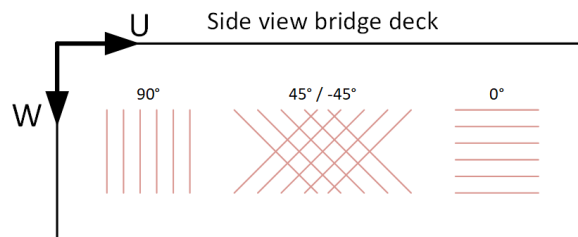


Figure 3.4: The definition of the fibre directions for the laminates in the webs.

3.2. Model

To investigate the shear force in the connectors, a model is constructed with SOFiSTiK. A parametric model in the Teddy text editor is used to be able to model different bridge configurations. The model consists of different modules (+PROG) which generate, calculate or collect results for the model. The modules are explained globally.

+PROG TEMPLATE

The input for the model is given in the module template. The layout of the model, the layout of the connections and the material properties is defined in this part. This is the only section that needs to be changed when a new calculation is required. The input data will be shown in chapter 4.

+PROG AQUA

The material properties defined in the module template are assigned to a new material in this module. In addition the cross section dimensions of the steel profiles are defined. For steel parts, S355 is used.

+PROG SOFIMSHC

The third module creates the geometric model. The steel girders and arches are modelled as beam elements (2 nodes). The FRP deck is modelled with quadrilateral elements (4 nodes). A line is required in SOFiSTiK to create beam elements. Areas are needed to create quadrilateral elements. The connectors are modelled with springs.

Creating areas in SOFiSTiK consists of three steps, for lines only the first two steps are needed. The first step is to create nodes (by using the command SPT), which will be the corners of the areas. These nodes will be connected with lines (SLN) to create the circumference of the area. The last step is to make an area (SAR) by selecting the lines. To translate a line into a beam element the cross section must be stated behind the SLN command. For an area the material type and thickness must be defined behind the SAR command.

Support conditions can be added to nodes by stating FIX and the boundary conditions that must be constrained behind the SPT, SLN or SAR command. When a beam element is generated with the help of a line, the boundary conditions of this beam elements are not necessarily at the location of the line. To locate the boundary conditions at the bottom of the girders, an extra node can be generated at this location. The extra node can be coupled with the beam to create a rigid connection with the command SPTP. Connectors are modelled as springs and can be generated by connecting two nodes (SPTS). Just like with the boundary conditions, it is possible that the node for a bolted connection in a beam or quadrilateral element is not located at the right spot. Again an extra node is generated and coupled with a rigid connection. A detail of a pair of rigid and spring elements that connect a steel girder to the FRP deck in the model can be seen in figure 3.5.

A bolt is located 100 mm from the centre of the girders at each side. The distance between the bolted connectors is 0.48 m. The transverse stiffness is a crucial parameter of the connectors as this influences the shear force transfer through the connectors. A value of 100 kN/mm is used. Different type of bolts have different transverse stiffnesses but this value is representative for injected steel reinforced resin (iSRR) bolts (Csillag & Pavlović, 2018). The over time change of the transverse stiffness of the connector is not taken into account.

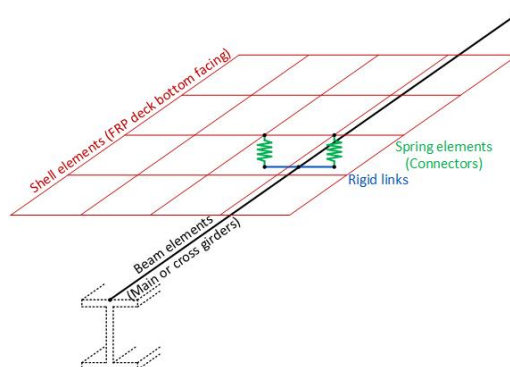


Figure 3.5: Detail of pair of rigid and spring elements that connect steel beam to FRP deck in model.

All bridges use the same type of support. They have a pinned support where movement in the x, y and z direction is prevented in only one cross section. Rotations are allowed in all directions. The remaining cross sections with supports have roller supports where only movement in the y and z direction is prevented. Movement in the longitudinal direction is now allowed just like rotations. In case of multiple spans, the cross section with pinned supports is located as close to the middle of the bridge as possible.

Because the model is parametric, loops are used to generate the model depending on the input. In order to prevent meshing problems, coupling of extra nodes in the middle of areas is not used. Instead the area is split in smaller areas so only the corners of the areas are coupled with other parts. An example how the lines (SLN) and areas (SAR) for the FRP webs are generated can be seen in listing 3.1. An example of an arch bridge which is generated with the model is shown in figure 3.6.

```

1 LOOP#i #L/#L_FRP+1
2   LOOP#j #B_points
3     SLN 70000+#B_points*#i+#j NPA 10000+2*#B_points*#i+#j NPE 40000+2*#B_points*#i+#j
4   ENDLLOOP
5 ENDLLOOP
6
7 LOOP#i #L/#L_FRP+1
8   LOOP#j (#B_points-1)
9     SAR NO 80000+(#B_points-1)*#i+#j MNO 3 T #t_web3*1000
10    SARB TYPE OUT 70000+#i*#B_points+#j
11    SARB TYPE OUT (11000+#B_points*#L/#L_FRP*2)+2*(#B_points-1)*#i+#j
12    SARB TYPE OUT 70001+#i*#B_points+#j
13    SARB TYPE OUT (41000+#B_points*#L/#L_FRP*2)+2*(#B_points-1)*#i+#j
14  ENDLLOOP
15 ENDLLOOP

```

Listing 3.1: SOFiSTiK code for the generation of the FRP webs.

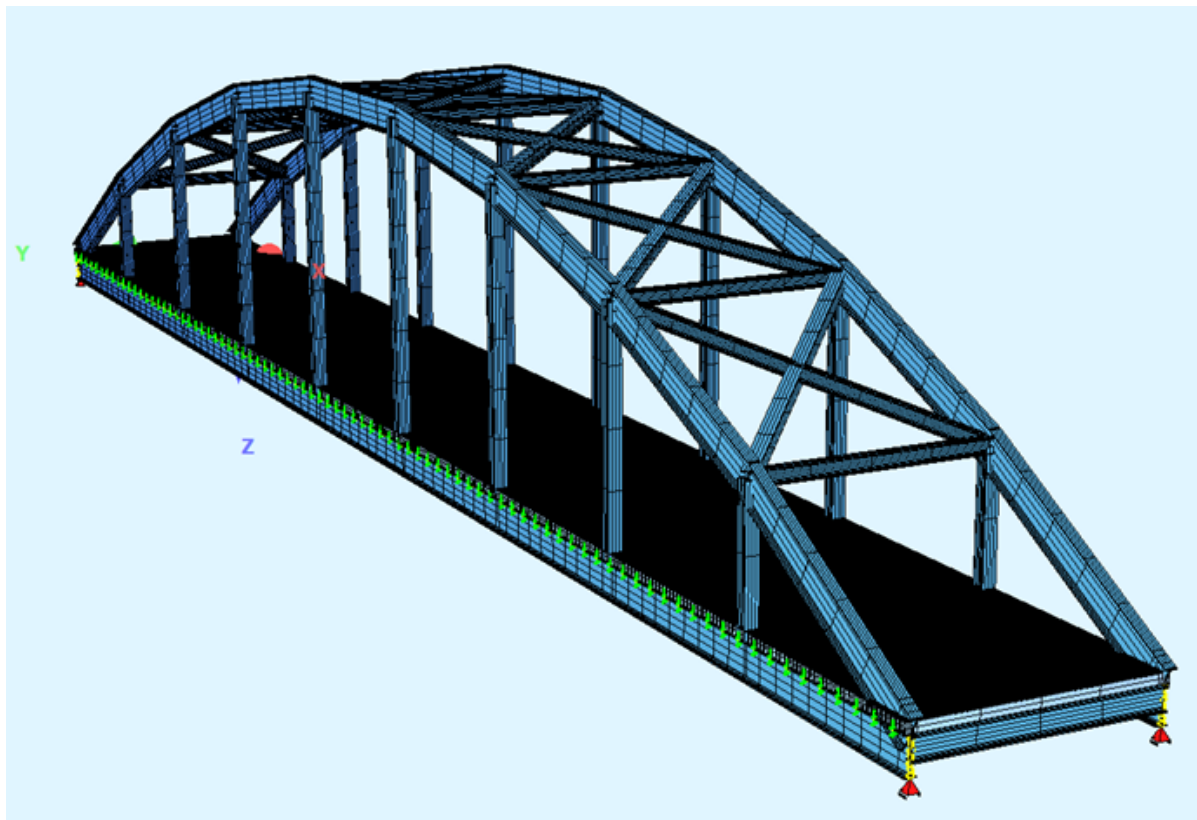
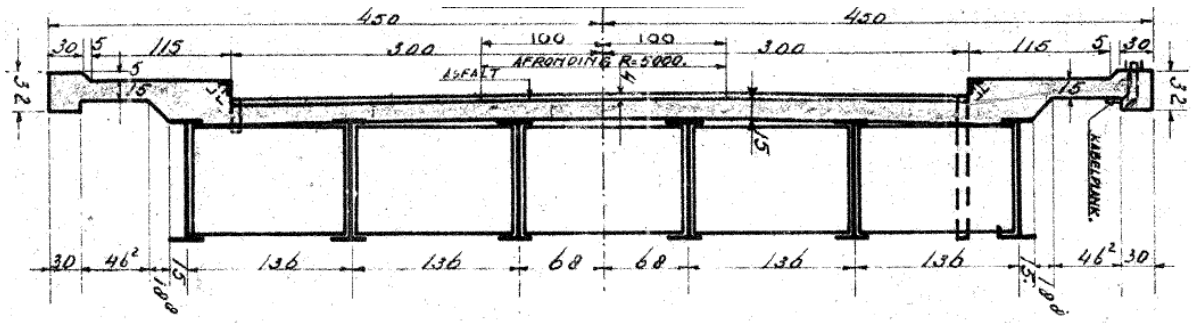


Figure 3.6: Arch bridge generated by the model.

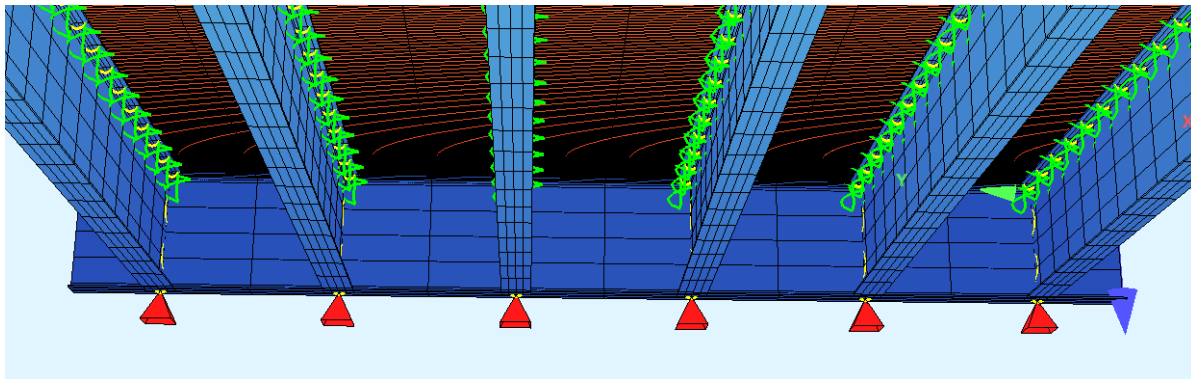
To compare the bridge model with existing bridges, an example of Brug Spannenburg is shown. Brug Spannenburg consists of two approach bridges and a movable bridge in the middle. The western approach bridge is one of the bridges that is investigated in this research. Figure 3.7 shows the cross section on the blueprint, what the bridge actually looks like and what it looks like in the model. The green lines between the new FRP deck in orange and the existing structure in blue are the connectors.



(a) Blueprint of the cross section.



(b) Picture of the bridge.



(c) Picture of the model.

Figure 3.7: Three different views of the cross section of Brug Spannenburg. A blueprint, a picture and the model.

+PROG SOFILOAD

This module places the loads on the bridge. Before traffic loads can be placed, the bridge must be separated into notional lanes. The number of lanes is defined in the module template. The loads are located according to the defined number of lanes. The load of a lorry consists of two or more axles. Each axle is placed as a separate load case. In the post-processing part the correct axles are combined to generate the load of the lorries. Also distributed loads are placed as a different load case. Beside traffic loads also temperature loads are applied. The loads definitions are given in the chapters where the loads are applied.

+PROG ASE

Now the model is built, it is time to do the analysis. A linear analyses is done that calculates all the forces and moments as well as the deformations of the bridge.

+PROG RESULTS

The last module is used to export the results from SOFiSTiK to an excel file. To prevent extreme amounts of data from all the runs only the data required for analyses is exported.

3.3. Linear finite element analyses

Different types of analyses can be applied. Two types of analyses were considered, linear finite element analyses and nonlinear finite element analyses. Nonlinear finite element analyses has some advantages over a linear analyses. There can be different sources of nonlinearity in a nonlinear analyses. Material nonlinearity in one of them. In this type of analyses it is for example possible to have material behaviour beyond the elastic design stage, the plastic stage. When the maximum elastic load is applied on a connector, it will start plastic deformation which will result in a transfer of forces to other connectors. Also cracking of the material could be investigated with this type of analyses.

A second form of nonlinear analyses is geometrical nonlinearity. In this type of analyses the deformation of the structure under the load is taken into account when calculating the equilibrium. A third form is contact nonlinearity in which gaps between adjacent parts may open or close. All these nonlinear analyses have iterative solution procedures to get the result within the convergence criterion. The advantage of using linear analyses is the simplicity of the analyses. It is easier and faster to apply in the FEM program.

The goal of this thesis is to find the magnitude of the shear force in the connectors. Because this is a first investigation, a faster working flow with a correct magnitude of the shear force, is more important than time consuming complicated methods. Additionally there are some simplifications in the model. It would be contradictory to use the most accurate calculation methods for the best result and at the same time do some simplification in the model that influence the results. One of those simplification is to suppose non-slip bolts. For this type of bolts linear analysis will give a correct representation of the behaviour. So only linear finite element analyses is used in this thesis.

3.4. Generic model

In this section the layout of the generic bridge will be explained. By only changing a few parameters on the bridge the influence of those parameters can be investigated. With the existing bridges it is more difficult to see the influence of a single parameter as almost every parameter is different. Besides, the small size of the generic model results in reduced calculation times, which was very useful when the model was developed. The relative simple layout of the generic bridge makes it also easier to understand the results.

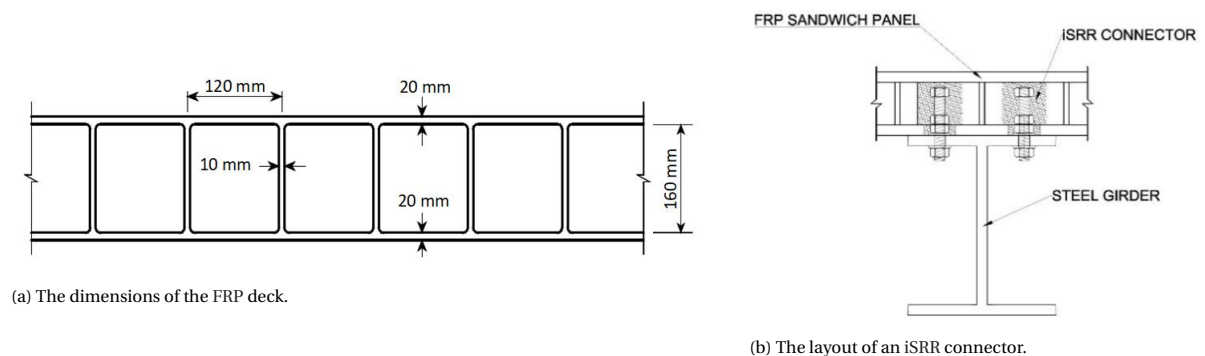
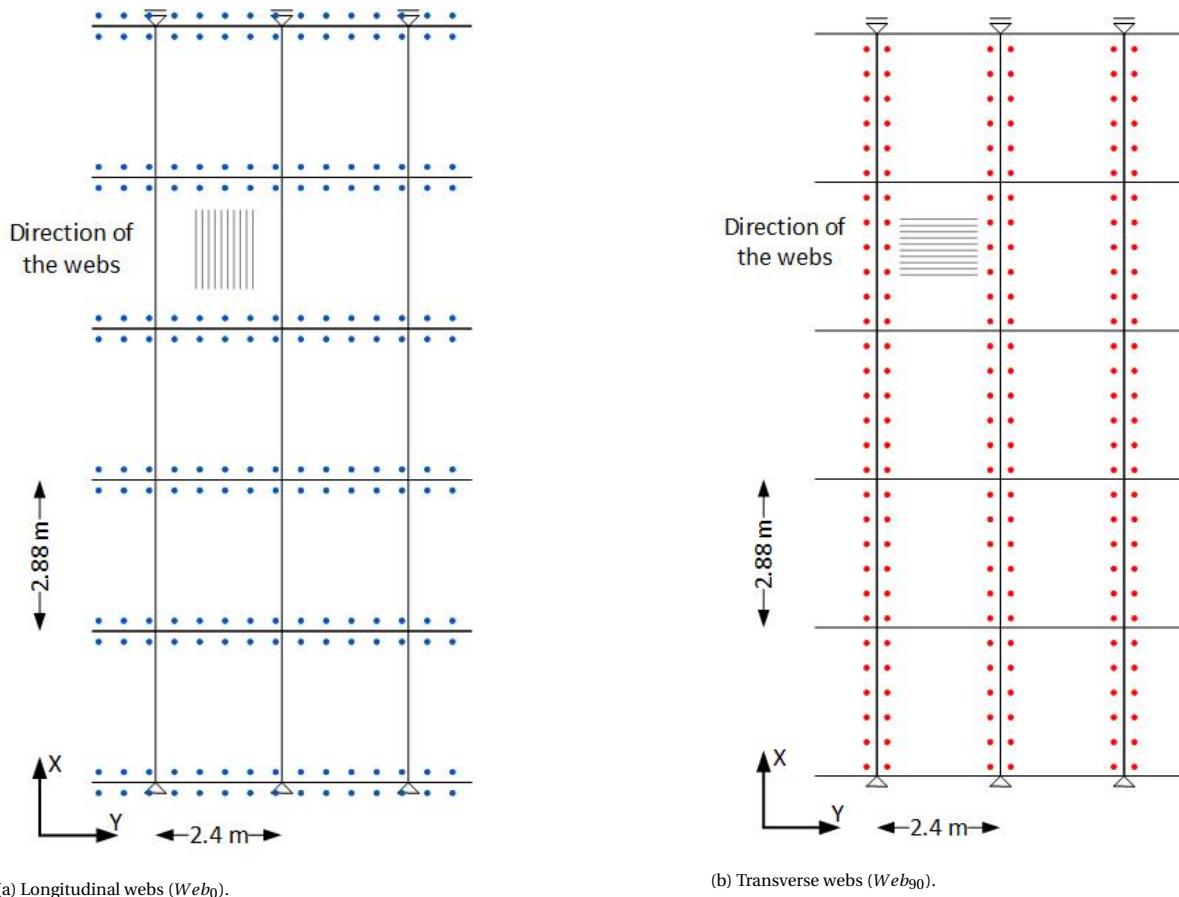


Figure 3.8: The dimensions of the FRP deck and layout of the connection to steel girder.

The dimensions of the generic bridge is fixed, namely a simply supported bridge with a width of 7.2 m and a length of 14.4 m. There are three main girders and six cross girders. All with a height of 1.0 m. The dimensions of the FRP deck is also fixed and can be seen in figure 3.8. In this figure it is also visible how the connector is placed in the FRP deck. The distance between the bolted connectors is 0.48 m. A bolt is located 100 mm from the centre of the girders at each side. A transverse stiffness of 100 kN/mm is used as this value is representative for iSRR bolts (Csillag & Pavlović, 2018).

The direction of the FRP webs influences the shear forces in the connectors, as the connectors are located in different positions. For practical reasons the bolted connectors must be located between the webs. In the case of longitudinal and transverse webs, this implies that connectors are placed on the cross girders and longitudinal girders, respectively, see figures 3.9.



(a) Longitudinal webs (Web_0).

(b) Transverse webs (Web_{90}).

Figure 3.9: Top view of the generic bridge layout, including connector layout, for the different web directions.

In this generic model three parameters will be changed namely the direction of the webs as mentioned before, the laminate of the FRP deck facing and the expansion coefficient of the resin. More about this will be explained when it is applied in chapter 6.

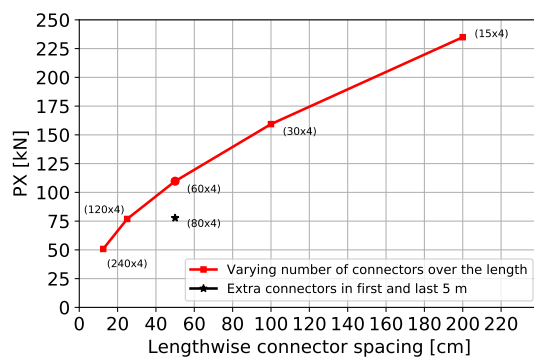
3.5. Connectors

In the rest of this research, the connector layout and the transverse stiffness of the connectors is kept the same. The distance between connectors is 0.48 m and the transverse stiffness of the connectors is 100 kN/mm (Csillag & Pavlović, 2018) as explained in the last section. However these parameters can influence the shear forces in the connectors significant as was shown in appendix A. The results in this section are obtained from the benchmark bridge.

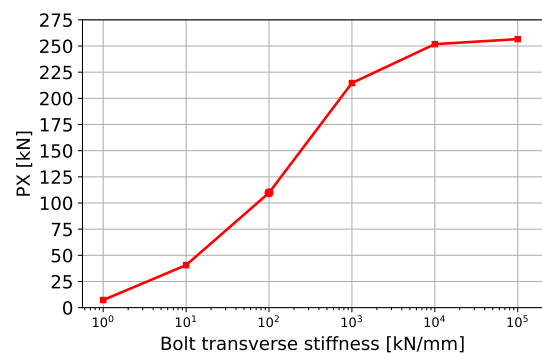
The reason for not changing the layout of the connector is to reduce the number of bridge parameters. Changing the distances between connectors makes it harder to compare the results for different bridges. The idea is that one can add or remove connectors in a later stadium if this is desirable to optimise the design. However, some results from the benchmark study are shown here to give an idea about the influence of the connector layout.

Decreasing the distance between connectors will reduce the maximum shear force in the connectors as shown in figure 3.10a. For each dot it is noted how many connectors are placed over the length of the bridge (first digit) and the number of connector per cross section (second digit). There are two main girders for the benchmark bridge, so the results presented here all have four connectors per cross section. One connector at each side of each main girder. Half the distance between girders does not mean the shear forces in the connectors is halved. How much it will decrease depends on the layout of the bridge and connectors. First of all, the direction of the webs results in different connector layouts. In addition is the number of (cross) girders and the distance between (cross) girders decisive in which layouts are possible. More girders and smaller distances between girders reduce the distance between connectors. These results are used to motivate the distance between connectors in the rest of the research (0.48 m) as these values are in the range what connectors can handle, although the shear forces will depend on the layout of the bridges.

In this research always a constant distance between the connectors is used, however the connectors in the middle of the bridge are loaded less than connectors close to the supports. A more cost effective design would be to get the same maximum shear forces in all the connectors and that they are used in full extent. To achieve this the distance between connectors in middle of the bridge must be higher than the distance between connectors close to the support. Indicated with a star in figure 3.10a, it is shown what the effect is of adding connectors at the edge of the bridge. In the first and last five meters of the bridge, the distance between the connectors is reduced from 0.5 m to 0.25 m. This means an extra twenty connectors are used (80x4) but the same maximum shear force is achieved as when 60 connectors were added (120x4). The connector layout could be further optimised as there is still a big difference in maximum shear forces in the connectors, see figure A.17 in the appendix. So placing connection in an optimised layout can make the design more cost effective.



(a) Sensitivity analysis of a changed number of connectors on the benchmark bridge.



(b) Sensitivity analysis of the transverse connector stiffness on the benchmark bridge.

Figure 3.10: In the benchmark study, see appendix A, bridge parameters of the benchmark bridge have been varied to investigate the influence.

The transverse stiffness also has a big influence on the results. The higher the transverse stiffness, the more shear forces it will transfer. A lower transverse stiffness will distribute the shear forces more evenly over the connectors. The transverse stiffness depends on the type and size of connector that is used. For this research a value of 100 kN/mm is used as this is the value for iSRR connectors but it can be changed as is done for the benchmark bridge, see figure 3.10b. The extreme transverse stiffness of the connectors are not realistic values but it can be seen that for example a transverse stiffness of 200 kN/mm already results in significant increase of the maximum shear force in the connectors. It should also be taken into account that during the lifetime of the bridge, the transverse stiffness of the connectors will decrease. So the shear force in the connectors is depending on the transverse stiffness of the connector.

So as shown in the graphs, doubling the distance between connectors will increase the shear forces by 45% due to static and fatigue loads. When the distance between connectors is halved, the shear forces due to static and fatigue loads will decrease by 30%. The stiffness of the connectors also influences the amount of shear force in the connector. A higher transverse stiffness of the connector results in higher shear forces, for example a doubled transverse stiffness of 200 kN/mm results in 25% higher shear forces. As not all connectors are loaded by the same amount of shear forces, the connector layout can be optimised. Connectors close to the supports have higher shear forces than connectors located at mid-span. Designs can be optimised to use the full capacity of each connector, this will reduce the number of connectors and makes at the same time a more cost effective design.

3.6. Mesh sensitivity

The size of the mesh determines the accuracy of a model. A finer mesh results most of the time in more accurate results. When a mesh is too large it can result in wrong results. The disadvantage of a finer mesh is the increase in computation time. To check if the chosen mesh is fine enough a convergence study is done.

In SOFiSTiK it is not possible to define the size of the mesh, SOFiSTiK will create the mesh by itself. However, it is possible to define some parameters which influence the size of the mesh. The first thing which is defined is the type of mesh. The beam and shells are all divided in quadrilateral elements only. The second parameter which can be defined is the maximum beam and shell length. It is not possible to define the exact length of the mesh, only the maximum length can be defined. This can be changed if the mesh is too big. Other parameters which control the mesh are turned of so there is no increasing mesh density at the edges, corners or structural areas.

The SOFiSTiK model is created with nodes. Where different elements of the model intersect, there are by definition nodes due to the way the model is constructed. Those elements can have a longer length than the maximum element length. In those cases, SOFiSTiK splits the elements in evenly distributed parts. Extra nodes are introduced to create more elements. The generic bridge has been used to check the sensitivity of the model. The bridge is loaded with first a single axle load of 100 kN in the middle of the slow lane and second with a distributed load of 10 kN/m² on the entire deck. Table 3.1 presents the shear force in connectors in longitudinal direction (PX) for different maximum element lengths. Also the number of nodes and elements is presented.

Maximum element size [m]	1	0.5	0.25	0.125	0.0625
Maximum PX due to axle load [kN]	6.8	6.8	6.7	6.7	6.7
Maximum PX due to distributed load [kN]	20.7	20.7	20.6	20.4	20.4
Number of nodes	20895	20943	38442	60435	118188
Number of shell elements (deck)	21636	21636	40868	64908	128138
Number of beam elements (girders)	141	189	360	693	1404

Table 3.1: Sensitivity analysis of the maximum shear force in a connector for the generic bridge.

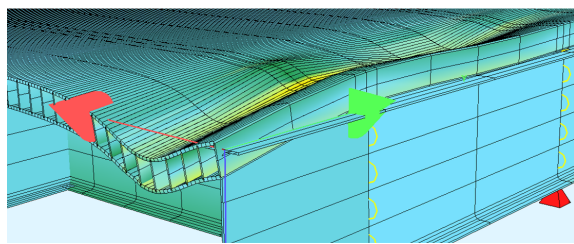
The sensitivity analyses shows that decreasing the maximum element size reduces the maximum shear force. However the difference between the largest and smallest element size is small with only 0.1 kN or 1.5% difference for the axle load and only 0.3 kN or 1.2% for the distributed load. In all cases the same connector had the maximum shear force. Other connectors showed the same pattern with a slightly decreasing shear force when the number of elements increased. The reason for the slight decrease is the way the model is created. The critical locations, for example where the connectors are connected, are by definition nodes which result in a mesh around those locations. Because of the small error with a maximum element size of 1 m and the much faster computational time, a maximum element size of 1 m is used in the rest of the report.

3.7. Limitations

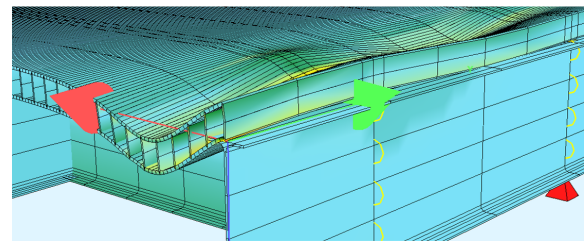
The model tries to represent reality but not everything is completely as it would be in reality. A few limitations of the model are explained in this section. The most important limitation, which affects the results on the maximum shear force in connectors, is the way the supports are constrained. Due to the chosen constraints at the supports, the shear forces in the connectors close to the support increases. Especially the shear force in the transverse direction is influenced. The shear force in the longitudinal direction is also influenced but the error margin is much smaller, within a few percent of the expected values. As the shear force in longitudinal direction is governing and the error margin is small it is accepted.

A second limitation of the model is the transfer of vertical forces. Contact areas between the deck and the support structure does not automatically mean that forces are transferred, see figure 3.11. The deck and girders are only connected via the connectors. There are results influenced by this simplification in the model but for the maximum shear forces in the connectors the influence is less than 1% so it is accepted as limitation.

Because only global effects are investigated in this research, the model should not be used to investigate local effects. The FRP sandwich panels are modelled with laminates. The build-up of the FRP laminates with different plies, and when InfraCore FRP panels are used the inclination of Z-shaped webs, are not modelled. Instead the properties of the laminates are calculated. The inclination is neglected as research showed that the influence on the stiffness properties of the deck is negligible (Lambrechts, 2019). Failure types cannot be investigated as the elements will never fail. These simplifications will not influence the shear force in the connectors but limit the possibilities of the model.



(a) The deformation of the superstructure and the deck not coupled.



(b) The deformation of the superstructure and the deck coupled at the corner.

Figure 3.11: The difference in deflection when the superstructure and the deck are and are not coupled. The deformation is magnified 140 times.

3.8. Model verification

The key parameter that is investigated in the thesis is the shear force in the connectors. To the best of the knowledge of the author, there is no experimental data about the shear forces in bolted connectors in hybrid steel-FRP bridges. With the current methods it is not possible to measure the shear force in connectors and as a result there is no data of shear forces in the connectors. So it is not possible to verify if the model is calculating the correct shear forces in the connectors. However it is possible to verify if other parameters of the model are calculated correctly.

If the deflection of the model is compared with experimental data and this is correct, it can be adopted that the shear forces in the connectors are also in the correct order of magnitude. The shear force in the connectors and the deflection are correlated with each other. Less hybrid interaction between the FRP deck and the steel girder results in more deflection and lower shear forces in the connectors. Contrariwise, more hybrid interaction results in less deflection and higher shear forces in the connectors.

The generic bridge will be verified with an analytical method proposed by Satasivam et al. (2017) and Gürtler (2004). The method is based on the mechanically jointed beam method from Eurocode-1995-1-1 (2005) and predicts the mid-span deflection. Partial hybrid interaction due to the connectors is taken into account with the method by calculating reduction factors. Gürtler (2004) used this method for an adhesively bonded steel-FRP deck and disregarded the shear stiffness as an adhesively bonded connection results in full hybrid inter-

action. Satasivam et al. (2017) adjusted the formula's by adding the slip surface so it is also valid for bolted connections. Both compared the method based on mechanically jointed beam with experimental data and the results showed good agreement. Satasivam et al. (2017) found a maximum difference of 5% for the deflection at mid span when bolted connections where used.

For the verification the layout of the generic bridge is used, which was explained in section 3.4. The layout of the FRP deck is as shown in figure 3.8a. Transverse webs are used, so the connector layout is as shown in figure 3.9b. The facings and deck have different compositions. Laminate 3 is used for the facings and laminate 4 is used for the webs as shown in table 4.5. The bridge is loaded with a distributed load of 10 kN/m^2 .

	Deflection at mid-span [mm]	Difference compared to model
SOFiSTiK model	14.807	
Analytical calculation	14.775	-0.2%

Table 3.2: Sensitivity analysis of the maximum shear force in a connector for the generic bridge.

For the verification, first the bending stiffness must be calculated. For this the cross section is divided into three parts: the top facing, the bottom facing and the steel girder. See also figure 3.12. The deflection at mid-span can be calculated. Equations 3.1 presents the equations for the bending stiffness and the deflection. The calculations are presented in appendix C. The deflection of the bridge calculated with the model and with the analytical method is shown in table 3.2. There is only a small difference of 0.2%. Knowing that the analytical method has a maximum measured difference of 5% compared to experimental data, the deflection of the model is in good agreement.

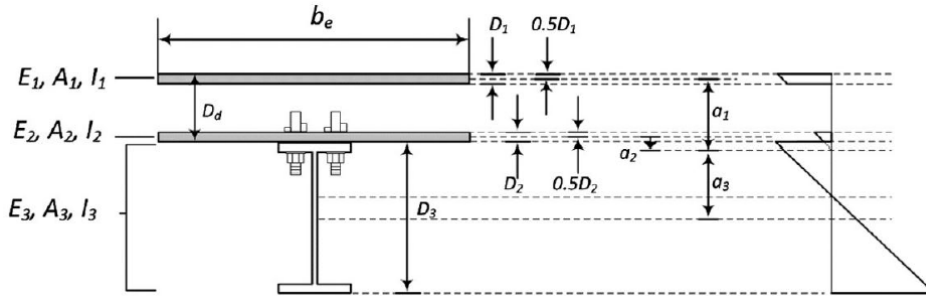


Figure 3.12: Cross section of the composite beam used (Satasivam et al., 2017).

$$EI_{eff} = \sum_{i=1}^n (E_i I_i + \gamma_i E_i A_i a_i^2) \quad (3.1)$$

$$u_z = \frac{5}{384} \frac{qbL^4}{EI_{eff}} + \frac{1}{8} \frac{qbL^2}{k_a G_a A_a}$$

(This page is intentionally left blank)

4

Bridge layout

This chapter describes the layout of the bridges included in this study. First the type of bridges is chosen. The dimensions of those bridges is described. Later, the method that determines the layout of the fibre reinforced polymers (FRP) decks for the bridges is presented. At the end of the chapter the composition of the web and facings for the bridges is presented.

4.1. Bridge type

Most bridges have an unique layout. Therefore choices have to be made which bridges will be included and which not. Replacing the deck of existing road bridge with FRP decks is a new phenomenon. Instead of investigating all type of bridges it is decided to focus on bridges with similar layouts.

To decide which layout will be investigated, the potential of the different type of bridges for getting an FRP deck is investigated. A database with the bridges owned and managed by Rijkswaterstaat is used to determine the potential. This database includes a quick scan which indicate if there are problems with the bridges based on expert judgement. Bridges with deck problems are relevant for renovation with an FRP deck. They are therefore the target group.

The database consist of 152 fixed bridged. Each bridge in this database is clustered in a group based on how the forces are transferred through the structure. Four main groups, namely girder bridges, arch bridges, cable-stayed bridges and truss bridges, can be distinguished. An example of the flow of forces through the girder bridges can be seen in figure 4.1.

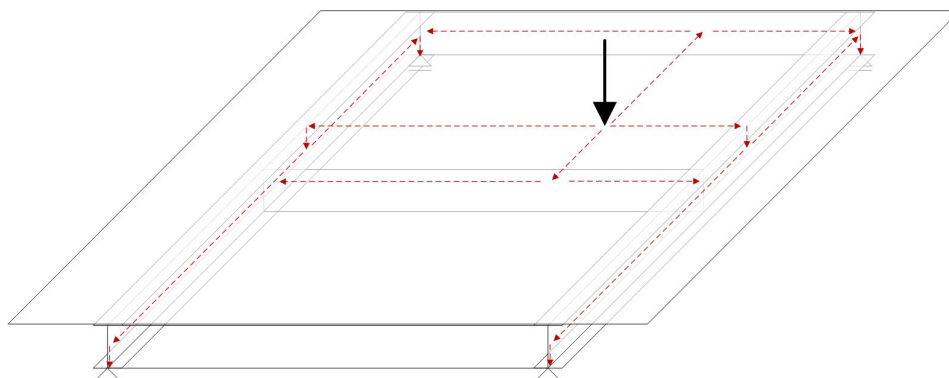


Figure 4.1: The flow of forces through the girder bridges.

Table 4.1 gives an overview of the results. 80 out of 152 bridges have been divided in one of the groups. The bridge that are excluded have unusual shapes. Also bridges with orthotropic decks (48) have been excluded. The orthotropic deck functions as top flange. Removing of the deck would result in girders without top flange so it is not possible to connect an FRP deck with bolts. As can be seen in table 4.1 girder and arch bridges are the most common bridges.

The main groups of the girder and arch bridges are divided in smaller groups. Girder bridge type 1 consists of multiple main and cross girders. Girder type 2 uses box girders and girder type 3 has concrete beams as superstructure. Girder type 4 consists of two girders with the deck hanging in between. The arch bridges are divided in two groups. Arch type 1 is an arch with vertical hangers and a lower deck, this means the deck is placed at the same height as the supports. Arch type 2 has an intermediate deck position. The deck is placed at about half the height of the arch.

	Number of bridges	Bridges with problems	Bridges with deck problems
Girder bridge	37	22	16
Type 1	29	18	12
Type 2	1	0	0
Type 3	5	3	3
Type 4	2	1	1
Arch bridge	27	16	16
Type 1	26	15	15
Type 2	2	1	1
Truss bridge	15	7	7
Cable-stayed bridge	1	0	0
Total	80	45	39

Table 4.1: Overview of the bridges in the Netherlands owned by Rijkswaterstaat. The table also shows if there are suspicions of (deck) problems.

In the table it is also mentioned how many of the different type of bridges have (deck) problems. Based on those results it has been decided to select girder bridge type 1 and arch bridge type 1 as most relevant type of bridges for this research. Those bridges are the most common bridges in the Netherlands and a large part of them have deck problems. By choosing these two type of bridges many existing bridges in the Netherlands with deck problems are included in the research. Examples of the two type of bridges can be seen in figure 4.2.



(a) Leemslagenbrug (arch bridge).



(b) IJsselbrug A12 (girder bridge).

Figure 4.2: The two bridge types which are investigated in this research.

The layout of girder and arch bridges can be seen in figure 4.3 and 4.4, respectively. The parameters which are used to model the bridges are also visible in the figures. The dimensions of the bridges are diverse, from four-lane highway bridges with spans over 200 m to one-lane bridges with spans of 30 m. The ranges of the bridge parameters can be seen in table 4.2. A complete list of the girder and arch bridges included in the research can be found in appendix D.

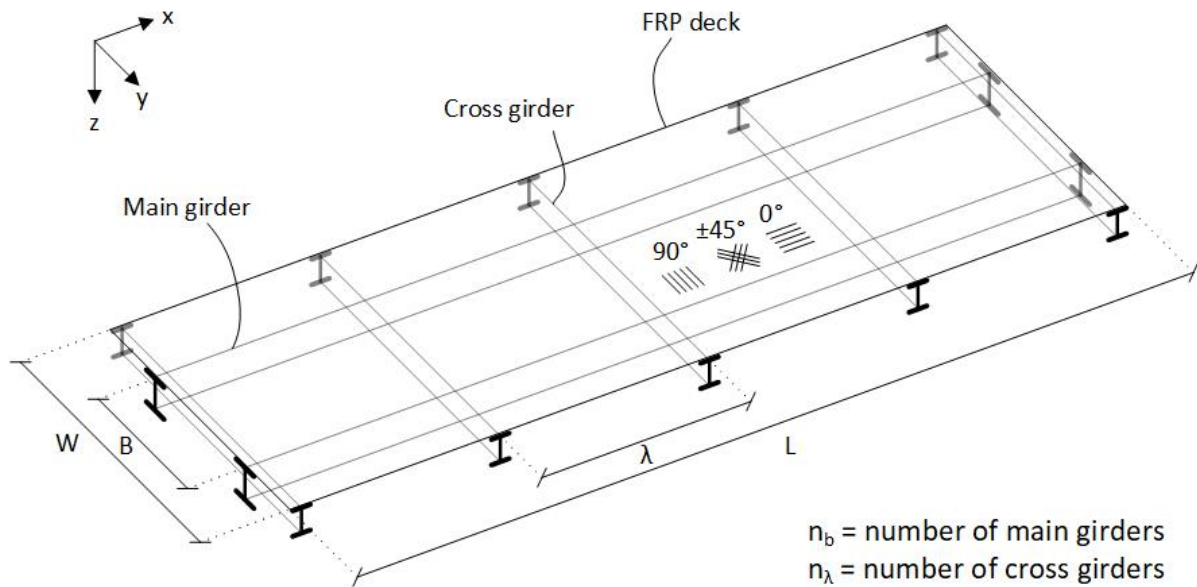


Figure 4.3: Parameters used for the girder bridges.

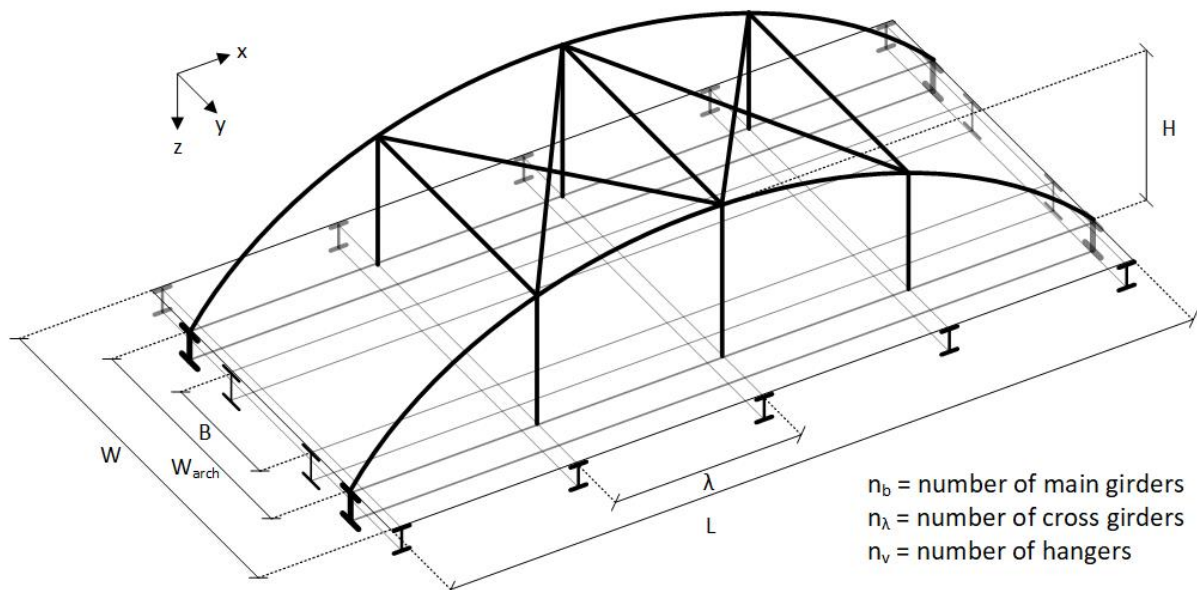


Figure 4.4: Parameters used for the arch bridges.

	Girder bridges	Arch bridges
Bridge length	13 - 530 m	60 - 300 m
Main span (L)	13 - 77 m	40 - 170 m
Width (W)	4.5 - 22.5 m	4.5 - 23 m
Number of longitudinal girders (n_b)	2 - 8	2 - 10
Number of cross girders(n_λ)	2 - 58	11 - 67
Distance between longitudinal girders (B)	1.28 - 9.85 m	0.9 - 5 m
Distance between cross girders (λ)	1.74 - 11.26 m	2.14 - 19.8 m

Table 4.2: The ranges of the bridge parameters.

4.2. FRP deck layout

When a company designs an FRP deck, the layout will be depending on the layout of the superstructure. To make the design cost efficient, a unique layout will be designed for each case with different dimensions and different fibre compositions. Because the FRP deck will be connected to the superstructure, hybrid interaction will occur, which means that the FRP deck will participate as top flange. Different FRP deck layouts result in different amounts of hybrid interaction.

Usually the webs of the FRP deck will be directed in the shortest distances between girders. This means that in some designs the webs will be parallel to the main girders and in some designs the webs will be parallel to the cross girders. Different web directions result in different cross sectional areas of the deck influencing the hybrid interaction between the superstructure and the deck.

For applicable results the FRP decks must have correct dimensions. With unique designs for each bridge it will be difficult to investigate the influence of the bridge layout. Besides it is a time consuming job to calculate the optimal FRP deck layout for each bridge. Therefore a simplified analytical method is used, based on previously research (Zarifis, 2018), to determine a design which is close to ideal. Buckling checks are not included as it is difficult to do them analytical. Requirements on the minimum thickness are included to prevent buckling.

4.2.1. FRP deck script

A script is used to determine with a simplified method the most cost effective FRP deck layout. The steps included in the script are shown in figure 4.7. Each step will be explained below.

Input

Bridge dimensions

Two dimensions of the bridges are determined, called B and λ . B is the longest distance between two main girders and λ is the longest distance between two cross girders, see also figure 4.5. If there are no cross girders the entire length of the bridge is used as value for λ . These bridge parameters are used as input for the analysis.

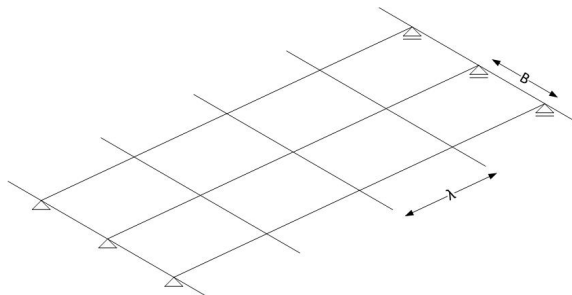
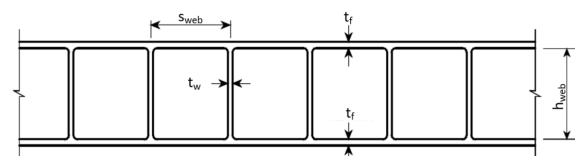
Figure 4.5: Bridge parameters B and λ .

Figure 4.6: FRP deck layout parameters which are varied.

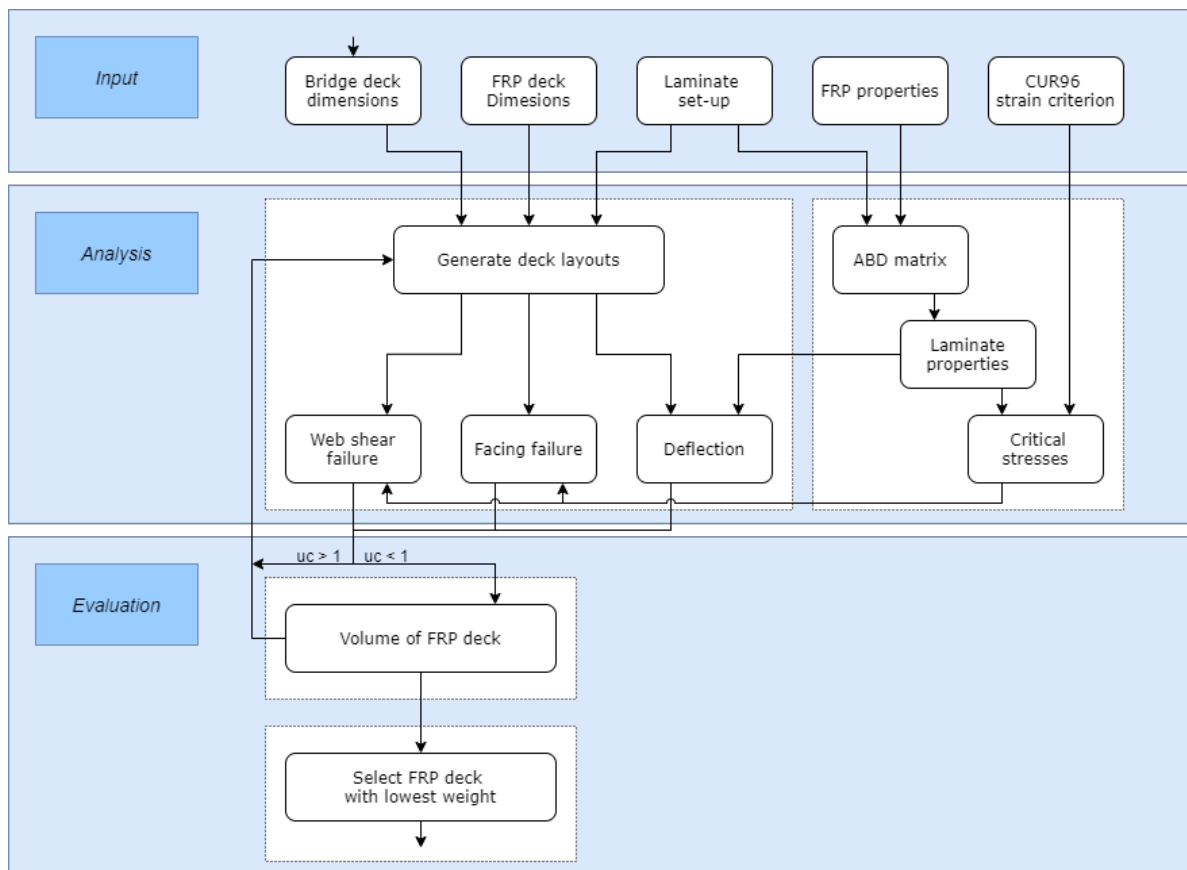


Figure 4.7: Scheme which explain how the script calculates the most cost effective FRP deck.

FRP deck dimension

Many different kind of FRP decks are possible. Only sandwich panels with all webs perpendicular to the facings are included in the analysis. This still leaves many options with different thicknesses for the facings and webs, different spacing between the webs and different heights of the webs. These variations can also be seen in figure 4.6. Minimum and maximum dimensions of the parameters are set in consultation with Fibercore. The requirements are present to make sure it is possible to construct the decks, buckling will not be possible and local stresses will not be too high. In table 4.3 the variations of the input parameters can be seen.

	Possible dimensions [m]
t_f	0.02, 0.022, 0.024, 0.026, 0.028, 0.03
t_w	0.01, 0.012, 0.014, 0.016, 0.018, 0.02
s_{web}	0.08, 0.01, 0.12
h_{web}	0.16, 0.18, 0.20, 0.22, 0.24

Table 4.3: The variations in the FRP deck dimensions.

Laminate set-up

The fibres can be orientated in four directions, 0° , 90° , 45° and -45° . Except for two conditions, all combinations are possible. In the CUR96 (2017) a minimum of 12.5% of fibres in each direction is recommended. Beside the 45° and -45° direction will always have the same percentage of fibres. The stacking sequence is not varied as Zarifis (2018) showed that no clear differences can be observed when there are fibres in all four directions.

FRP properties

Not all properties have been varied. The volume fibres fraction, V_f , which describes the ratio between the volume fibres and volume resin is kept constant at 50%. The properties of an E-glas unidirectional (UD) ply can be seen in table 4.4.

V_f	E_1 [kN/mm ²]	E_2 [kN/mm ²]	G_{12} [kN/mm ²]	ν_{12}
50%	37.2	11.4	3.4	0.29

Table 4.4: Properties of an E-glas UD-ply.

CUR96 strain criterion

The strength of FRP is high in comparison with steel and concrete. Disadvantage is the strain of the material that occurs when loading the FRP. The CUR96 (2017) sets a limit on the strain of 1.2% and a shear strain limit of 1.6%.

Analysis

Generate layout

For each input parameter, one of the options is selected to create the FRP deck. This is repeated until all deck designs were analysed.

ABD matrix

Before the laminate properties can be calculated, first the ABD matrix of the laminate must be calculated. This 6x6 ABD matrix tells something about the relation between the applied load and the associated stains. How the ABD matrix is calculated is explained in appendix B. The final result, a symmetric 6x6 matrix, can be seen in equation 4.1.

$$\begin{bmatrix} A_{11} & A_{12} & A_{16} & B_{11} & B_{12} & B_{16} \\ A_{12} & A_{22} & A_{26} & B_{12} & B_{22} & B_{26} \\ A_{16} & A_{26} & A_{66} & B_{16} & B_{26} & B_{66} \\ B_{11} & B_{12} & B_{16} & D_{11} & D_{12} & D_{16} \\ B_{12} & B_{22} & B_{26} & D_{12} & D_{22} & D_{26} \\ B_{16} & B_{26} & B_{66} & D_{16} & D_{26} & D_{66} \end{bmatrix} \quad (4.1)$$

Laminate properties

The ABD matrix must be used to calculate the laminate properties and the critical stresses. In-plane engineering constants are used to calculate the laminate properties. It uses the assumption that the laminate is predominately loaded in its plane. Flexural engineering constants should be used if bending is the dominant type of loading. Equation 4.2 shows how the laminate properties are calculated in which t is the thickness of the laminate.

$$\begin{aligned} E_1 &= \frac{A_{11}A_{22} - A_{12}^2}{A_{22}t} \\ E_2 &= \frac{A_{11}A_{22} - A_{12}^2}{A_{11}t} \\ G_{12} &= \frac{A_{66}}{t} \\ \nu_{12} &= \frac{A_{12}}{A_{22}} \end{aligned} \quad (4.2)$$

Critical stresses

When the laminate properties are known, the critical stresses can be easily calculated as shown in equation 4.3. The laminate properties must be multiplied with the strain criterion.

$$\begin{aligned}
 \sigma_1 &= E_1 * 0.012 \\
 \sigma_2 &= E_2 * 0.012 \\
 \tau_{12} &= G_{12} * 0.016
 \end{aligned}
 \tag{4.3}$$

Facing failure

The first verification done during the analysis is on facing failure. The maximum stress in the facing is determined with equation 4.4. z is the vertical distance between the neutral axis of the FRP deck and the furthest point. I is the moment of inertia and M is the maximum moment. The stress must be smaller than the critical stress in the direction in which the load is transferred to the support. Two situations can be distinguished. The situation in which $B < \lambda$ and $B \geq \lambda$. Figure 4.8 explains how the maximum bending moment is determined. The edges of the plate to which the forces are transferred is depending on the location of the load. It is assumed that the FRP deck is simply supported on only two sides. This is an overestimation of the resulting bending moment. The triangular loads are transformed into a rectangular load so it can be simplified into a 2D beams. The maximum moment can be calculated and is different for point loads and for distributed loads. The distributed load that is applied is equal to 9 kN/m^2 and the point load is equal to 300 kN . These values are based on load model 1 (LM1) from the Eurocode-1991-2 (2003). The stress from the point and distributed load are added together to check the stress.

$$\sigma = \frac{Mz}{I}
 \tag{4.4}$$

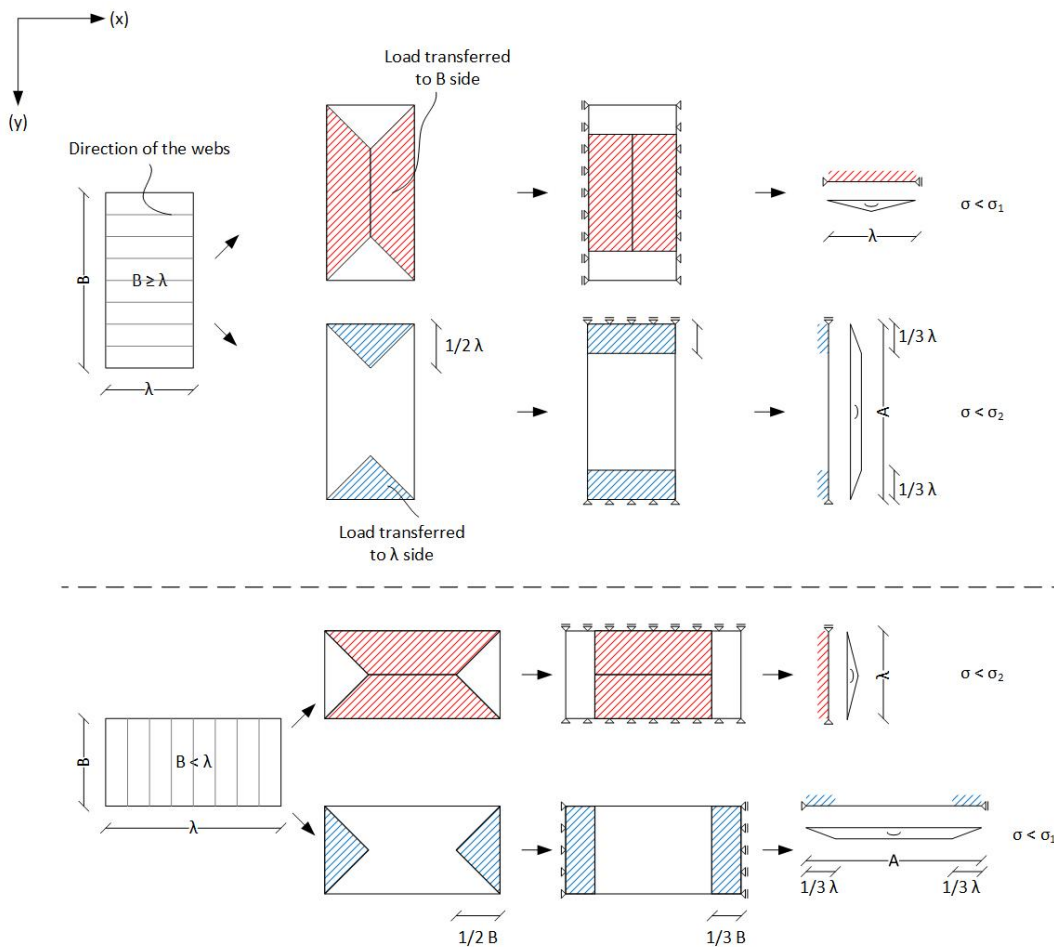


Figure 4.8: Simplified method how the maximum moment is calculated which is needed for the facing check.

Web shear failure

The second verification is for web shear failure. This is done with equation 4.5. Again a 2D simply supported beam is assumed just like with the facing check. In the first equation a single wheel is loading the webs. All forces are distributed on the webs below the wheel. The wheel has a weight F of 150 kN according to LM1. The force of the wheel is spread over an area of 400x400 mm. In the second equation a distributed load q of 9 kN/m^2 is loading the webs. h is the height of the webs and t_w is the thickness of the webs. n_{web} represent the number of webs that is loaded. The length L is depending on which situation is investigated. When $B \geq \lambda$ the length of the webs is λ and when $B < \lambda$ the length of the webs is B . The combined stress of these two equations must be smaller than the critical shear stress τ_{12} .

$$\begin{aligned}\tau_F &= \frac{F}{(400/s_{web})ht_w} \\ \tau_q &= \frac{0.5qL}{n_{web}ht_w}\end{aligned}\quad (4.5)$$

Deflection

The last verification checks if the deflection is within the limits. Again to make it easy to check a 2D simply supported structure is assumed just like with the facing check. The deflection can be checked with equation 4.6. As the longest span is checked, L is the largest value of B and Λ . Depending on the type of load the f_1 and f_2 in the formula change. Point loads and distributed loads have an respectively added F and q to the subscript. The loads are again an axle load of 300 kN and distributed load of 9 kN/m^2 . Shear deflection is also included. The total deflection is the sum of the deflection due to the distributed load and the point load. The maximum deflection is equal to $L/250$.

$$\begin{aligned}f_{F1} &= \frac{FL^3}{48} \\ f_{F2} &= \frac{FL}{4} \\ f_{q1} &= \frac{5qL^4}{384} \\ f_{q2} &= \frac{qL^2}{8} \\ G_c &= \frac{n_w t_w}{w} G_{12} \\ w &= \frac{f_1}{EI} + \frac{f_2}{G_c h}\end{aligned}\quad (4.6)$$

Evaluation

ULS and SLS checks

The facing failure, web shear failure and deflection have been verified. An unity check is calculated to determine if the FRP deck fulfills the requirements. In case the unity check is above 1, the option is removed from the list with all possibilities and the next option is investigated.

Volume of FRP deck

The volume of FRP deck is calculated. Costs are difficult to determine as companies are reluctant to disseminate information about cost. Labour cost is always present but not so much depending on the FRP layout. The amount of material on the other hand is depending on the amount of fibres and resin. As the volume fraction and density is constant for both the fibres and resin the volume of the FRP deck will be a good equivalent to the cost. The design with the lowest volume is selected as 'cheapest'.

4.2.2. FRP deck results

When the FRP deck layouts were calculated for all bridge, bridges with comparable FRP deck layouts have been grouped. The FRP deck layout of each bridge in a group is changed in such a way that all the bridges

in the group have the same layout. The layout differs little to the most cost efficient design calculated with the simplified method and still fulfills the requirements that were set. Now it is possible to compare results independent of the FRP deck layout.

Three facing layouts will be used when modelling bridges. The layouts can be seen in table 4.5 as laminate 1 to 3. The only difference is the amount of fibres in each direction. The webs always have most fibres in the 45° and -45° resulting in laminate 4 as can be seen in 4.5. This makes sense because the only check that is done for the webs is on shear. The lowest unity checks are obtained when G_{12} is as high as possible. This is the case when there are more fibres in these directions. The distance between the webs will be 0.12 m and the height of the webs will be 0.16 m.

Facing 1 is used for bridges with the cross girders closer to each other than the main girders. Facing 2 and 3 are used for bridges where the main girders are closer to each other than the cross girders. If facing 2 or facing 3 is used depends on the ratio B/λ . Facing 3 will become a better option when the ratio is getting closer to 1. The webs are directed in the shorted span between girders, so the smallest value of B or λ . For the generic model laminate 3 is the best option with webs in the transverse direction, although for this model only some other layouts will be investigated to show the influence of the design parameters.

	$t[mm]$	$0^\circ[\%]$	$\pm 45^\circ[\%]$	$90^\circ[\%]$
Laminate 1 (facing)	20	62.5	12.5	12.5
Laminate 2 (facing)	20	12.5	12.5	62.5
Laminate 3 (facing)	20	25	12.5	50
Laminate 4 (webs)	10	12.5	37.5	12.5

Table 4.5: The composition of the laminates that will be used in the remaining of this thesis for the FRP decks.

(This page is intentionally left blank)

5

Hybrid interaction

In this chapter, it is shown what the effect of hybrid interaction is by comparing two models of the generic bridge. The first model is just as described in chapter 3 and uses hybrid interaction. The second model will be adjusted at some points to create a non-hybrid model. The deflection, slip and stress of the two models will be compared. Before the hybrid and non-hybrid models are compared, first the effect of hybrid interaction is explained.

5.1. Effect hybrid interaction

A formal definition for hybrid interaction is the amount of horizontal forces that is transferred between the beams. Full hybrid interaction is achieved when 100% of the horizontal forces is transferred and no hybrid interaction is achieved when 0% of the horizontal forces are transferred. When connected with bolts, there will be partial hybrid interaction. These cases can be seen in figure 5.1. Only the no hybrid interaction, with the non-hybrid model, and partial hybrid interaction, with the hybrid model, will be compared.

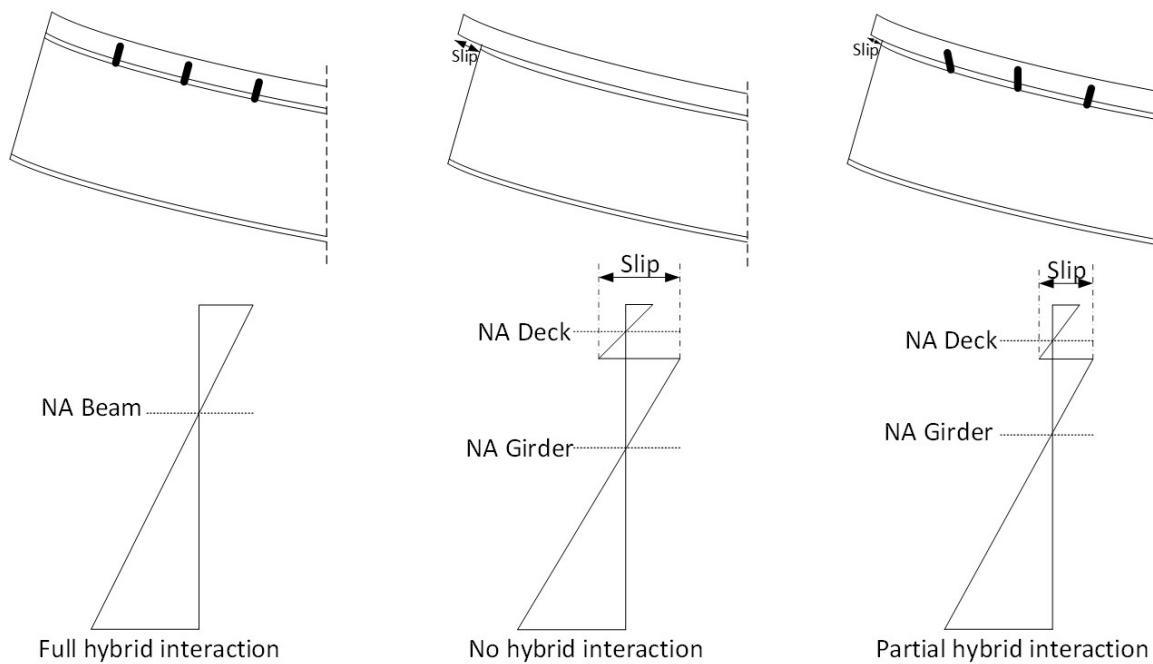


Figure 5.1: Different situations of hybrid interaction.

The effect of hybrid interaction can be explained with a simple example of a timber beam as shown in figure 5.2. One can imagine that the deflection of the beam will be lower when the height of the beam doubles. The bending stiffness (EI) of the beam is increased. When two beams are placed on top of each other and glued together, the beams will behave as a single beam with a doubled height, so again the deflection is lower. In the fourth case, again two beams are placed on top of each other but this time a mechanical connection is made. The height of the beam is doubled, but due to the spacing between mechanical connectors, the beams are not completely interacting together. In the Eurocode it is stated that when timber beams are jointed mechanically, a reduction factor must be applied when the bending stiffness of the beam is calculated. This reduction factor is taking into account that the beams are not completely interacting. For glued timber beams this reduction factor is equal to 1. When a bridge is constructed with steel girders and a fibre reinforced polymers (FRP) deck, connected with bolts, there will be some hybrid interaction reducing the deflection. Just like with the timber beam mechanically connected.

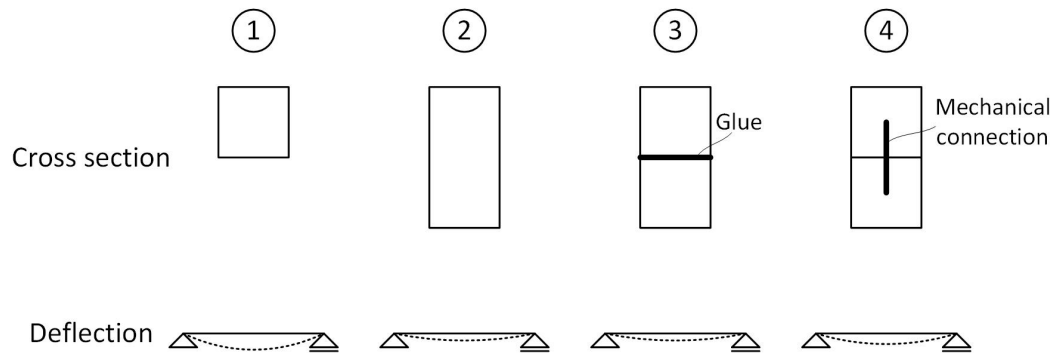


Figure 5.2: The deflection for timber beams with different cross sections.

5.2. Non-hybrid Model

The non-hybrid model is similar to the hybrid model, there are only some changes in the connectors. The idea is to have no interaction between the deck and the girders. But the two need to be connected in such a way that the deck cannot float away. First the transverse stiffness of the original connectors is reduced to almost zero, it is changed from 100 kN/mm to 0.01 kN/mm. This prevents that shear forces are transferred through the connectors. To prevent the deck from floating away because the shear forces cannot be transferred, three connectors have other properties. First in the middle there is a connector which is fully fixed between the deck and the girder. Secondly there are two connectors at the begin and end of the bridge which only allow movement in the longitudinal direction. The three connectors prevent the deck from floating away in the longitudinal and transverse direction but still allow movement in both direction. In addition rotations of the deck in the horizontal plane is prevented. Movement and rotations in the other directions are prevented by the axial stiffness of the original connectors. An overview of the non-hybrid model with the changes for transverse and longitudinal decks can be seen in figure 5.3.

The shear force in the connectors is investigated in this research. The transverse stiffness is one of the most important parameters for the shear force in the connectors. A higher value attracts more shear force while a lower value transfers the shear to other connectors. When the transverse stiffness is zero, no shear forces can be transferred. Because the transverse stiffness of the connectors is changed in the different models, it is not possible to compare the hybrid and non-hybrid model by comparing the shear forces in the connectors. Therefore a different parameter must be used.

The deflection is chosen as parameter to compare the hybrid and non-hybrid model. One can imagine that the moment of inertia of the girders is smaller than the moment of inertia of the girders and the deck combined when they are working as one. A higher moment of inertia will reduced the maximum deflection. Connectors will not make the girders and deck work together for 100 % but interaction will be achieved. This results in less deflection. In addition, if a part of the FRP deck is not fully contributing to the hybrid interaction, this will influence the deflection as well. So when the hybrid model is compared with the non-hybrid

model, the maximum deflection of the non-hybrid model is expected to be larger because there is no interaction between the deck and the girders. Therefore the deflection is a good parameter to investigate if there is hybrid interaction and how much it influences the results.

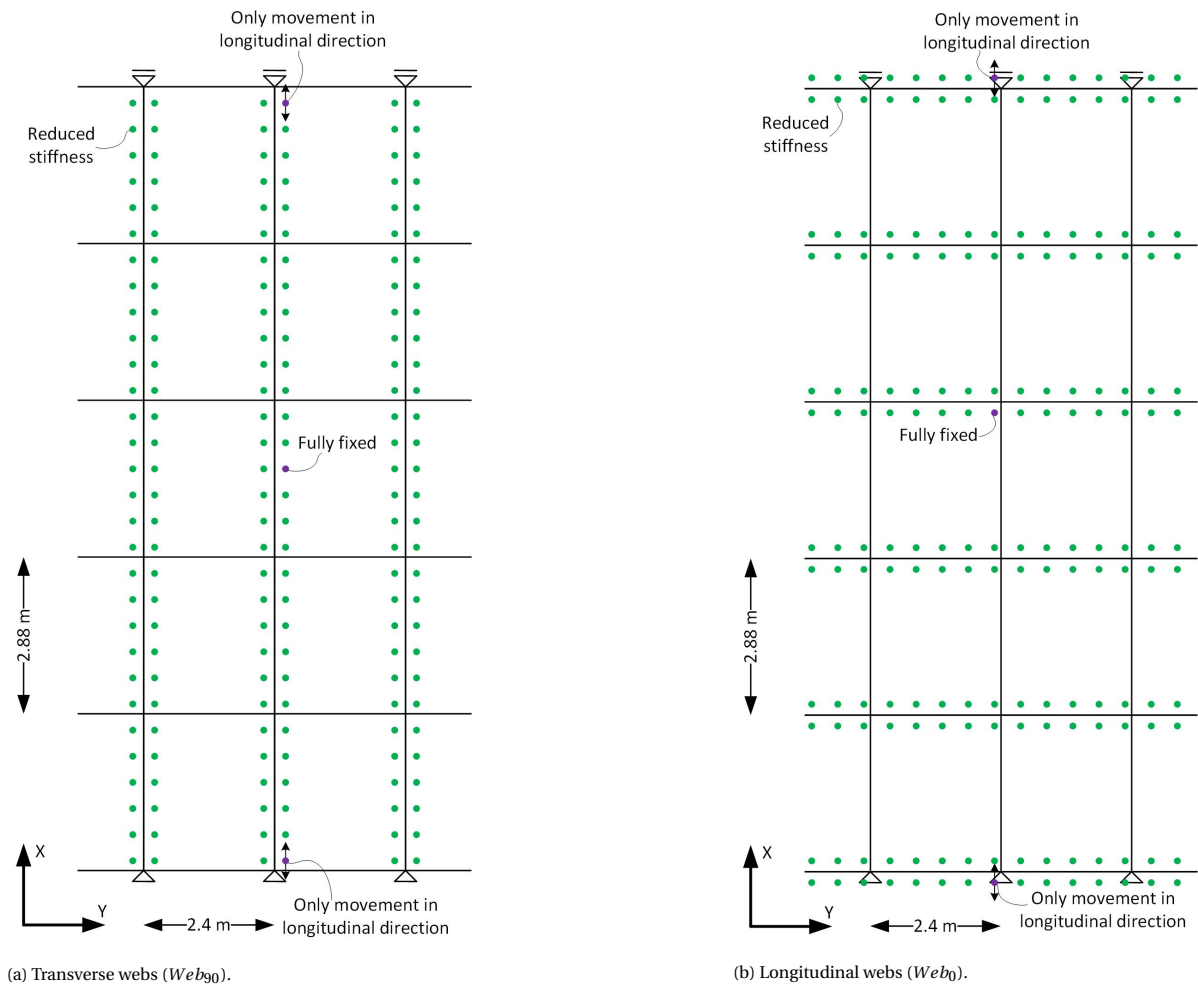


Figure 5.3: The non-hybrid interaction model. The transverse stiffness of the connectors is reduced and the boundary conditions of three connectors is changed.

In addition to the deflection, the transverse displacement of the connectors or slip is investigated as well as the stress distribution along the height of the beam. Figure 5.4 shows the definition of the slip. It is the transverse displacement between the middle of the steel girder and the middle of the bottom FRP facing of the deck. In case of full hybrid interaction there would be no slip. The amount of slip can indicate how close to full hybrid interaction the hybrid model is. The stress distribution along the height of the beam also indicate how much hybrid interaction is achieved but also if every part of the FRP deck is contributing.

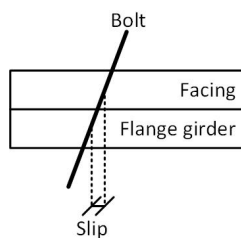


Figure 5.4: The definition of the slip of the bolted connectors.

5.3. Hybrid vs Non-hybrid

The hybrid and non-hybrid version of the generic bridge for longitudinal and transverse webs will be compared. The dimensions and layout of models are identical for the hybrid and non-hybrid models. The only difference is the reduced stiffness of the original connectors and three adjusted connectors in the non-hybrid model as indicated in figure 5.3. The maximum deflection of the girders will be compared as well as the slip and stress distribution along the height of the beam. The models are loaded by self-weight and an axle load in the middle of the slow lane.

Deflection [mm]	Hybrid model				Non-hybrid model			
	Axle load		Distributed load		Axle load		Distributed load	
	Web_0	Web_{90}	Web_0	Web_{90}	Web_0	Web_{90}	Web_0	Web_{90}
	6.960	5.418	18.878	14.807	8.506	8.643	21.565	21.764

Table 5.1: The maximum deflection of the girders for the hybrid and non-hybrid model due to different loads.

The deflection for the eight different cases is presented in table 5.1. It can be seen that the deflection of the non-hybrid model loaded is larger than the deflection of the corresponding hybrid models. However there is a difference visible when comparing the models with web_0 and web_{90} . The deflection of the non-hybrid models with web_0 is about 1.2 times larger compared to the hybrid models for both the axle and distributed load. The deflection of the non-hybrid models compared to the hybrid models with web_{90} is 1.6 and 1.5 times larger for respectively the axle load and distributed load. So the transverse stiffness of the bolted connections, present in the hybrid model, increases the interaction between the steel girders and the FRP deck and reduces the maximum deflection of the bridge for all models. The larger reduction of the deflection for web_{90} models means that there is more hybrid interaction in case of transverse webs. Figure 5.5 compares the deflection of the web_{90} hybrid model with the deflection of the web_{90} non-hybrid model, both loaded with a distributed load. The deflected models are pasted over each other. The non-hybrid model is made a bit transparent. As a result it is visible that there is more deflection for the non-hybrid model.

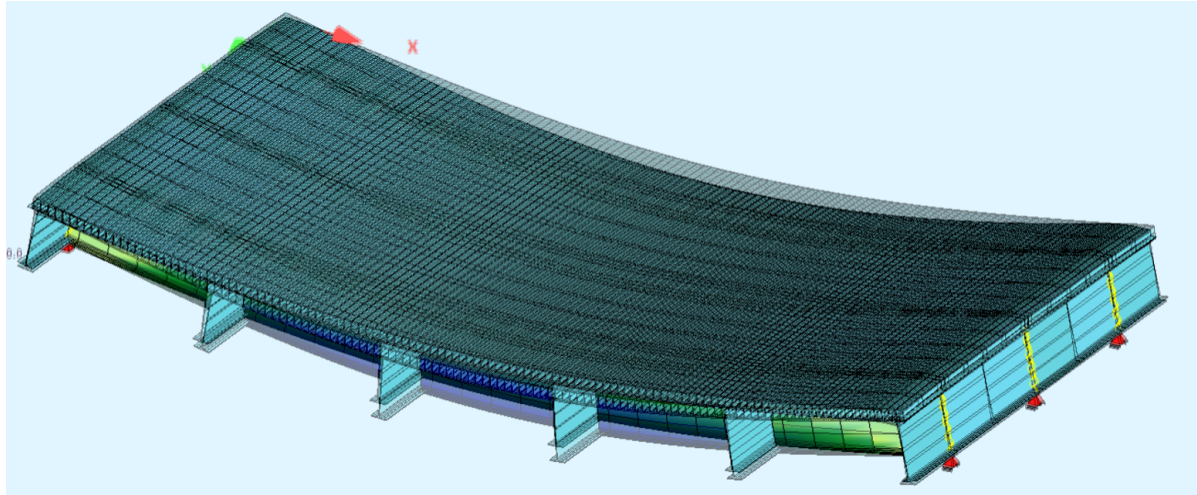


Figure 5.5: The deflection of the hybrid and non-hybrid model due to a distributed load with web_{90} . The non-hybrid model is made a bit transparent to be able to compare the deflections and see there is more deflection for the non-hybrid model. The deflection is exaggerated to make the difference better visible.

Slip [mm]	Hybrid model				Non-hybrid model			
	Axle load		Distributed load		Axle load		Distributed load	
	Web_0	Web_{90}	Web_0	Web_{90}	Web_0	Web_{90}	Web_0	Web_{90}
	0.049	0.068	0.144	0.207	1.644	1.314	3.838	2.862

Table 5.2: The maximum slip of the connectors for the hybrid and non-hybrid model due to different loads.

Table 5.2 presents the maximum slip found in one of the connectors for the hybrid and non-hybrid model. Both the axle load and the distributed load for web_0 and web_{90} are shown. It is clear that the slip is much larger in the non-hybrid models. The reduction of the slip in the hybrid models compared to the non-hybrid models is larger for web_0 models than for web_{90} models. This indicates that, at least the bottom facing of the FRP deck, is more activated in case of web_0 although the difference is small. Figure 5.6 also shows the slip in the two models for the distributed load. It can be clearly seen that the connector in the non-hybrid model is much more slanted than the connector in the hybrid model. The slip in the hybrid models is not zero, so there is no full hybrid interaction.

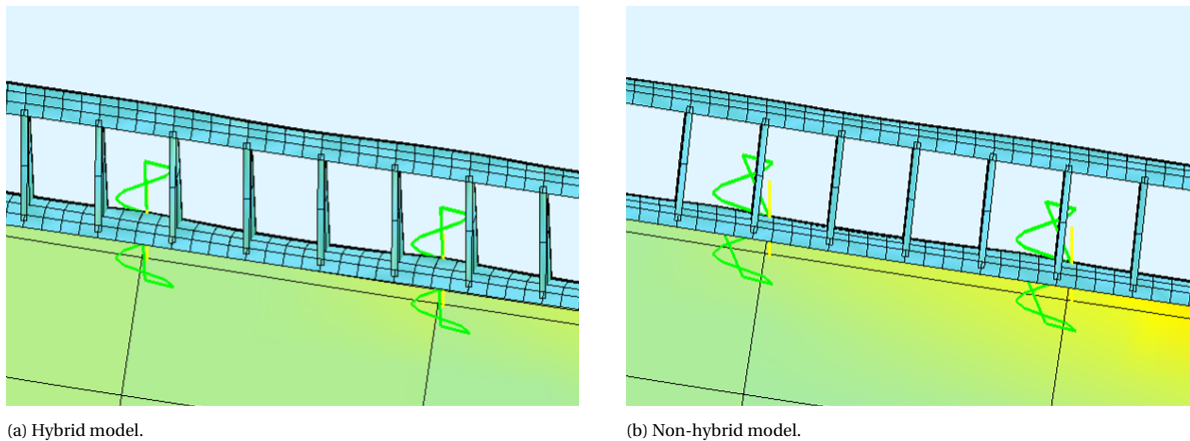


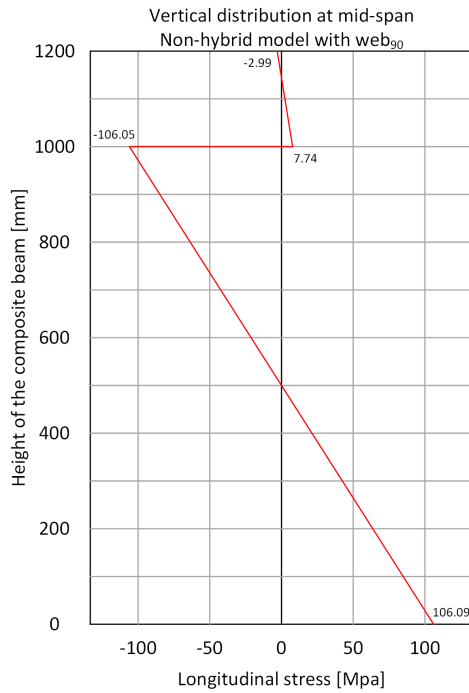
Figure 5.6: The slip of the bolted connections of the hybrid and non-hybrid model due to a distributed load with web_{90} .

The last parameters that is investigated is the stress. The longitudinal stress over the height of the beam is determined in the lengthwise middle of the central main girder for the models with a distributed load. The results can be seen in figure 5.7. The first 1000 mm is the stress in the steel girder and the stress from 1000 to 1200 mm is the stress in the FRP deck. The steel girders are expanded at the bottom and compressed at the top resulting in respectively tension and compression. In the non-hybrid models, the FRP deck does not interact with the steel girders and as a result there is also tension in the bottom facing and compression in the top facing. For the non-hybrid model it would be expected that the compression stress in the top facing is equal to the tension stress in the bottom facing. In the hybrid models there is interaction between the girders and deck. The stress distribution of the deck is therefore not standing on its own, resulting in compression in both the top and bottom facing. However the stress in the top facing is smaller than the stress in the bottom facing. It would be expected for the hybrid model that there is a higher compression stress in the top facing compared to the bottom facing of the FRP deck.

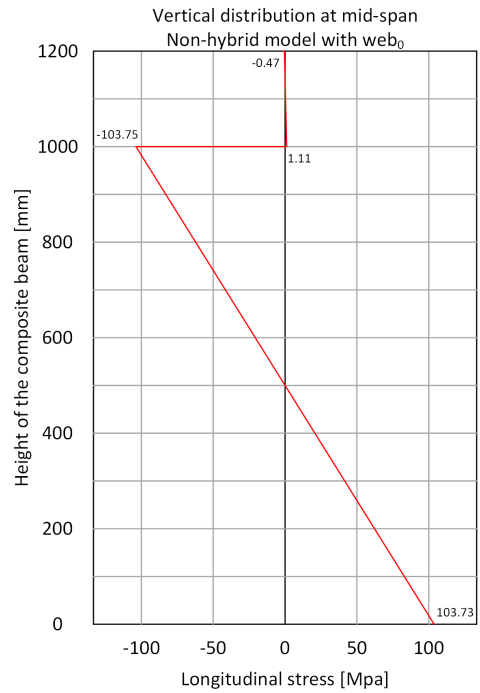
In all cases the stress in the top facing is smaller than expected and is therefore not contributing as much as would be expected. Swinnen (2020) had the same observation during his research and found two reasons for the lower compression in the top facing. Swinnen (2020) isolated both effects in additional models. First the effect of transverse bending of the FRP deck was investigated. Transverse bending of the deck results in tension forces in the top facings above girders and compression forces in the top facing between girders. This had a significant effect on the longitudinal stress in the top facing. Second there is the secondary moment effect. The distributed load causes bending of the composite beam, the bottom facing of the FRP deck acts together in compression with the top flange of the steel girder. Because of the low in-plane shear stiffness of the FRP panel, the top facing is not engaged and practically not mobilised. This results in tension stress in the top facing although of minor magnitude. Both effects reduce the compression forces in the top facing of the FRP deck at the measured location.

In order to increase engagement of the top facing and transfer more stresses between the top and bottom facing, several improvements can be proposed. A larger centre-to-centre distance of the facings of the deck, makes the core less stiff and therefore less able to transmit stresses. This means there is a greater shear lag effect leading to a lower effective width and subsequently lower composite stiffness (Dreaves, 2018). A smaller web height reduces the flexibility and increases the deck stiffness and transfer of stress between the facings.

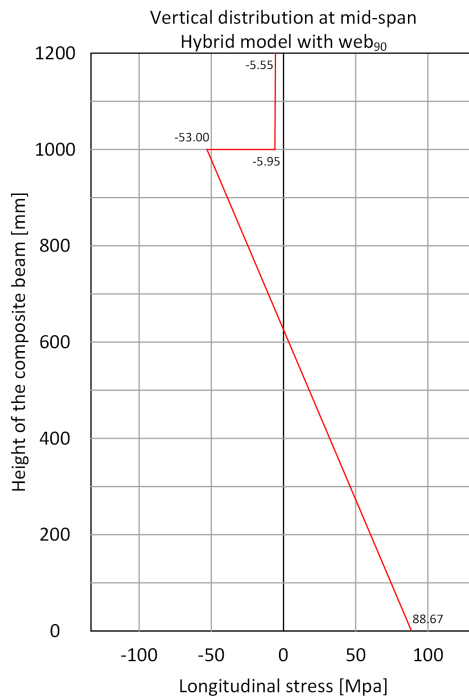
However, the height of the deck cannot be decreases without checking the strength of the deck as the inertia of the deck increases with a higher deck and so does the strength. Another option is to increase the stiffness of the webs. This can be done by reinforcing the webs, using a different material or by using different composition. Dreaves (2018) also investigated the effect of the core stiffness by adding the foam, located between the webs for feasibility reasons, to his model. A 5% greater stiffness was achieved.



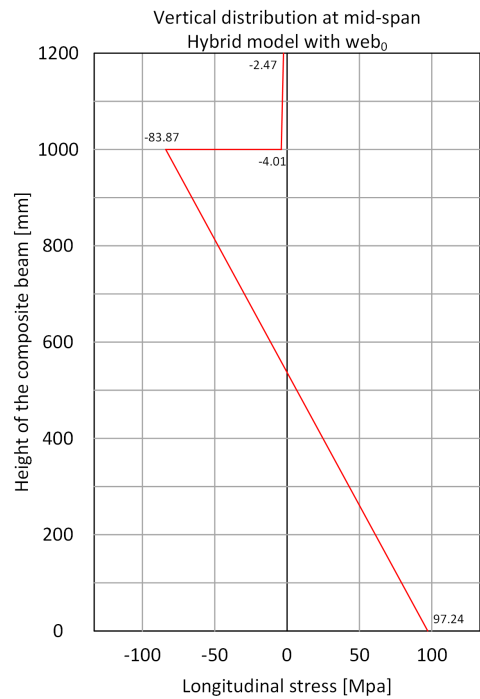
(a) Non-hybrid model, web_{90} .



(b) Non-hybrid model, web_0 .



(c) Hybrid model, web_{90} .



(d) Hybrid model, web_0 .

Figure 5.7: The stress along the height of the beam at the middle of the central main girder.

In case there is more hybrid interaction, there will be more forces transferred through the connectors resulting in higher shear forces. Web_0 has a higher reduction in stress in the top facing compared to the web_{90} variants. This means less forces are transferred through the connector and there is less hybrid interaction. So because there is less hybrid interaction when the webs are in the longitudinal direction, it is also expected that there will be lower shear forces compared to using webs in the transverse direction.

The SOFiSTiK model uses hybrid interaction, the model is compared with a variant without hybrid interaction. As a result the deflection and slip are reduced and the FRP deck is loaded in compression. The deflection results show that there is more hybrid interaction in case of transverse webs. The deflection is in the hybrid model a factor 1.5 smaller for transverse webs compared to a factor of 1.2 for longitudinal webs. The maximum slip is significantly reduced, through there is still slip so full hybrid interaction is not achieved. The reduction in slip when the hybrid model is used is a little bit larger for longitudinal webs, indicating that the bottom facing is activated a bit more compared to transverse webs. The stress in the top facing is not fully activated. In case of longitudinal webs the top facing is activated less than when transverse webs are used. This means there is more hybrid interaction in case of transverse webs and as a result the shear forces in the connectors are expected to be higher. Depending on the layout of the bridge the difference in deflection between the hybrid and non-hybrid model can change. Also the layout of the FRP deck influences the amount of hybrid interaction.

(This page is intentionally left blank)

6

Static shear force

The aim of this chapter is to investigate the shear force in non-slip bolted connectors with hybrid interaction. Two type of loads will be taken into account, namely traffic load according to load model 1 (LM1) and temperature load. When it comes to analysing the shear forces there are more types of loading to be considered. However, the influence of the other loads is negligible compared to the selected ones. This was proved during a Benchmark study at the start of this project and the results can be found in appendix A. The goal of this chapter is to subsequently gain knowledge into the influence of traffic and temperature on the shear forces in connectors between fibre reinforced polymers (FRP) decks and indicate what is the magnitude of forces to be expected.

Regarding the geometry of the bridges, the following cases will be analysed. First the generic bridge and second the real bridges in the Netherlands as presented in chapter 4. The generic case is considered in order to have a reference point that is easy to understand and fast to calculate. Besides the generic case can be used for parametric analyses to investigate the effect of design parameters on the magnitude of the shear forces in the connectors. Then the real bridges are analyzed to gain knowledge on the magnitude of expected shear forces on actual geometries. These results can be beneficial for evaluating the applicability of different types of connectors.

In this research the layout of the bolts, i.e. the number of connectors per meter girder, is kept the same for each bridge and results from only the most heavily loaded connectors are used. Most of the times those connectors are close to the supports. Optimisation of the layout is possible to reduce the number of connectors. In situations where shear forces in the connectors are higher than feasible, extra connectors can be placed on the locations where required but this is not done in this report.

This chapter is structured as follows. First the definition of the loads is explained. Then it is explained how the results from the SOFiSTiK model are processed. Subsequently the result for the generic bridge are presented, which include parametric analyses to investigate some design parameters. The last section shows the results of the highway bridges in the Netherlands.

6.1. Load definition

6.1.1. Traffic load

Traffic results in different loads on the bridges. Eurocode-1991-2 (2003) should be used to verify the bridges. The benchmark study, see appendix A, showed that horizontal loads caused by accelerating and braking barely have influence on the shear force in the connectors and are therefore neglected. Bridges need to be verified with four different models for vertical loading. Because the benchmark study showed that LM1 results in the highest shear forces in the connectors, only this load model is investigated in this chapter.

LM1 is a static traffic load which is used to analyse global effects. It consists of a tandem system with two axles. The load of each axle is 300 kN in lane 1, 200 kN in lane 2 and 100 kN in lane 3. The remaining lanes have no axle load. The distributed load is equal to 9 kN/m^2 for lane 1 and the remaining lanes and the remaining area have a distributed load equal to 2.5 kN/m^2 . The distance between the axles is 1.2 m and an axle is 2 m wide. The contact area of a wheel is 0.4 by 0.4 m. The loads must be applied in each lane on the worst part for each detail that is investigated. The layout of the tandem system can also be seen in figure 6.1. A cross section of the generic bridge with the loads according to LM1 can be seen in figure 6.2.

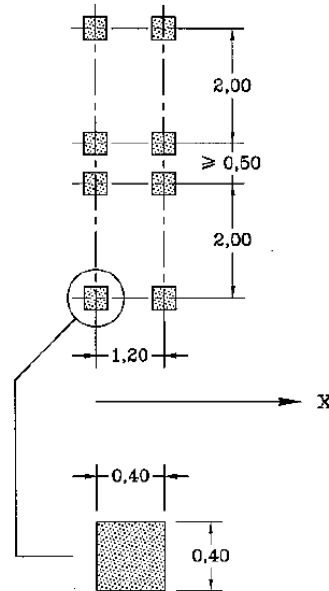


Figure 6.1: Definition of the geometric dimensions of the wheels and axles for LM1.

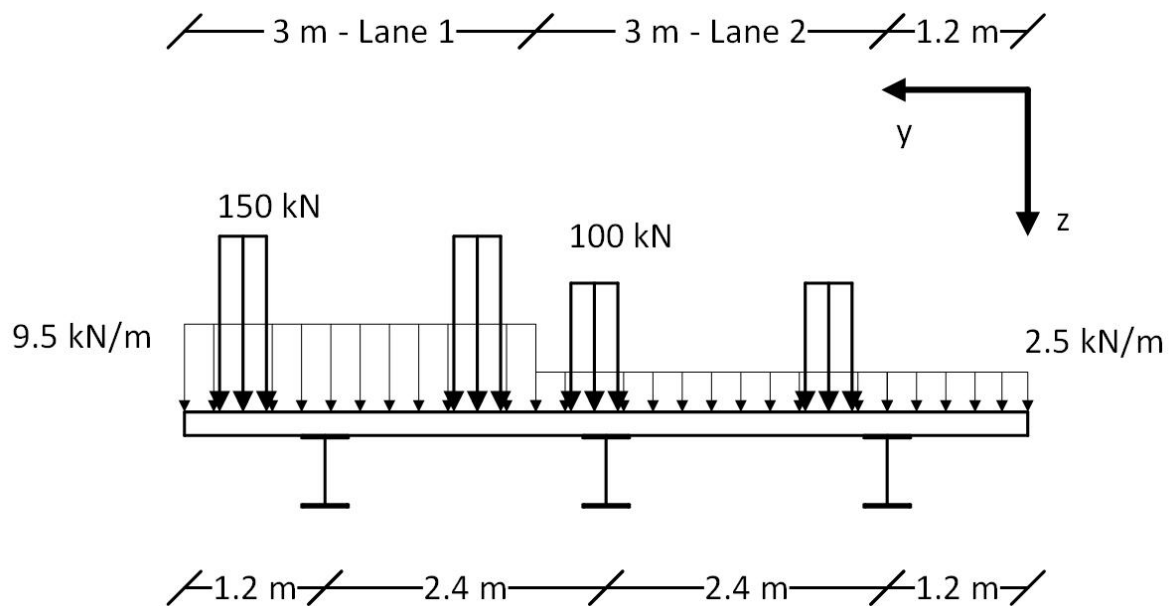


Figure 6.2: Cross section of the generic bridge with loads according to the Eurocode.

6.1.2. Temperature load

Thermal action on bridges should be assessed with an uniform temperature component and a temperature difference component according to Eurocode-1991-1-5 (2003). The effect of both components on the bridge is shown in figure 6.3. The uniform temperature component results in extraction or contraction of the bridge parts. When the expansion coefficient of the deck and girders have the same value there will be no forces in the connectors due to temperature load. The temperature difference component results in bending of the bridge.

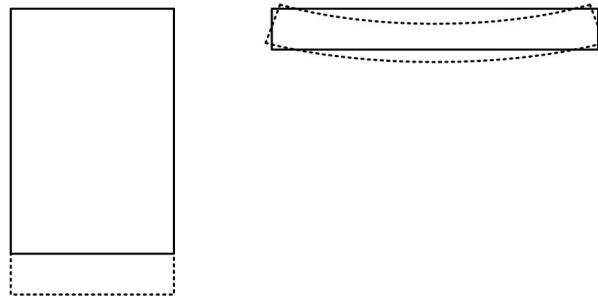


Figure 6.3: The expansion due to uniform temperature component (left) and due to temperature difference component (right).

The FRP deck and steel girder have different expansion coefficients. The uniform temperature component will result in different expansions of the deck and the girders. Connectors will try to keep everything together but as a result shear forces will occur. The temperature difference component will have different temperatures over the height of the bridge. The top of the girders and bottom of the deck will have the same temperature as they are located above each other. So in the connectors there will be a more or less uniform temperature difference resulting in shear forces. The temperature that needs to be applied for the temperature difference component is smaller than the temperature that must be applied for the uniform temperature component.

As a result the uniform temperature load will be the governing temperature load as this creates the largest displacements between top and bottom of the connectors and consequently leads to the largest shear forces in the connectors. Different types of uniform loading can result in expansion or contraction of the bridge parts. For the shear forces in the connector the only difference will be the direction of the load. Because the direction of the load in the connector is not important, the absolute largest uniform temperature load is the governing case. A uniform temperature load of $+38^{\circ}\text{C}$ has been applied to the generic bridge (Eurocode-1991-1-5, 2003).

6.2. Methodology for static analyses

To determine the static shear forces in the connectors, several steps are followed which are explained in this section. The analyses start with running the model in SOFiSTiK. The results obtained with the model are loaded in a python script that calculates the influence line of the connectors. From these results the magnitude of the heaviest loaded connector is obtained.

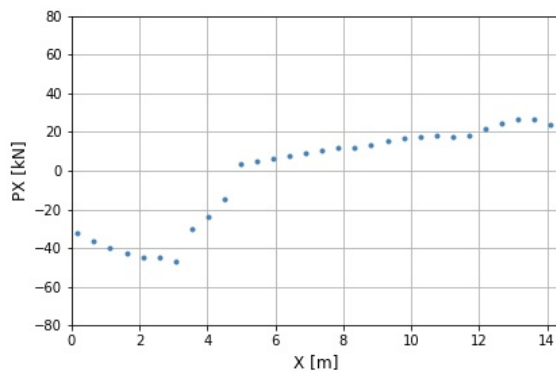
Model

When a bridge is investigated, it is modelled as described in section 3.2. In the input of the model, the layout is entered. The load definition of the static traffic load and the static temperature load are described earlier in this chapter. The model only calculates the shear forces due to axle loads, not the entire tandem system. The magnitude of the axles load depends on the lane. The axle load is applied every 0.4 m in each lane of the bridge. The temperature load consists of a temperature difference. The temperature load is applied in the form of extension or contraction of the bridge elements. The extension or contraction is equal to the temperature difference multiplied with the expansion coefficient of the material. Each axle load and temperature load is saved as a separated load case. The calculated shear forces in the connectors for each load case are saved and can be used in the next step.

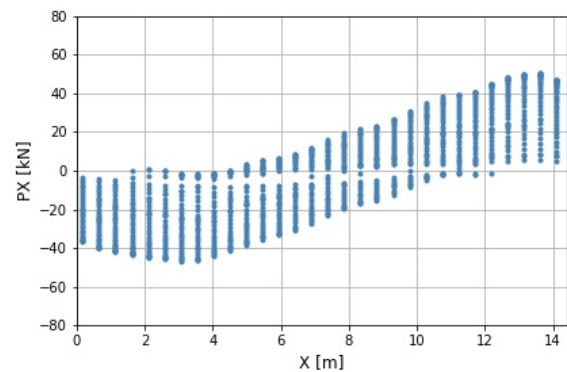
Envelope of shear forces

The static shear forces due to an axles load driving over the bridge or due to temperature load are calculated. To plot the envelope of shear forces, several steps are undertaken with a python script. The steps are plotted in figure 6.4. First for a load case, so a single axle or temperature load, the shear forces in the connectors are imported. For the traffic load, tandem systems are needed so two load cases 1.2 m from each other are combined. The connectors on the bridge are plotted in rows, connectors with the same y-coordinate are in the same row. The shear force due to the tandem system or temperature load is plotted for a single row of connectors. The connector row below the slow lane will be the governing row as these connectors are closest to the heaviest loads, but each row can be plotted. Each dot represents the shear force in a different connector due to a single tandem system or temperature load. Temperature load does not require different axles to be combined, and also does not have different locations where the loads can be located. Therefore for temperature loads only this first step is needed.

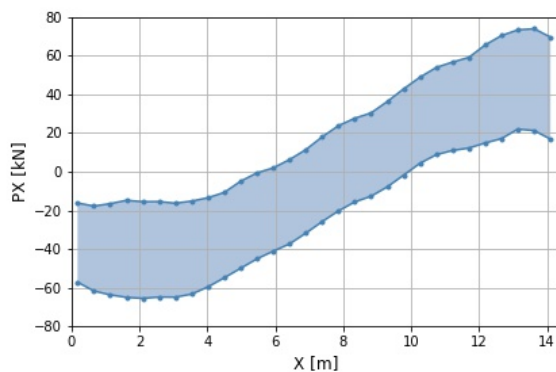
In the second step the tandem system starts moving to different locations. Every time the tandem system shifts 0.4 m further over the bridge. Each dot again represents the shear force in a connector due to a load case. Dots in the same vertical line are the same connectors but the dots are loaded with loads (tandem system) at different location on the bridge. The first two steps are repeated for all the lanes. In the third step, the different lanes are combined. For each lane the minimum and maximum shear force of the connectors is selected. By superposition the different lanes are added up. Also the distributed load is added. The minimum and maximum shear force of each connector is marked and the area in between is shaded. This is the envelope for the connectors of a single row. The minimum and maximum shear force for each connector can now be read in the graph. In the last step multiple connector rows are combined. This graph can be used to read the extreme shear force that can be expected.



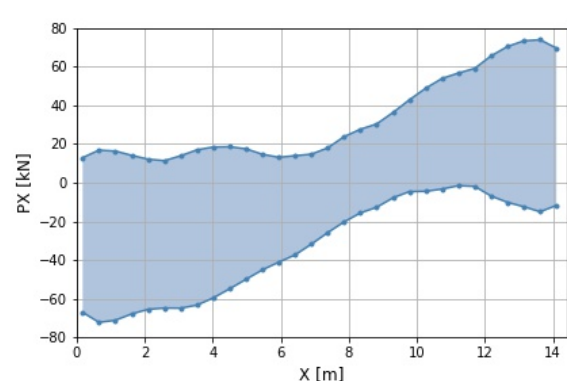
(a) The shear forces due to a single tandem system for the connector row under the slow lane.



(b) The shear force due to the tandem system moving along the slow lane for the connector row under the slow lane.



(c) The different lanes and distributed loads combined for the connector row under the slow lane.



(d) All connector rows combined.

Figure 6.4: The generation process of the envelope of the static shear forces in the connectors of the generic bridge with laminate 3 and *web90*.

Compare bridges

For the static analyses the extreme shear forces are relevant. The extreme shear forces can be read from the envelope of the static shear forces. This is the maximum shear force that is expected in a connector. Changing the layout of the bridge will result in changes in the maximum shear force so each layout change in the model will result in a different maximum shear force. To compare different bridges, the maximum shear force can be plotted against bridge parameters like the span.

6.3. Static results on the generic bridge

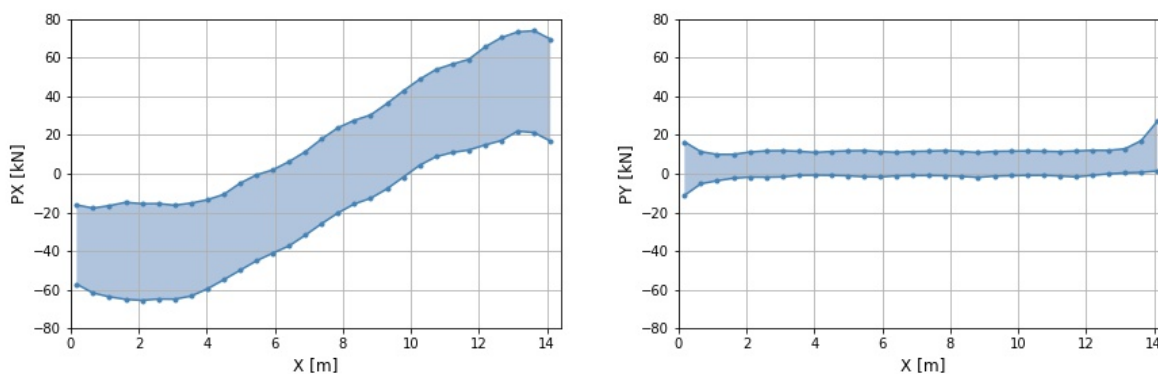
The static shear force of the generic bridge differs depending on the layout of FRP deck. Some variations in the layout of the generic bridge are applied to investigate the influence of the bridge parameters. There are two variations in the direction of the webs and three variations with different facing laminates that are investigated with traffic load. For temperature load also three variations in the coefficient of thermal expansion (CTE) is investigated. The three variation in the CTE of the resin have no influence on the results due to traffic load because the expansion coefficient can be changed without changing other properties. So eventually the shear force in the connectors is investigated for six generic cases when loaded with traffic load and eighteen cases when loaded with temperature load. In case the optimal FRP deck layout would be selected with the method as described in chapter 4, the generic bridge would have facings made with laminate 3 and webs perpendicular to the main girders (web_{90}).

6.3.1. Traffic load

PX vs PY

SOFiSTiK can present the results of the shear force in the connectors in two components, namely shear force in connectors in longitudinal direction (PX) and shear force in connectors in transverse direction (PY). The advantage is that it will be visible in which direction the shear forces are working. Different loads can result in shear forces in different directions. When the forces are working in different directions the maximum shear force is not amplified. By comparing the shear force working in a fixed direction, it can be seen which loads on the bridge do or do not amplify the maximum shear force in the connectors. Also the magnitude can be compared.

The PX and PY due to LM1 are compared for the generic bridge with the optimal FRP deck. The results for the heaviest loaded connector row can be seen in figure 6.5. It can be seen that the magnitude of the maximum PX is about a factor 5 larger than the maximum PY. This was also found in a more extensive investigation during the benchmark study as can be seen in appendix A. Thus the PX will give the governing shear forces.



(a) The PX of the connector row under the slow lane.

(b) The PY of the connector row under the slow lane.

Figure 6.5: The PX and PY are compared for the connectors under the slow lane.

In both the graphs of the PX and the PY it can be seen that the maximum shear force in the connectors in the middle of the bridge follows a more or less straight line. However at the edges of the bridge this pattern is not followed anymore. Especially the PY shows some peaks at the edge. These peaks are due to the way the model is created. At the supports there are strict boundary conditions. These constraints result in increasing shear forces at the edges of the bridge. A more extensive elaboration can be found in appendix A. Because the error due to the deviations of the PX at the edges is permissible, and the magnitude of the PX is larger than the PY. It was decided to move on with the model but only investigate PX when loaded with traffic loads.

Different deck layouts

Six different FRP deck layouts are investigated. For each case the connector with the most severe combination of axle loads on each lane is determined. The connector with the highest shear force is selected and shown for each of the generic cases in table 6.1.

	PX laminate 1 [kN]	PX laminate 2 [kN]	PX laminate 3 [kN]
Web_0	50.6	50.0	50.1
Web_{90}	87.3	69.6	73.9

Table 6.1: The shear force in connectors in longitudinal direction due to traffic load.

Laminate 1 has most fibres in the longitudinal direction, increasing the hybrid interaction. This results in higher shear forces compared to the other laminates. Webs parallel to the main girders (web_0) will increase the cross sectional area and so the hybrid interaction. The cross sectional area of the webs perpendicular to the main girders (web_{90}) cannot be completely included and therefore there will be less hybrid interaction. Despite this, it was found that the case wherein webs are parallel to the main girders, lower shear forces in the connectors were observed. This discrepancy is attributed to the connector layout and bending of the cross girder. Traffic load results in lateral bending of the cross girders reducing the hybrid interaction between the connected cross girders and deck. Moreover, the largest shear forces are located close to the supports. Connectors on the cross girders result in a more equal distribution of the forces over the connectors.

Figure 6.4c shows the envelope of the static shear forces in the connectors of the generic bridge, with web_{90} and laminate 3, below the slow lane. The maximum shear force is found in connectors at the begin and end of the bridge. Connectors connecting the girder below the slow lane with the FRP deck are the governing connectors as it will experience higher shear forces compared to connections located at the other side of the bridge. The envelope of the connectors on the other side of the bridge will have the same shape, only the magnitude is lower as the loads are further from the connectors. This results in figure 6.4d when all connector rows are combined in a single graph. In the middle of the bridge, the envelopes will overlap in the same area in the graph resulting in a smaller range while at the beginning and ending of the bridge there is less overlapping between the different connector rows resulting in wider range.

6.3.2. Temperature load

Compared to the traffic load also the CTE of the resin has an influence on the shear forces in the connectors. Due to hybrid interaction between the FRP panel and the girders, the magnitude of the largest force in the connector will depend on the orientation of the fibres in the facings and whether the panel is connected to the longitudinal or the cross girders. Different types of resins can be used which results in different CTE for a unidirectional (UD) ply. The range of CTE as mentioned in the CUR 96 (2017) has been used and is listed in table 6.2. Depending on the CTE of the plies and the percentage of fibres in each direction, different CTE for the laminates are obtained. The CTE of the laminates has been calculated with the classical laminate theory for the x and y direction, see appendix B for more information how this is done. The results are shown in table 6.3. For the temperature load eighteen different FRP deck layouts are investigated.

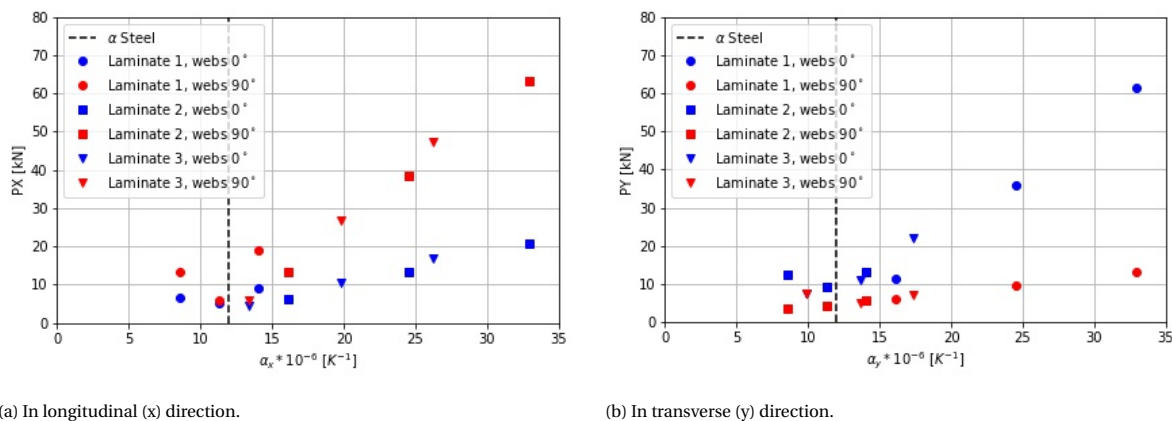
	$\alpha_r = 50[\cdot 10^{-6} K^{-1}]$	$\alpha_r = 85[\cdot 10^{-6} K^{-1}]$	$\alpha_r = 120[\cdot 10^{-6} K^{-1}]$
α_1	7.2	8.9	10.5
α_2	23.2	37.0	50.8

Table 6.2: The coefficient of thermal expansion of the UD ply.

Resin	$\alpha_r = 50[\cdot 10^{-6} K^{-1}]$		$\alpha_r = 85[\cdot 10^{-6} K^{-1}]$		$\alpha_r = 120[\cdot 10^{-6} K^{-1}]$	
	$\alpha_x[\cdot 10^{-6} K^{-1}]$	$\alpha_y[\cdot 10^{-6} K^{-1}]$	$\alpha_x[\cdot 10^{-6} K^{-1}]$	$\alpha_y[\cdot 10^{-6} K^{-1}]$	$\alpha_x[\cdot 10^{-6} K^{-1}]$	$\alpha_y[\cdot 10^{-6} K^{-1}]$
Laminate 1 (facing)	8.6	16.1	11.3	24.5	14.0	32.9
2 (facing)	16.1	8.6	24.5	11.3	32.9	14.0
3 (facing)	13.4	9.9	19.8	13.7	26.2	17.3
4 (web)	11.5	11.5	16.4	16.4	21.2	21.2

Table 6.3: The coefficient of thermal expansion of the laminates.

All cases have been calculated and the results are shown in figure 6.6. Distinction has been made between the shear force in connectors in longitudinal direction (PX) and the shear force in connectors in transverse direction (PY). Each marker represents a generic case that has been investigated. The various laminate types used are indicated by means of different marker types, whereas the colour represents the direction of the webs. For each colour and marker shape combination, three dots are presented representing the different expansion coefficients of the resin.



(a) In longitudinal (x) direction.

(b) In transverse (y) direction.

Figure 6.6: The shear force in the connectors due to temperature load of the generic bridge with eighteen variation in FRP deck.

The anisotropic material behaviour of FRP results in different CTE in the longitudinal and transverse direction, subsequently yielding different shear forces in these directions. A wide range of shear forces is found in the connectors with values varying from 3.4 kN to 63.3 kN. In general, the closer the CTE of the facings is to the expansion coefficient of steel, the lower the shear forces in the connectors. Therefore laminate 1 results in the lowest connector forces since its CTE is closest to that of steel. However, since the analysed laminates all have one dominate fibre direction, the other direction has a notably different CTE than steel. This results in higher connector forces in one direction as opposed to another. In general it would be best practice to design the FRP panel by taking into account both directions with regards to fibre orientation as well as considering the means by which the panel is connected (i.e. to longitudinal or cross girders), in order to minimize the connectors forces in both directions. Figure 6.6 indicates that the case with laminate 3 and a $50 \cdot 10^{-6} K^{-1}$ CTE of the resin is optimal in the case of the generic bridge loaded with temperature load.

The direction of the web also influences shear forces in the connectors. When the webs are directed in the transverse direction, higher shear forces in the connectors in x-direction are obtained compared to webs placed in the longitudinal direction. This difference can be explained with respect to the bolt layout. In the

case of longitudinal webs, the bolts are located on the cross girders. This allows the deck to extend between the cross girders reducing the shear forces in the connectors. For transverse webs the bolts are located on the longitudinal girders which limits the extension of the deck in the longitudinal direction and results in higher shear forces in the connectors. For the shear forces in y-direction the results are reversed.

The CTE of the resin and the percentage of fibres in each direction determines the CTE of the laminate and together it influences the shear force in the connectors. The volume fraction is kept constant in these cases but this parameter could be changed to adjust the CTE of the laminate and stiffness properties. Upon the inclusion of temperature effects, a large variation in connector shear forces are obtained. This highlights the importance of including temperature loading during designing. It is possible to adjust the laminate in such a way that the shear forces in the connectors due to temperature loading are relative low.

Following the notion of webs and most fibres in the directions of the load transfer, bridges with many cross girders will have most of the fibres and webs orientated in the longitudinal direction and will therefore use laminate 1. This means that the shear forces in the longitudinal direction will be small but in the transverse direction significant shear forces can occur. Bridges with nearly no cross girders will have most of the fibres and the webs orientated in the transverse direction and therefore will use laminate 2. This will, depending on the type of resin, result in high forces in the connectors in the longitudinal direction, whereas in transverse direction the forces are relative low.

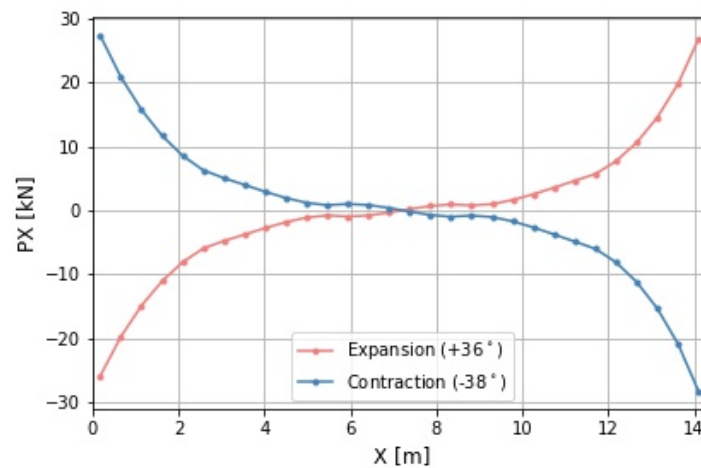
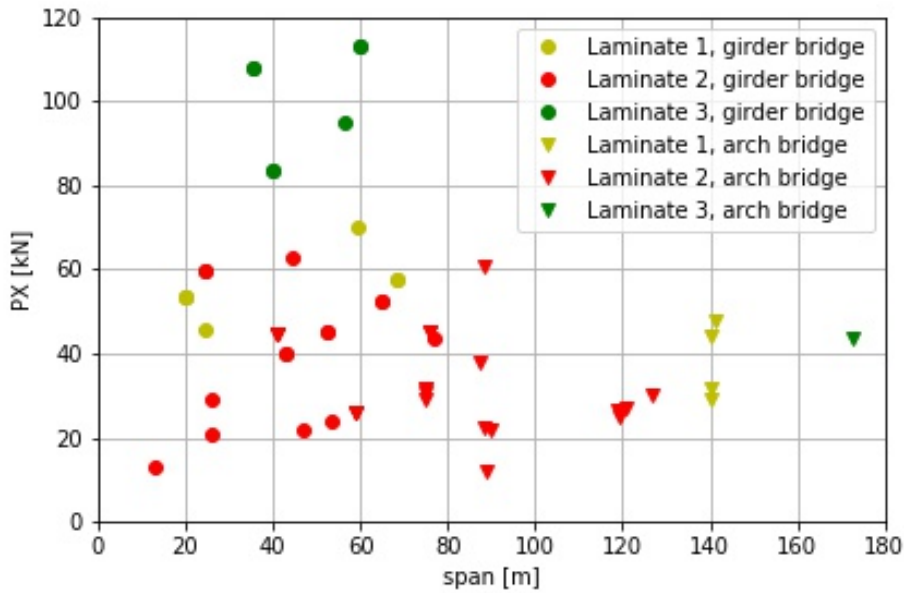


Figure 6.7: The shear forces in a row of connectors due to expansions or contraction in the generic bridge with laminate 3, web_{90} and a $85 \cdot 10^{-6} K^{-1}$ CTE.

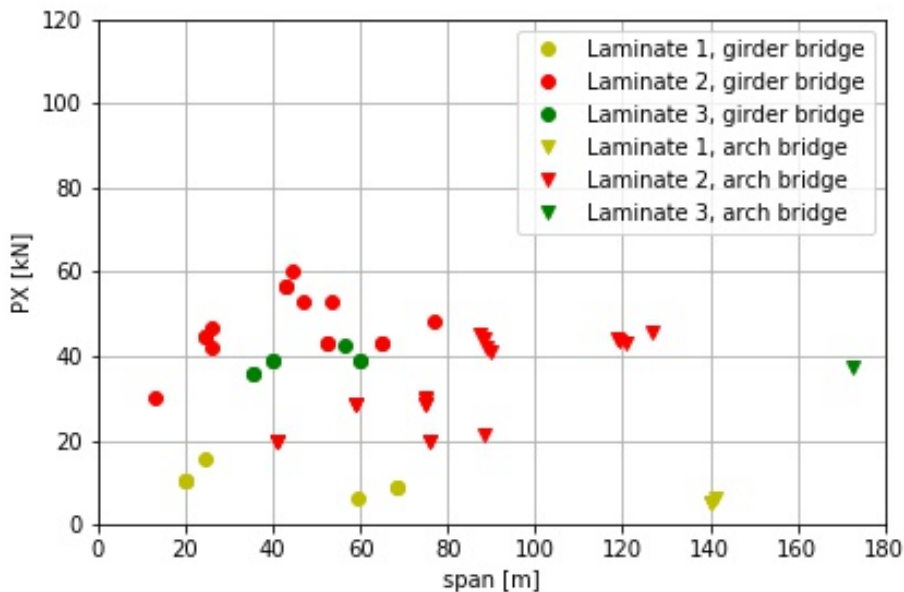
Just like with the traffic load, the connectors loaded by temperature load at the begin and end of the bridge experience the highest shear forces. This can be seen in figure 6.7 where the generic bridge with laminate 3 and web_{90} is loaded by a positive and negative temperature difference. There are differences between different rows of connectors. The connectors at the outer main girder have higher shear forces than connectors on the middle main girder. This applies to the shear force in longitudinal and transverse direction. As shown expansion or contraction does not have an influence of the results, only the sign of the shear force changes. The highest temperature difference is governing.

6.4. Static results on highway bridges in the Netherlands

Maximum shear forces in the connectors due to traffic and temperature loads are determined for each of the bridges included in the database as discussed in chapter 4. The applied load is the same as for the generic case. For the temperature load the expansion coefficient of the average resin is used: $85 \cdot 10^{-6} K^{-1}$. The webs are for laminate 1 directed in the longitudinal direction and for laminate 2 and 3 in the transverse direction as those are the shortest distances between girders. The results can be seen in figure 6.8 where the shear force in the connectors is plotted against the span of the bridge.



(a) Due to traffic loads.



(b) Due to temperature loads.

Figure 6.8: The maximum shear force in the connectors in highway bridges in the Netherlands when an FRP deck would be applied.

The maximum shear force in the girder bridges varies from 10 to 110 kN due to traffic load and from 5 to 60 kN due to temperature load. Bridges with laminate 2 as facings, which are bridges with a relative large distance between cross girders, perform better under traffic loading but worse under temperature load compared to bridges with other laminates.

In most cases, arch bridges have larger spans than the girder bridges. In general this does not results in larger shear forces in connectors compared to girder bridges. This can be explained because the hangers function as intermediate supports. The arch bridge behave as bridges with multiple smaller spans. The maximum shear force in arch bridges varies from 10 to 60 kN due to traffic loading and from 5 to 50 kN due to temperature loading. There is not a facing laminate on the arch bridges that performs best for traffic load, mainly because the number of lanes varies. Bridges with laminate 1 have lowest shear forces due to temperature loading.

6.4.1. Discussion of static shear force results

The regular design practice would be to place the FRP deck in the direction of the local shortest span, i.e. over the cross or longitudinal girders. Placing the webs and most fibres in the direction of the load transfer using the dimensions of the generic bridge results in webs in the transverse direction and laminate 3 for the facings. In terms of shear forces in the connectors due to traffic load this would not be the ideal configuration as webs in the other direction result in lower forces. Similarly, this configuration is not optimal with respect to temperature loading. The ideal configuration for the generic bridge for the lowest possible shear forces in longitudinal direction in the connectors is to use longitudinal webs and laminate 1 with an average CTE of the resin or longitudinal webs and laminate 3 with a low CTE of the resin. This differs to the optimal configuration, which was transverse webs and laminate 3, when only taking into account the failure modes of the FRP deck. The same applies to the existing highway bridges in the Netherlands. The results presented show that the shear force in the connectors is one of the aspects to be considered when designing a bridge where hybrid interaction between the deck and the steel superstructure is engaged.

7

Fatigue shear force

This chapter is about the fatigue shear forces in the connectors. Fatigue forces are the repeating forces due to cyclic loading. Different parameters can be distinguished in cyclic loading as shown in figure 7.1. For an steel-fibre reinforced polymers (FRP) connection two of those parameters are important: the amplitude and the mean value. The amplitude is the largest deviation from the mean value during a loading cycle. The mean value is the average value during a loading cycle. The goal is to determine the maximum shear force ranges and the type of load cycles.

This chapter start with the definition of the fatigue loads. It is followed with an explanation of the fatigue evaluation method. Thereafter it is explained how the results from the SOFiSTiK model are processed. Next, the fatigue analysis is applied on the bridge Nieuw Vossemeer. Also the case when multiple lorries are on the bridge is investigated.

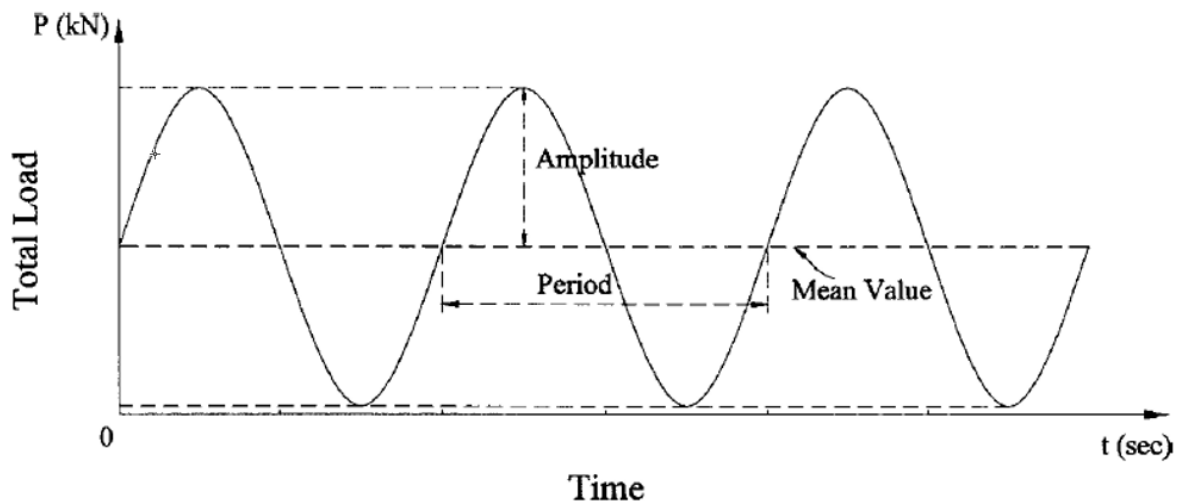


Figure 7.1: Parameters of cyclic loading (Cheng & Karbhari, 2006).

7.1. Load definition

Just like with static traffic load definition as described in section 6.1.1, for fatigue verification there are different loading models and the worse model is governing as described in Eurocode-1991-2 (2003). Five fatigue load model (FLM) are described in the Eurocode which can be used to check the fatigue life of the bridge.

FLM 1 and 2 are used to check whether the fatigue life may be considered as unlimited when a constant stress amplitude fatigue limit is given. This is the case for steel but not for FRP. FLM 3, 4 and 5 use fatigue strength curves to determine the fatigue life. FLM 3 uses a simplified method for the verification. FLM 4 uses a set of standard lorries to produce effects equivalent to those on the road. FLM 5 uses real traffic data to determine the fatigue life.

Fatigue load model 4 (FLM4) as described in the dutch National Annex will be used in this chapter. Two different sets of lorries are available. FLM4a is for materials that only depend on the stress range for fatigue damage and FLM4b is for materials that not only depend on the stress range but also on the mean stress. For FRP FLM4b must be used as the fatigue resistance depends on the stress range and the mean stress.

The set of lorries for FLM4b includes seven lorries with each different geometry, axle load and axle spacing. Because the existing bridges in this report are highway bridges, the distribution of the lorries is based on long distance transport which has more heavier lorries than the shorter distance distribution. An overview of the lorries can be seen in table 7.1. The layout of the wheels can be seen in figure 7.2.








	Vehicle type		Traffic type	Wheel type	
	Lorry	Axle spacing [m]	Equivalent axle load [kN]		Long distance [%]
1		4.50	70 130	20.0	A B
2		1.50	70	7.0	A
		2.40	120		C
		1.30	120 120		B B
3		3.20	70	37.0	A
		5.20	130		B
		1.30	100		C
		1.30	100		C
		1.30	90		C
4		3.40	70	20.0	A
		6.00	140		B
		1.80	90		C
		1.80	90		C
5		4.80	70	10.0	A
		3.60	150		B
		4.40	80		C
		1.30	80		C
		1.30	70		C
6		3.20	80	4.5	A
		1.30	160		B
		4.40	100		C
		1.80	100		C
		1.80	100		C
		1.80	100		C
7		3.20	70	1.5	A
		1.40	180		B
		4.40	170		B
		1.30	80		C
		1.30	80		C
		1.30	80		C
		1.30	90		C

Table 7.1: Set of equivalent lorries for FLM4.

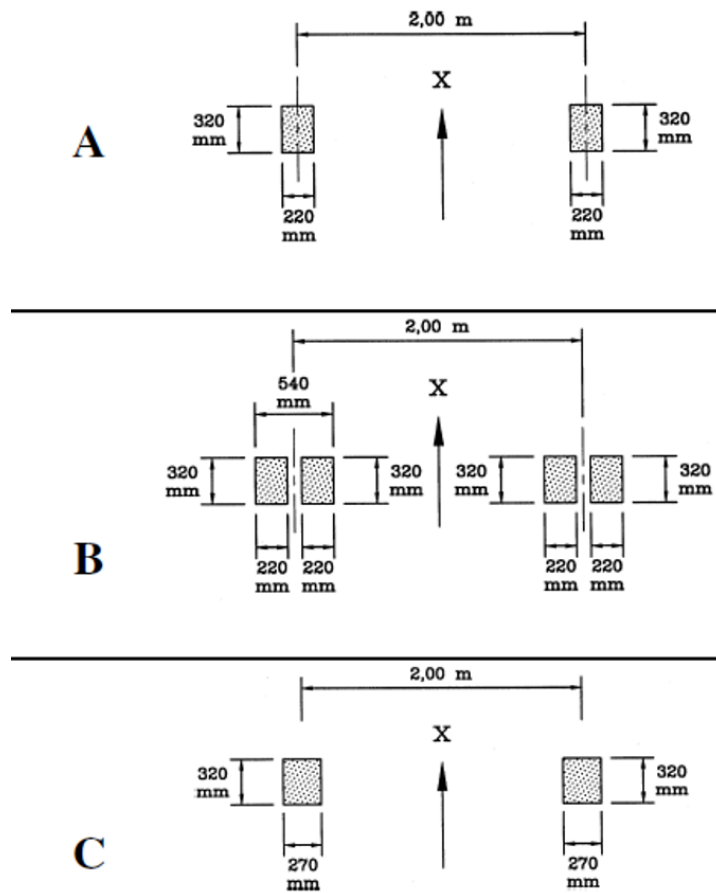


Figure 7.2: Definition of the geometric dimensions of the wheels and axles for FLM4.

The number of lorries passing the bridge of course has a major influence in the fatigue damage. For highway bridges a maximum of two million passing lorries are expected per year in the slow lane. With an expected lifespan of 100 years for the bridges the number of passing lorries can be calculated. Near expansion joints an additional amplification factor $\Delta\varphi_{fat}$ should be taken into account as can be seen in figure 7.3. Bridges with spans longer than 60 meter should include some passages with two lorries at the same time, next to each other or behind each other. These cases are discussed later this chapter, in section 7.5.

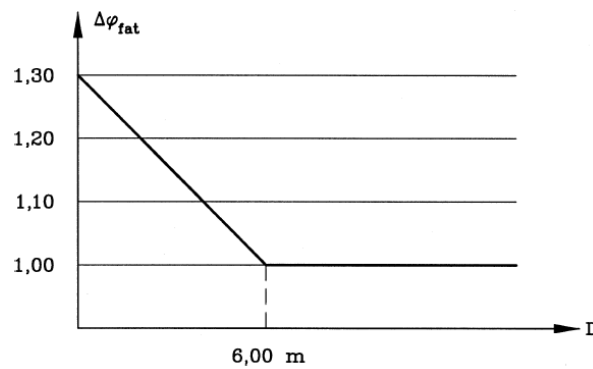


Figure 7.3: Representation of the additional amplification factor near expansion joints.

7.2. Process for evaluation

Fatigue verification usually follows Eurocode-1993-1-9 (2006) guidelines, which consists of six steps. First typical load cycles are defined, these load cycles are translated into stress histories at the detail that is under investigation. The third step counts the number of stress cycles. The magnitude and amount of cycles can then be plotted in a histogram called the stress range spectrum. The fifth step uses cyclic stress (S) against cycles to failure (N) (S-N) curves to determine for the occurring stress ranges the number of cycles to failure and calculates the damage due to the real number of cycles. The last step is to verify if the damage does not exceed the criterion, it must stay below 1 during the lifespan of the detail.

Connectors connecting the steel superstructure with an FRP deck is a detail that must be investigated on fatigue. However, there are a few problems with the fatigue procedure described in the previous paragraph. First of all, each detail requires its own specific S-N curves that must be created with numerous lab experiments. At the moment of writing there are no S-N curves for injected steel reinforced resin (iSRR) connectors connecting steel with FRP. This makes it impossible to calculate the damage in the connectors due to different loads. Since the ordinary way is not possible, a different method is used: R-ratio. The amplitude has a major effect on the fatigue performance. The amplitude of a cycle is expressed as the R-ratio. The minimal stress is divided by the maximum stress during a cycle ($R = \sigma_{min} / \sigma_{max}$). More about the R-ratio is explained later in this section.

Moreover, fatigue verification uses stress in the detail. This makes sense as stress is a good measurement to tell when a material will fail, regardless of the dimensions. In the iSRR connector it is difficult to define the cross sectional area. Due to the resin and small steel balls around the top of the bolt the cross sectional area is not constant over the height of the connector. It is decided to calculate forces in the connector instead of stresses to avoid the discussions about stress peaks that can occur and what cross sectional area should be used. Additionally force ranges can be easily compared with lab experiments as force ranges are applied in the experiments. This also means that for the formula of the R-ratio the stresses are exchanged for forces, see 7.1.

$$R = \frac{F_{min}}{F_{max}} \quad (7.1)$$

With the definition of the R-ratio known, it is important to understand what it means, this is explained in figure 7.4. The graph in the top left corner represents a load diagram over time. The load diagram in the right top corner is the same graph but it is vertically flipped to show the difference between positive and negative peaks. Positive or negative refers to the direction of loading. In the second row four peaks are highlighted in both graphs. In the left graph the peaks are positive, in the right graph the peaks are negative. In the third graph each highlighted case is shown and the R-ratio is calculated according to formula 7.1 and presented below the graph.

In case of positive peaks, it can be seen that a theoretical range from -1 to 1 can occur. In case of -1 the compression and tension force are equal in magnitude. As long as the number stays negative there is reverse loading. A positive number refers to only tension. The higher the R-ratio, the smaller the difference between the minimum and maximum force. Division by 0 is not allowed so the denominator cannot be 0 in the formula for the R-ratio. In addition an R-ratio of 0 does not give any information about the magnitude of the peak. To prevent this also the numerator cannot be 0. To solve this all F_{min} and F_{max} values within 10% of 0% load are changed to 10%. So a peak from 0% to 100% load results in an R-ratio of 0.1. Negative peaks result in a theoretical range from $-\infty$ to ∞ . The boundary of $-\infty$ can be changed to -10 when taking into account that values close to 0% are changed to 10% resulting in a range varying from -10 to ∞ .

The direction of loading is in most cases important as this will result in tension or compression and the materials have different responses on those types of loading. However in connectors, taking into account the assumption of non-slip connectors that is used in this report, the direction of loading is not important. This means the R-ratio of negative peaks can be translated to R-ratio of positive peaks with the following formula: $R_{positive} = 1/R_{negative}$. This makes the overview of different load peaks that can be expected clearer.

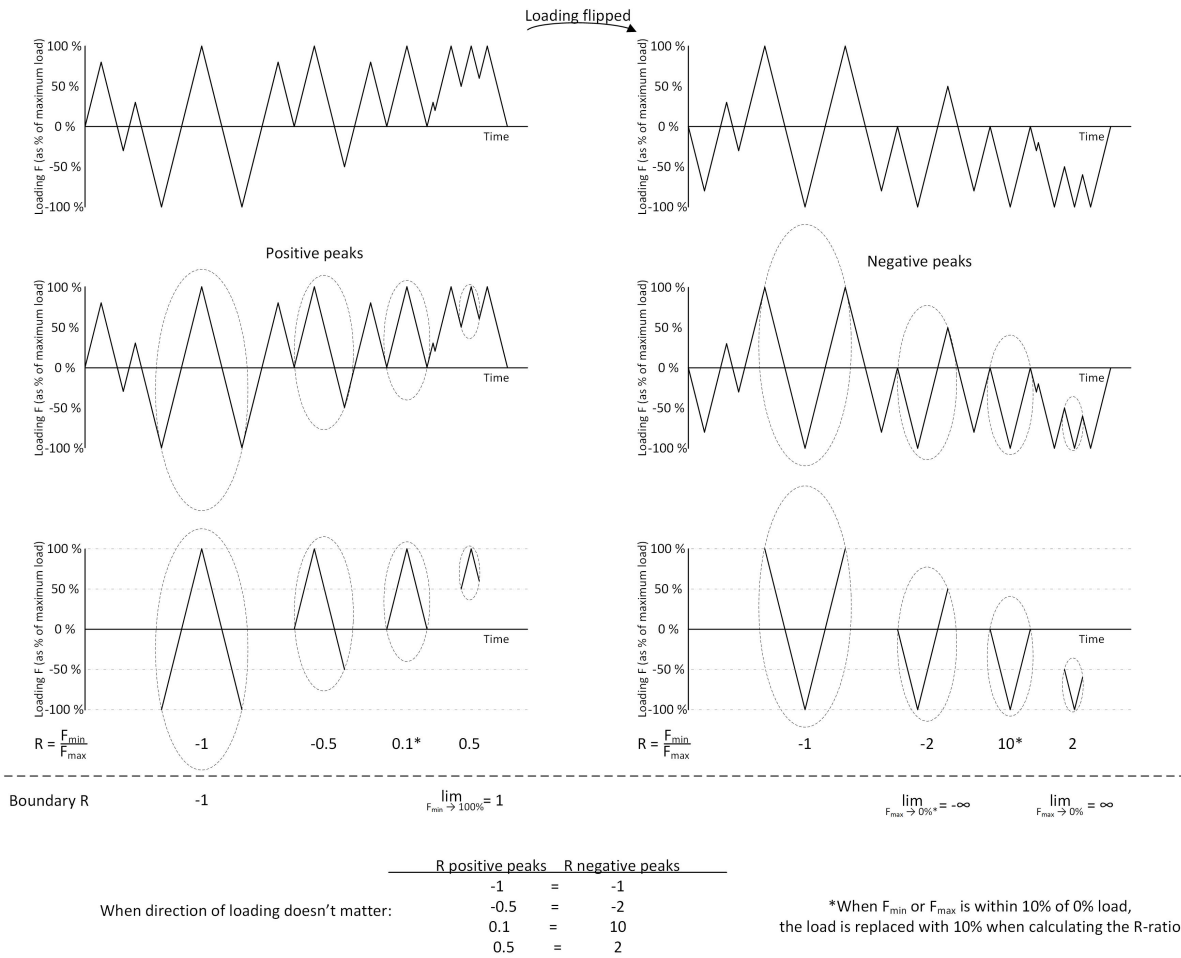


Figure 7.4: Explanation of the R-ratio.

So damage calculation is not possible but the R-ratio can be used as an alternative. It is possible to present the R-ratio of each load cycle with the corresponding load range and the total number of cycles. All cycles will be subdivided in four groups, depending on the R-ratio with each bin having a range of 0.5. This will give an overview of what type of load cycles are appearing most often and what the magnitude of the load is for the different type of load cycles. These results will help to know in which bins of R-ratios the experiments must be done. Experiments are needed to create S-N curves and different R-ratios will result in different S-N curves. With those curves it will be possible to calculate the damage of the connectors. It is expected that R-ratios of -1 are the most damaging, as previous experiments showed that reverse loading is more damaging for the fatigue live than loading from a single direction, but experiment must demonstrate that this is also the matter in this case Vassilopoulos & Keller (2011).

7.3. Methodology for fatigue analyses

The fatigue analyses consist of different steps which are explained in this section. The analyses starts with running the SOFiSTiK model, the data obtained with the model will be used to create influence lines of the lorries driving over the bridges. Thereafter the cycles in the influence lines are counted. The last step is to create the graphs presenting the force range versus the number of cycles for the different bins of R-ratio.

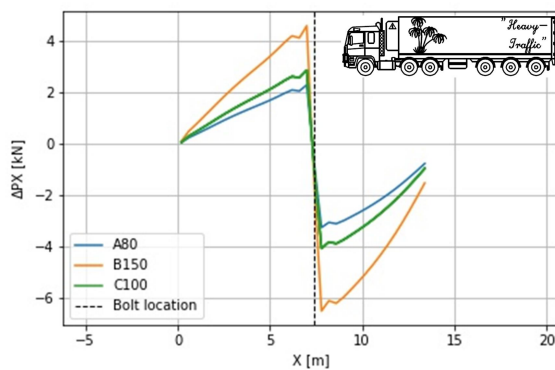
Model

The bridge that is investigated is modelled as described in 3.2. The layout and FRP deck are entered as input. Earlier in this chapter the load definition for the fatigue analyses is described. Seven different lorries are

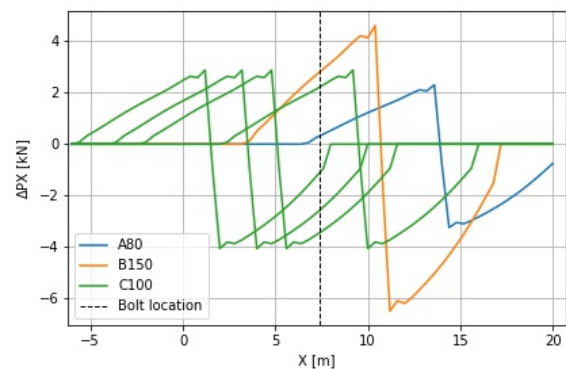
needed with three different type of wheels on the axles. Instead of modelling all the lorries, only the three different axles are modelled with an unity load of 100 kN. The axle load is applied every 0.4 m over the entire length of the bridge in the middle of the slow lane. Each axle load is saved as a separated load case. The model calculates the shear forces in the connectors and for each load case, the shear forces in all the connectors are saved. This data is used in the next step.

Influence line

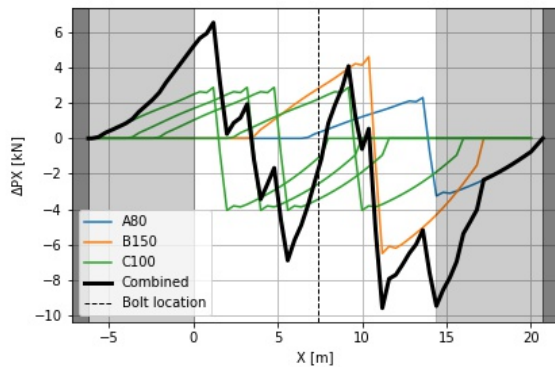
The model has calculated an axle load driving over the bridge. For each connector, the influence line due to an axle load can be plotted, this is done with a python script. The goal is to get an influence line that shows the shear force in connectors in longitudinal direction (PX) in a selected connector caused by the lorries axle loads along the length of the bridge (x-axis). The vertical dotted line will be used to show the location of the connector. To get from the influence line of the axle load to the influence line of the lorry, first the influence line of each axle of the lorry is plotted and the unity load is converted to the equivalent axle load by multiplication. An example of this can be seen in figure 7.5a where the axles of lorry 6 are driving over the generic bridge. The second transformation includes the axle spacing and shifts the axles to the correct position relative to each other as seen in figure 7.5b. Now all lorry axles are in the correct position, all that is left is to sum the influence lines of the different axles as seen with the black line in 7.5c. For fatigue analyses the influence lines for all seven trucks are needed.



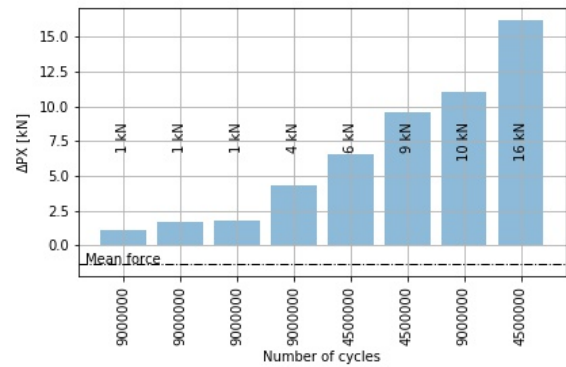
(a) Influence line of the axles of lorry 6.



(b) The axles are shifted to the correct axle spacing.



(c) The axles are summed to create the influence line.



(d) The force range spectrum.

Figure 7.5: Steps to create the influence line and the force range spectrum. The connector is located in the middle of the bridge. This example uses the generic bridge and lorry 6. Notice that four axles have the same axle load.

The influence line of the lorries is taken from the middle of the lorry. Imagine that each lorry is driving from the right of the graph to the left. Before the middle of the lorry enters the bridge at the right of the graph, there are already axle(s) on the bridge resulting in shear forces in the connectors. Therefore an extra area, marked with light grey, is added at the beginning of the bridge. So when the middle of the lorry enters the light grey area in the graph the first axle enters the bridge. When the lorry enters the white area the middle of the lorry is on the bridge, but not yet all axles. When the lorry leaves the bridge the same happens. The middle of the

lorry leaves the bridge when it enters the light grey area, some axles are at this point already off the bridge, but some axles are still on the bridge. When the last axle leaves the bridge, the middle of the lorry enters the dark grey area.

Cycle counting

The influence line of the lorries are used to count the cycles, also this part is done with a python script. For cycle counting the rainflow method is used. The rainflow method analyses fatigue data and reduces a spectrum of varying force into an equivalent set of force reversals. The rainflow method can be done by hand as shown in figure 7.6. The force history is reduced to a set with peaks and valleys. For manual counting the force history is rotated 90° clockwise. Imagine rain flowing over the force history. When the flow falls off the graph, it continues on the next peak if possible. When flows are merging, the flow with the largest magnitude has priority. This is done on both sides of the graph. Each water flow is counted. The force range, denoted with the blue numbers, is listed and counts for half a cycle. An overview can be made of all the force ranges and the number of times each cycle appear during the passage of a single lorry as shown on the right side of the graph.

During the analyses, the counting of the influence lines of all seven lorries is done with a python script. With the results of the passage of a single lorry known, it is calculated how often each lorry type will pass using the lifespan of 100 years, two million lorry passages per year and the known distribution between the different type of lorries as shown in table 7.1. The number of passages of each lorry is multiplied with the number of cycles that one passage of that lorry causes. All cycles that will happen during the lifetime of the bridge can be added together and presented in the force range spectrum. An example of the force range spectrum is shown in figure 7.5d. This force range spectrum is created for a connector in the middle of the generic bridge, with lorry 6 driving over it. The influence line that is used to create the force range spectrum can be seen in figure 7.5c. Also the means force is presented in the force range spectrum graphs.

R-ratio

The force range spectrum of all seven lorries are calculated. In the last step the R-ratio of each bin of the force range spectrum is calculated. Depending on the R-ratio, the results are added to one of the four force range spectrum graphs. So the force range spectrum graphs of all seven lorries are combined and split into four graphs based on the R-ratio. Force ranges close to each other are grouped. The number of cycles of each group of force ranges is counted and presented on a logarithmic scale.

The four graphs can be used to see what type of load cycles are applied on the details that are investigated. Also the number of cycles and magnitude of the load cycles can be seen. This information can be used to investigate what type of loading can be expected in connectors and so what type of loading need to be tested in the lab. When enough lab tests are done it is possible to create S-N curves for the connectors and do damage calculations.

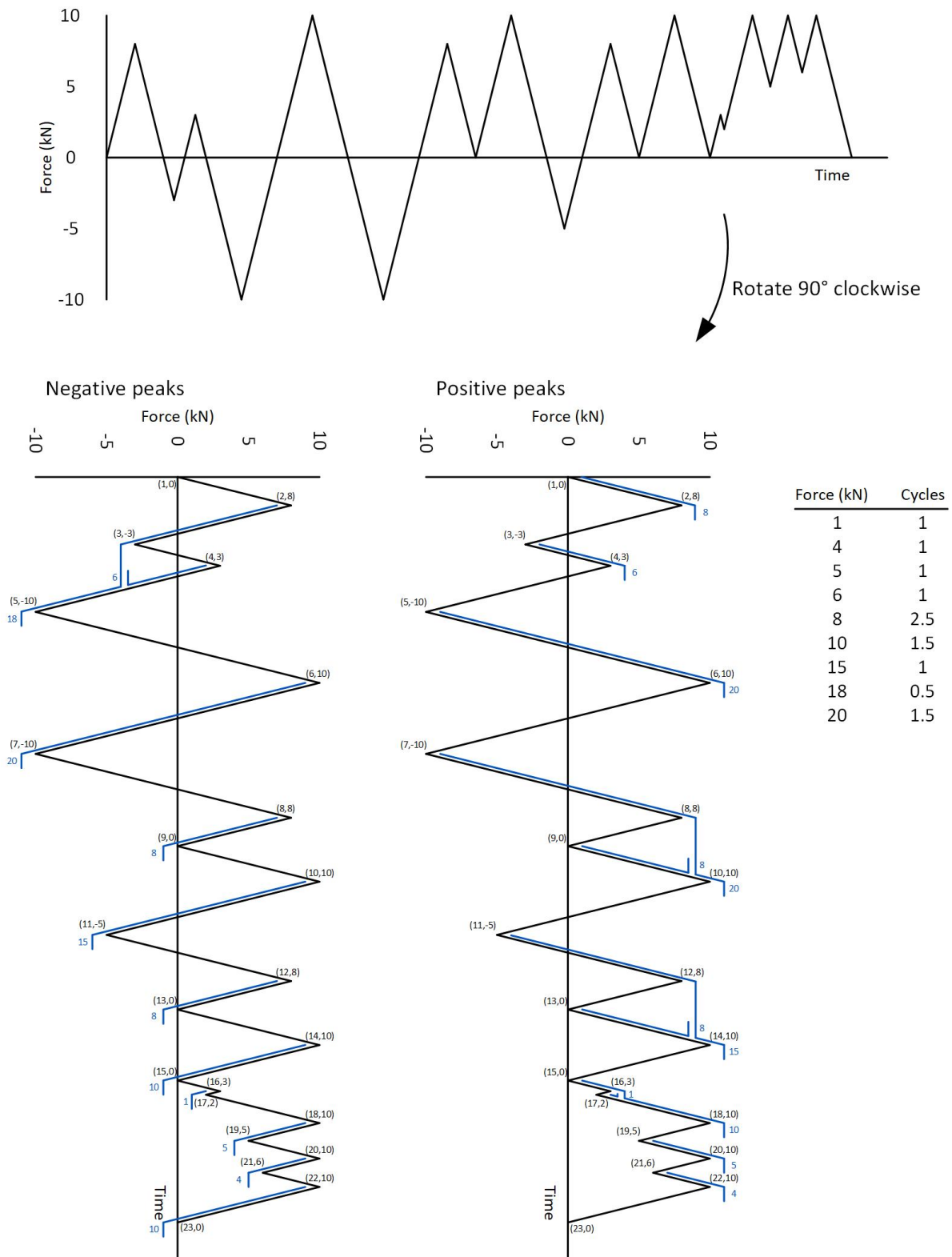


Figure 7.6: Cyclic counting with the rainflow method. In the table on the right side the results shown.

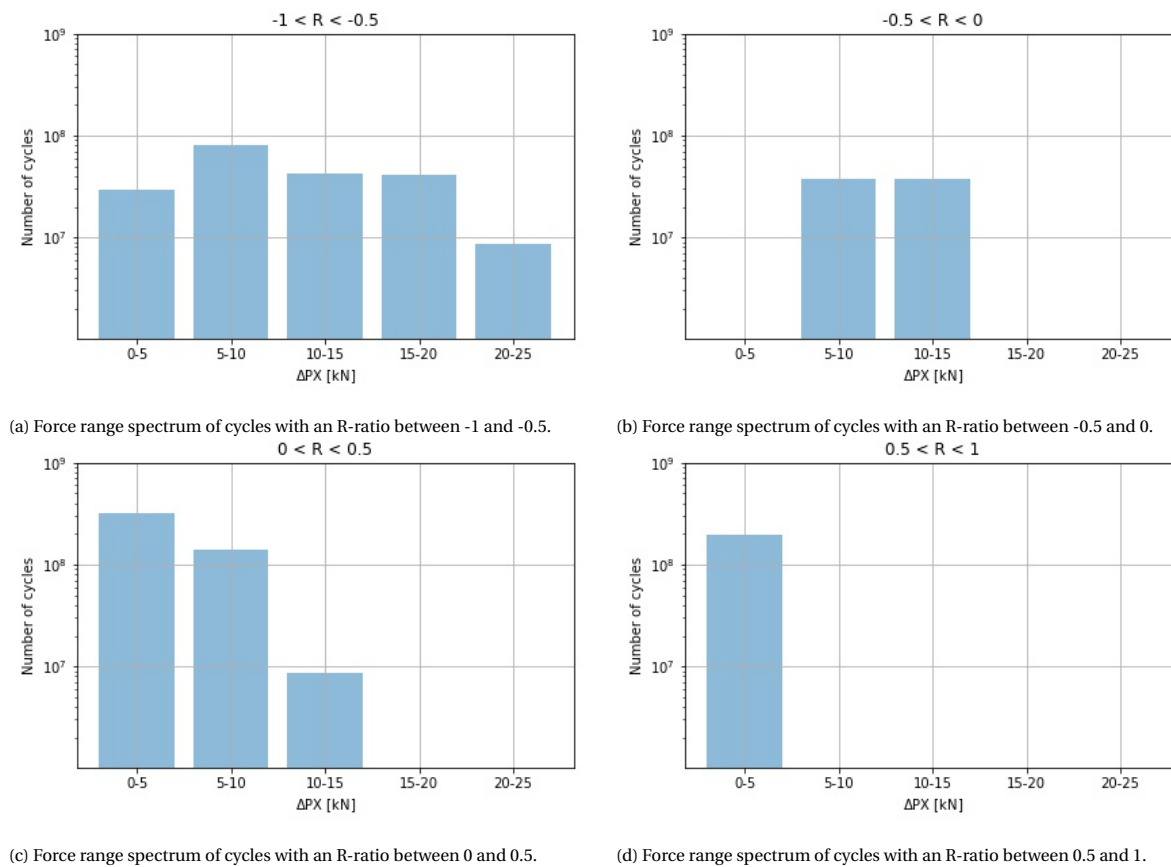


Figure 7.7: The force range spectrum of a connector in the middle of the generic bridge. The results are split in four groups based on the R-ratio.

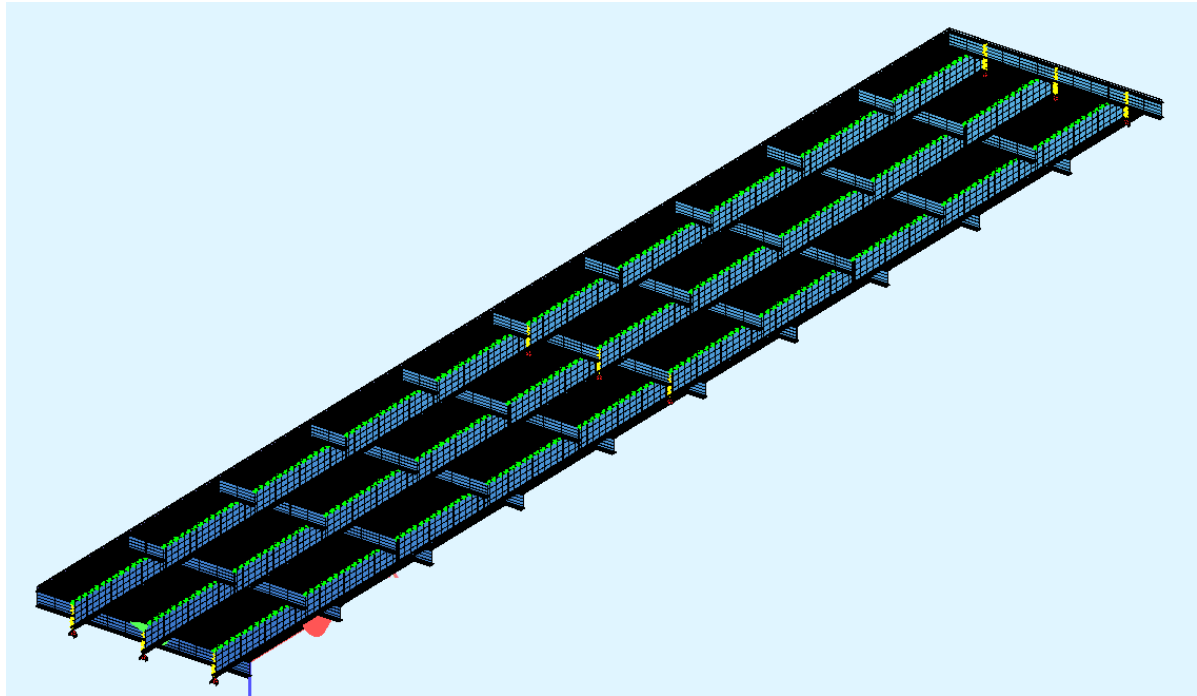
7.4. Evaluation of a heavy loaded static bridge

The fatigue evaluation process that is described in this chapter can now be applied on existing bridges. Instead of evaluating all the bridges, only the results from one bridge will be discussed. Both the static traffic load and the fatigue analyse use axle loads as input for the calculations of the shear force. The number of lanes has an affect on the relation between the static traffic load and the fatigue analyses. During static analyses up to three lanes are loaded while only the slow lane is loaded during fatigue analyses. Nevertheless there will be a correlation between the shear force in the connectors due to static traffic load and due to fatigue load. The bridges with the highest shear forces in the connectors are therefore the most interesting for fatigue analyses. Different bridges that have been checked all had the same behaviour under fatigue load, only the magnitude was different.

So only the results of one bridge are shown in this section, namely the approach bridge Nieuw Vossemeer. The bridge is shown in figure 7.8a and is one of the heaviest loaded bridges in terms of shear force in the connectors during static traffic analyses. The bridge consist of multiple spans of each over 35 m long and is the approach bridge for an arch bridge over a river. The total length is about 212 m. In the model only two spans are modelled to reduce modelling time. This will have an effect on the results. Axle loads on different spans than the connector will still create shear forces in the connectors. However the force range is relative small compared to when the axle is on the same span as the connector. Furthermore there are no more fluctuations due to passing of the axles. Taking everything in considering there are some cycles not counted because not all spans are modelled but these cycles have a relative low force range. The model can be seen in figure 7.8b.



(a) Side view of the approach bridge Nieuw Vossemeer.

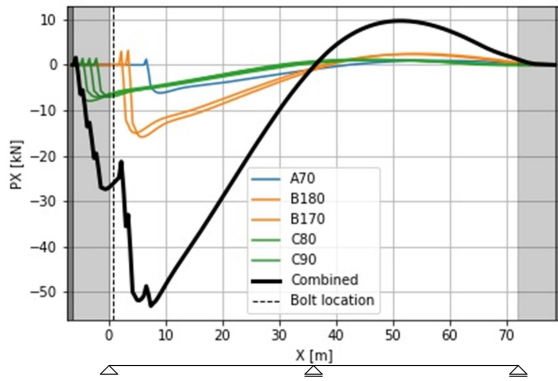


(b) Two spans of the approach bridge Nieuw Vossemeer, seen from below. The green lines are the connectors connecting the blue steel superstructure with the black FRP deck.

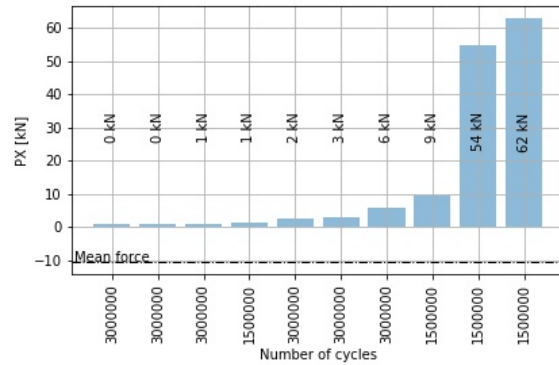
Figure 7.8: The picture and the model of the approach bridge Nieuw Vossemeer.

The results of three connectors at different locations on the bridge are calculated. The locations are at the beginning of the bridge, in the lengthwise middle of the first span and at the end of the first span. The influence lines due to lorry 7 for the connectors at these locations are shown in figure 7.9 as well as the corresponding force range spectrum.

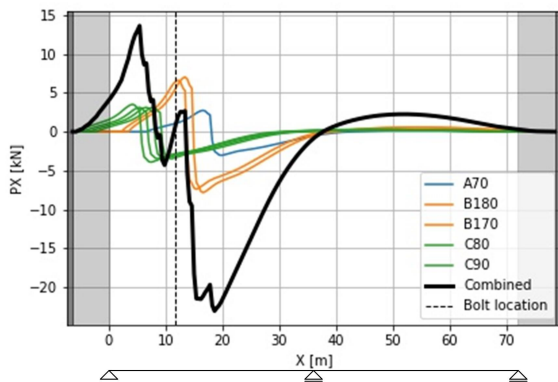
The influence lines have different shapes, depending on the location of the connector. The influence line for connectors at the beginning or ending of a bridge span are characterized by gradual increase and decrease to the maximum shear force. The closer the lorry gets to the connector, the higher the absolute shear force in the connector. Axles entering or leaving the bridge result in small disruption of the gradual flow. The maximum shear force on a connector due to lorry 7 is about 50 kN. The steady increase and decrease results in two half cycles in the force range spectrum. The disruptions due to entering or leaving the bridge results in multiple extra cycles in the force range spectrum but all with a small magnitude.



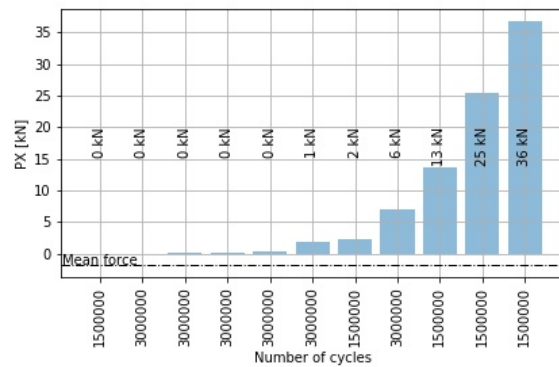
(a) The influence line of a connector at the beginning of the bridge due to lorry 7.



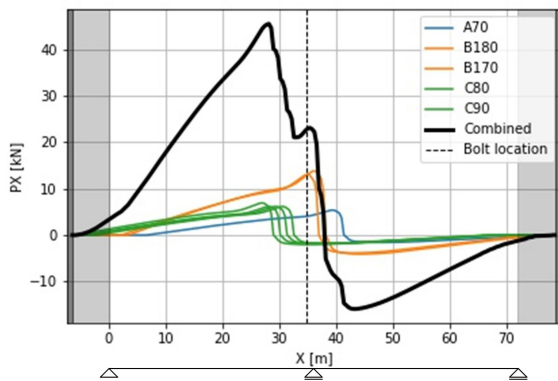
(b) The force range spectrum of a connector at the beginning of the bridge.



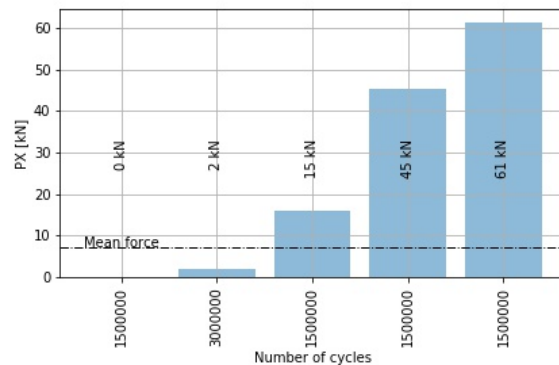
(c) The influence line of a connector at the middle of the bridge due to lorry 7.



(d) The force range spectrum of a connector at the middle of the bridge.



(e) The influence line of a connector at the end of the first span of the bridge due to lorry 7.



(f) The force range spectrum of a connector at the end of the first span of the bridge.

Figure 7.9: The influence line and force range spectrum of different connectors for the bridge Nieuw Vossemeer. Lorry 7 is used for these examples.

A lorry on the second span also results in shear forces in the connectors, influencing the force range spectrum. The shear force in the connector due to the lorry on the second span has a different sign. This increases the magnitude of the largest cycle in the force range spectrum to about 62 kN and adds an extra cycle to the force range spectrum. The extra cycle has a magnitude of about 30% of the maximum shear force for the connectors close to the intermediate support and about 20% of the maximum shear force for the connector at the entrance of the bridge. Even though it does not matter for the connectors in what direction it is loaded. It can be seen that the sign depends on the location of the axles. Axles right of the connector result in a negative peak and axles left of the connector result in a positive peak. When the lorry is on the next span it is reversed.

When the connector is located in the middle of a span lengthwise, the shear force in the connector changes direction when the lorry passes the connector. The magnitude of the shear force will gradually increase when the lorry is driving over the bridge with drops when axles pass the connector. These drops result in both a positive and a negative peak. Between the axles small force ranges appear, the magnitude depends largely on the distance between the axles. When axles are close to each other there is only a small increase in shear force, resulting in a small force range cycle. Axles further from each other result in more significant force range cycles. The maximum shear force is about 22 kN and more important the maximum force range cycle is about 36 kN. A lorry on the second span of the bridge has the same effect on connectors in the lengthwise middle as it has on connectors at the beginning or ending of the span. It increase the magnitude of a cycle but now it is not the cycle with the largest magnitude that is influenced.

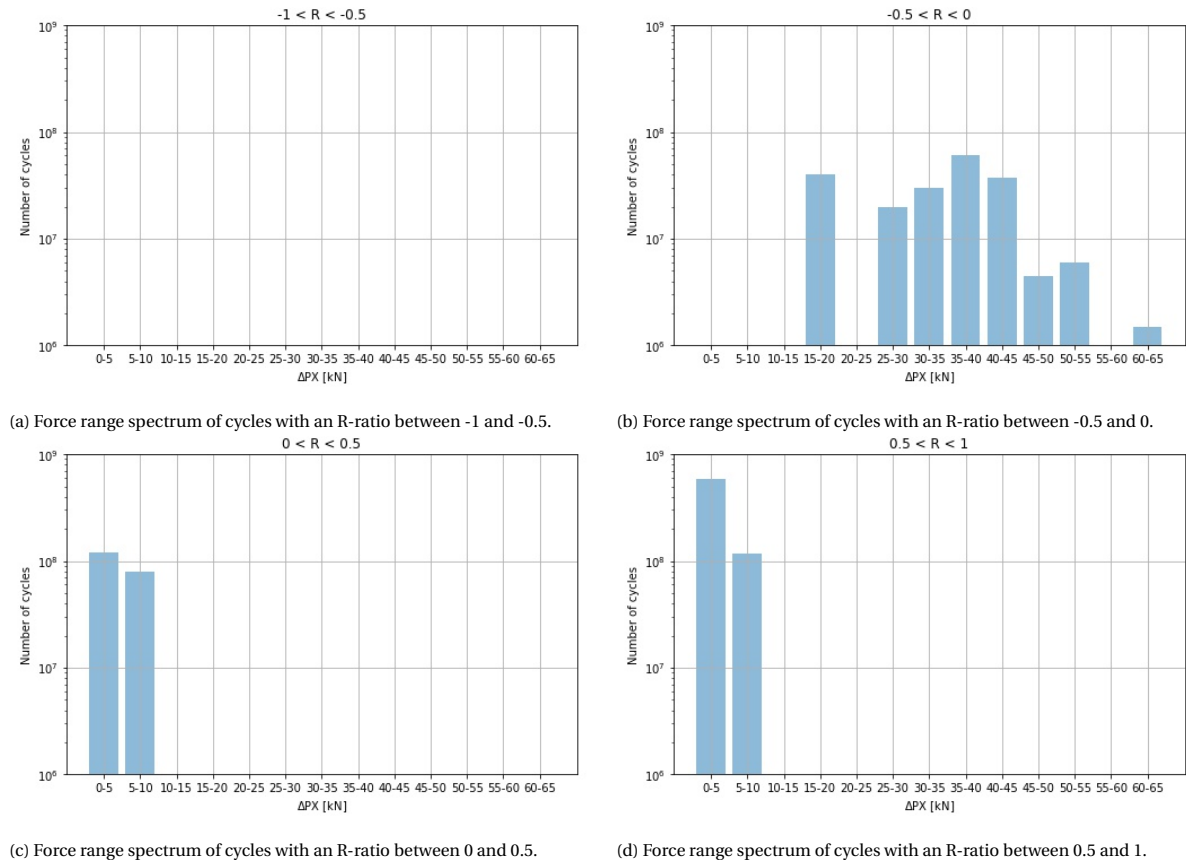


Figure 7.10: The force range spectrum of a connector in the beginning of the bridge Nieuw Vossemeer. The results are split in four groups based on the R-ratio.

For connectors at both the start and the lengthwise middle, the R-ratio can be calculated taking into account all different lorries driving over the bridge. The largest force ranges start at a shear force of 0 kN, it reaches its maximum value and goes back towards 0 kN. This results in R-ratios close to 0. Therefore most cycles are in the spectrum of -0.5 to 0.5. The fact that there is a second span has influence on the results. Some cycles now change sign and as a result it gets an R-ratio just below 0, so it is organised in the group -0.5 to 0. Passage of the lorries axles result in small force ranges with an R-ratio in the spectrum between 0 and 1.

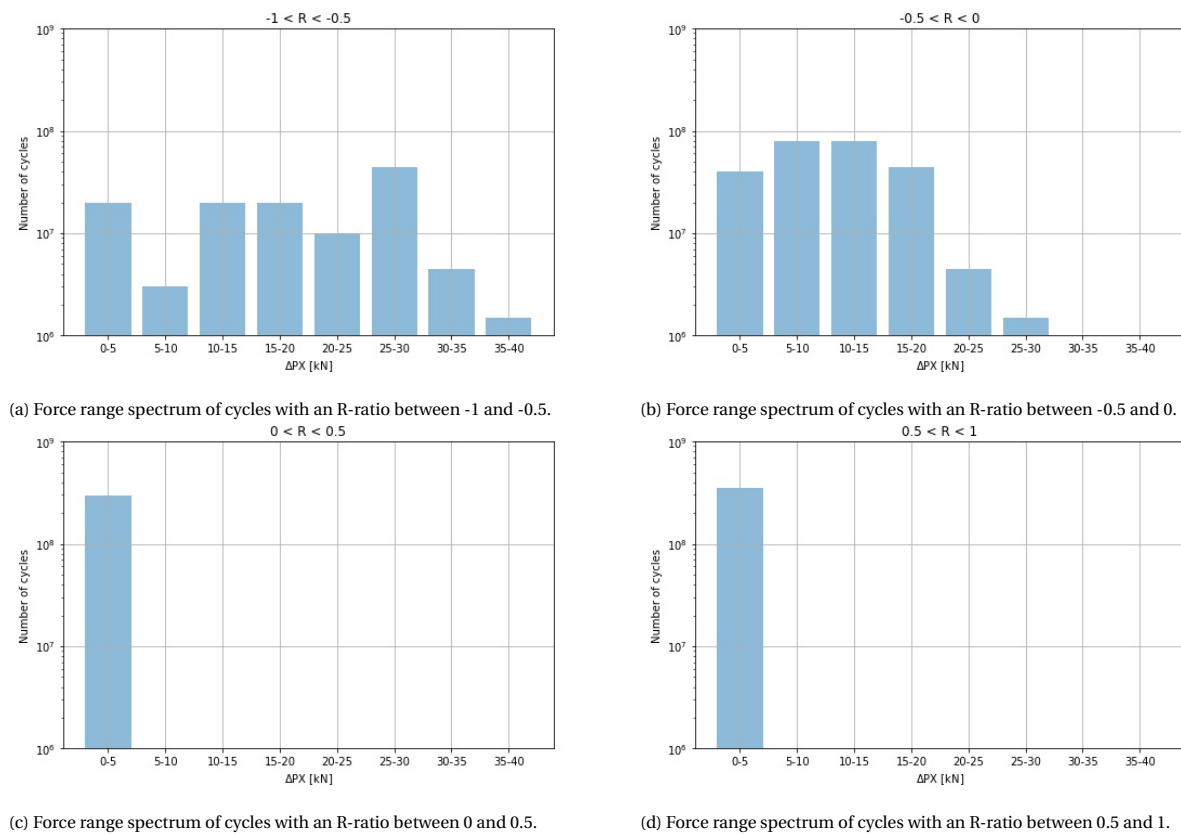


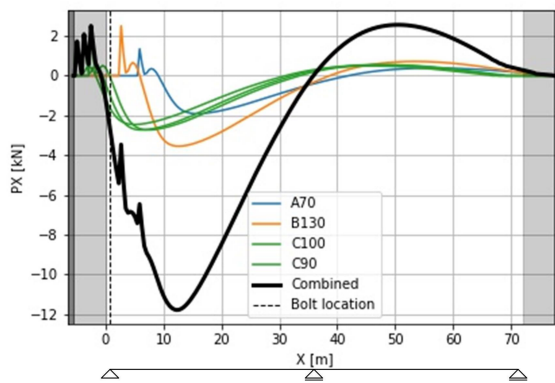
Figure 7.11: The force range spectrum of a connector in the middle of the bridge Nieuw Vossemeer. The results are split in four groups based on the R-ratio.

The R-ratio for connectors in the lengthwise middle of the bridge can be seen in figure 7.11. As can be seen, all relevant load cycles have an R-ratio between -1 and 0. The higher the magnitude of the force range, the more cycles shift to the group of R-ratios between -1 and -0.5. This makes sense as the connectors absolute extreme positive and negative shear force values are almost equal. The force ranges that occur when axles pass the connector have R-ratios in the entire R-ratio spectrum. In general the passage of the axles of the front and back of the lorries results in R-ratios between 0 and 1. The passages of the axles in the middle of the lorries results in R-ratios between -1 and 0 as it happens when the shear force in the connector is close to 0 kN and is changing sign. Despite the number of cycles there is probably no significant fatigue damage effect due to the passages of the axles as the force ranges are most of the time below 5 kN. For other bridges the same phenomena are observed, the largest force ranges have an R-ratio in the range of -1 to -0.5. Most of the other force ranges are in the spectrum of -1 to 0. Force ranges due to the passages of axles can have all R-ratios but the magnitude of those force ranges is low.

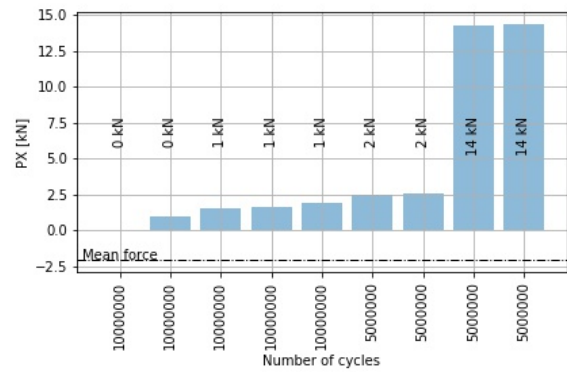
7.5. Multiple lorries

The slow lane on a highway full of lorries driving behind each other is a common event in the Netherlands. Therefore in the dutch annex load combinations are added for bridges that include multiple lorries. First there is the possibility of lorries driving behind each other. Second there is the possibility of lorries overtaking each other. Third there is the possibility of lorries passing each other in the opposite driving direction. These cases can increase the peak cyclic load and for that reason it should be included. There are rules which lorries should be used in which situations and how often it should be taken into account. A lorry in the second lane should be applied 5% of the time, for this lorry 3 should be used. As damages cannot be calculated, it is particularly interesting to see what the influence of a second lorry is on the peak cyclic load. Regulators are always looking for methods to better describe the real loading situation of bridges. Without real loading data this is not possible but it is interesting to see what the influence of a second lorry is. This is calculated in this

section.



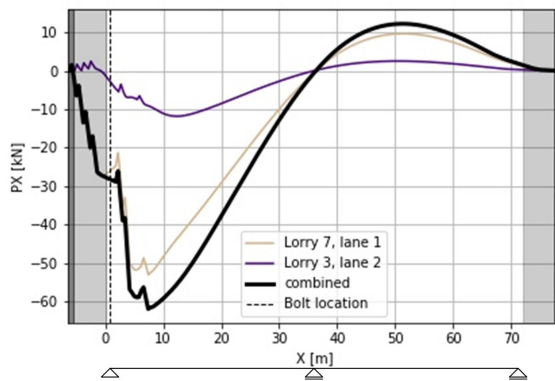
(a) The influence line of a connector at the beginning of the bridge.



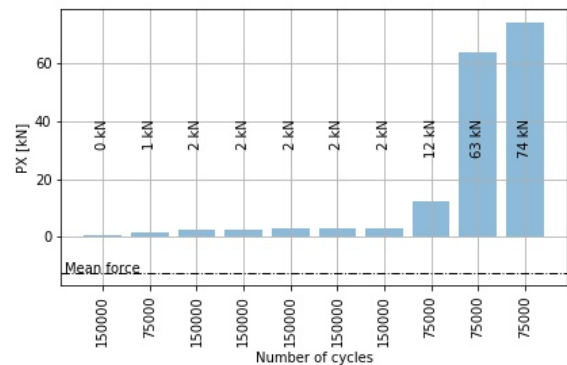
(b) The force range spectrum of a connector at the beginning of the bridge.

Figure 7.12: The influence line and force range spectrum of a connector at the beginning of the bridge due to lorry 3 in the second lane of the bridge Nieuw Vossemeer.

When lorry 3 is passing the bridge in the second lane, the magnitude of the shear force in the investigated connector is smaller compared to lorry 3 passing the bridge in the slow lane. This can be seen in figure 7.12. The reason for this is that the investigated connector is below the slow lane. There are three main girders for this bridge. Lorry 3 is now further away from the investigated connector and other connectors closer to the lorry also take part of the load.



(a) The influence line of a connector at the beginning of the bridge.



(b) The force range spectrum of a connector at the beginning of the bridge.

Figure 7.13: The influence line and force range spectrum of a connector at the beginning of the bridge due to lorry 7 in the slow lane and lorry 3 in the second lane of the bridge Nieuw Vossemeer. Figure 7.9a and 7.12a are combined.

In figure 7.13, the results of lorry 7 in the slow and lorry 3 in the second lane are combined. It can be observed that the magnitude of the largest force ranges increases slightly. There are two reasons for the slight increase. First lorry 3 is, compared to lorry 7, a lighter lorry. Second, because it is driving in the second lane, it is further away from the investigated connector. Other connectors are now closer to lorry 3 and already take a big part of the load. The connectors below the slow lane are still the heaviest loaded connectors.

The R-ratio of the two lorries, see figure 7.14, can be compared with the R-ratio due to lorry 7 only, see figure 7.10. Notice that in only 5% of the passages of lorries, there are two lorries. So originally there were 7 lorries passing, table 7.2 shows how often each lorry passes. Now for each lorry, 5% of the time there is a second lorry which is always lorry 3. The cases with a second lorry resulted in increased force ranges but the distribution between the different R-ratio groups is still the same. Only 5% of the time there is a second lorry and there are no big differences in the R-ratio. There is a small increase in magnitude of the force range when there is a second truck but the distribution between R-ratio groups is the same.

The layout of the bridge can influence the effect of a second lorry. In this example there is a main girder below the second lane. Bridges without main girders also have no connectors close to the second lane. In these cases it is possible that the connectors that transfer most of the shear forces from the lorry on the slow lane also transfer the shear forces from the lorry on the second lane. In these cases the magnitude of the force range will increase more than was the case in the example.

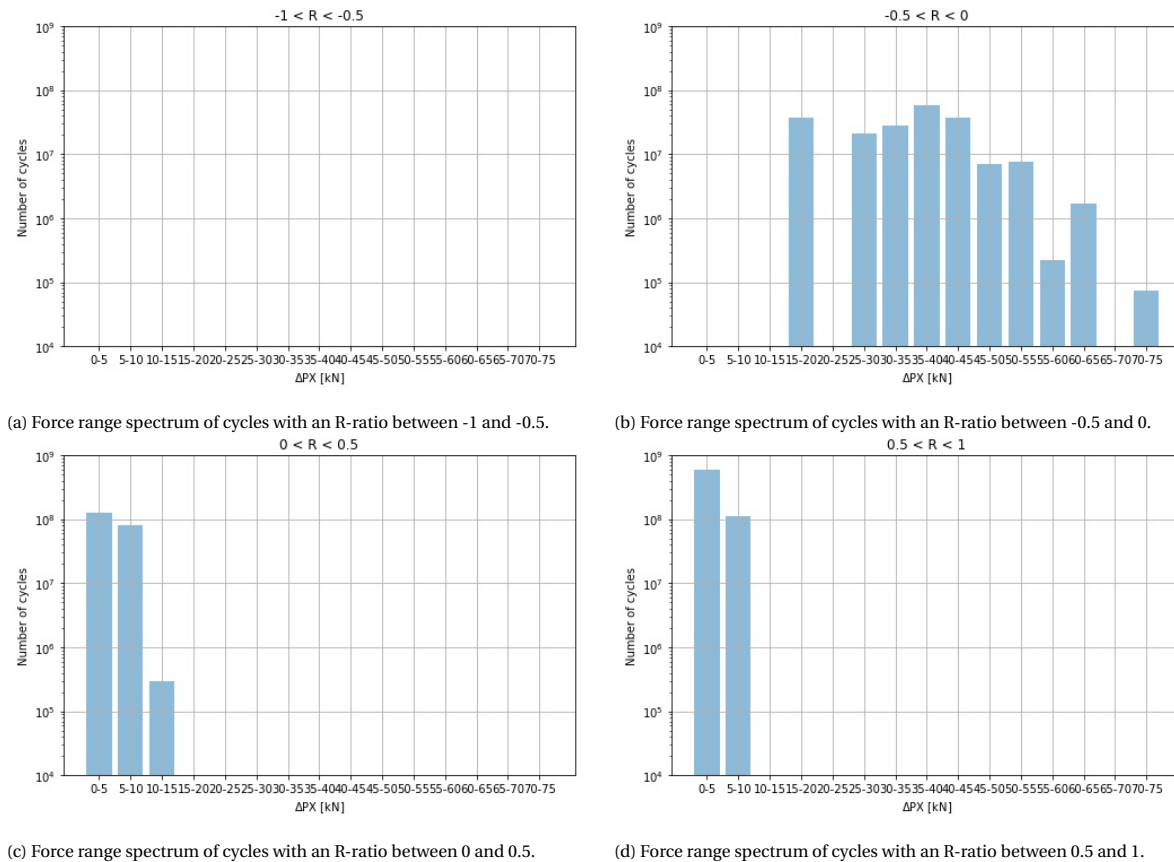


Figure 7.14: The force range spectrum of a connector in the beginning of the bridge Nieuw Vossemeer. The results are split in four groups based on the R-ratio.

7.6. Discussion of fatigue shear force results

Comparing connectors in the lengthwise middle of the bridge with connectors at the beginning there are a few differences that can be mentioned. First there is a big difference in the magnitude of the force range cycles. For this bridge the maximum force range for connectors in the middle is 36 kN while the connectors at the edge need to deal with cycles of 62 kN. This difference is partly the result of the multiple spans, although even with a single span the connectors at the edge would have the highest maximum force range. On the other side connectors in the middle will experience more load cycles than connectors close to supports. However, the magnitude of those extra cycles is most of the time small.

The R-ratio for connectors in the lengthwise middle is for the higher force ranges in the range between -1 and 0. For connectors close to the supports the R-ratio is for the larger forces ranges close 0. Multiple spans will shift the R-ratio of connectors close to the supports a bit more negative ending in the range -0.5 to 0. Passages of axles close to each other will result in force ranges with small magnitudes. This can result in a wide range of R-ratios between -1 and 1.

Summarizing, the magnitude of the force range of connectors close to supports is larger than for connectors in the lengthwise middle of spans. The R-ratio of normative force ranges for connectors close to supports is close to 0. For connectors in the lengthwise middle of spans these R-ratios are in the spectrum between -1

and 0. Multiple spans increases the maximum shear force range for connectors close to the supports while for connectors in the lengthwise middle of spans some force ranges is increased but not the largest. The R-ratio for connectors in the middle span will shift a little towards the -0.5 to 0 spectrum. Passages of axles will result in small force ranges. Multiple lorries result in larger force ranges but no shift in the R-ratio. The same observations can be made for bridges with other dimensions. For further investigations in damage, S-N curves are needed for different R-ratios.

8

Conclusions & recommendations

In this chapter the conclusions and recommendations of the research are presented. The conclusions are given by answering the research questions.

8.1. Conclusions

The main research questions are composed of sub-questions. Before the main research questions can be answered, the sub-questions are discussed.

1. What is the effect of the hybrid interaction on bolted connections in hybrid steel-FRP bridges.

Hybrid interaction between the steel girders and the fibre reinforced polymers (FRP) deck results in less deflection. For the generic bridge the deflection is 1.5 and 1.6 times lower for the distributed load and axle load respectively. The iSRR connectors do not reach full hybrid interaction as there is still slip, but compared to the model without hybrid interaction it is more than 10 times smaller.

2. What are the maximum shear forces in the bolted connections of hybrid steel-FRP bridges due to traffic loading.

The maximum shear force in the bolted connectors due to traffic load depends on the layout of the FRP deck. For six investigated generic cases its in the range 50-87 kN. Changing the direction of the webs from web_0 to web_{90} , and therefore the bolt configuration, increases the maximum shear force with a factor of about 1.5.

For the existing highway bridges owned and managed by Rijkswaterstaat there is a large scatter in the maximum shear forces in the connectors with values ranging from 10 to 110 kN. The dimensions of the bridge influence the maximum shear force but also the type of laminate that is chosen. Those laminates influence the magnitude of the shear force. The hangers of the arch bridges function as intermediate supports, decreasing the maximum shear force in the connectors.

3. What are the maximum shear forces in the bolted connections of hybrid steel-FRP bridges due to temperature loading.

Temperature load must be taken into account when designing the FRP deck. Incorrect orientation of the laminate in the facing can result in significant shear forces in the connectors up to 63 kN.

For the existing highway bridges owned and managed by Rijkswaterstaat the maximum shear forces due to temperature load are ranging from 5 to 60 kN. The fibre directions in the facings, which is defined with the distance between girders, determines to a large extend what the magnitude of the shear force will be.

4. What is the maximum shear force ranges in bolted connections of hybrid steel-FRP bridges due to fa-

tigue loading.

The maximum shear force range in the bolted connection depends on the location of the connector. In this context the approach bridge Nieuw Vossemeer, which showed during static traffic loading one of the highest shear forces in the connectors, was investigated. Connectors in the lengthwise middle of this bridge experience maximum shear force range up to 36 kN and connectors at the edge of the bridge have maximum shear force range up to 62 kN. Multiple spans increases the maximum shear force range for connectors close to the supports.

5. What type of load cycles are most dominant in the bolted connections of hybrid steel-FRP bridges due to fatigue loading.

The type of load cycles is defined with the R-ratio. The most harmful load cycles for connectors in the middle of the bridge lengthwise have an R-ratio close to 0, the most harmful load cycles for connectors at the edge have an R-ratio between -1 and 0. Two parallel lorries will change the magnitude of the shear force range cycle but do not change the R-ratio.

Research question:

What are the relevant static and fatigue forces on bolted connectors in hybrid steel-FRP bridges?

The results presented show that the shear force in the connectors is one of the aspects to be considered when designing a bridge where hybrid interaction between the deck and the steel superstructure is engaged. Incorrect deck design can result in unnecessarily high shear forces in the connectors. For the existing highway bridges the maximum shear forces in the connectors are 110 and 60 kN due to traffic and temperature loading respectively.

8.2. Recommendations

- Experimental study on the fatigue behaviour of iSRR connectors to create S-N curves for different R-ratios would be needed to quantify the damage in the connectors. In this research it was not possible to quantify the damage but this should be included in further research when S-N curves are available.
- The transverse stiffness of the iSRR connectors is kept constant in this research. However the transverse stiffness will decrease over time. This will influence the distribution of shear forces over the connectors. Further research can investigate how the maximum shear forces will change over time.
- The SOFiSTiK model that is used has a small margin of error for the shear forces close to the supports. The model can be improved to avoid those peaks of shear forces in the connectors.
- Only linear finite element analyses is used in this report. To allow for redistribution of shear forces between connectors it can be interesting to do non-linear finite element analyses.
- Experimental results are needed to verify the magnitude of the shear forces in the connectors. However, further research on how to measure the shear force in connectors is required.
- In this research the connector layout is not changed. It would be interesting to optimise the design of the connector layout and locate the connectors where they are needed, e.g. more connectors close to the supports.
- Only two type of bridges, namely fixed girder and arch bridges, are included in this research. FRP deck replacement on other type of existing bridges or movable bridge has also potential. These can be investigated as well.

References

- Alampalli, S. & Kunin, J. (2003). Load testing of an frp bridge deck on a truss bridge. *Applied Composite Materials*, 10(2), 85–102.
- Alnahhal, W., Aref, A. & Alampalli, S. (2008). Composite behavior of hybrid frp-concrete bridge decks on steel girders. *Composite Structures*, 84(1), 29–43.
- Ascione, F. (2010). A preliminary numerical and experimental investigation on the shear stress distribution on multi-row bolted frp joints. *Mechanics Research Communications*, 37(2), 164–168.
- Bishara, A. G., Liu, M. C. & El-Ali, N. D. (1993). Wheel load distribution on simply supported skew i-beam composite bridges. *Journal of Structural Engineering*, 119(2), 399–419.
- Chen, A. & Davalos, J. F. (2014). Design equations and example for frp deck–steel girder bridge system. *Practice Periodical on Structural Design and Construction*, 19(2), 04014003.
- Cheng, L. & Karbhari, V. M. (2006). Fatigue behavior of a steel-free frp–concrete modular bridge deck system. *Journal of Bridge Engineering*, 11(4), 474–488.
- Chiewanichakorn, M., Aref, A. J. & Alampalli, S. (2007). Dynamic and fatigue response of a truss bridge with fiber reinforced polymer deck. *International Journal of Fatigue*, 29(8), 1475–1489.
- Csillag, F. (2018). Demountable deck-to-girder connection of frp- steel hybrid bridges (Tech. Rep.). Delft: TU Delft.
- Csillag, F. & Pavlović, M. (2018). Push-out behaviour of demountable shear connectors for steel-frp hybrid beams – part 1 : Experiments. Submitted to *Composite Structures*.
- Cur96. (2017). Delft: SBRCURnet.
- Davalos, J. F., Chen, A. & Zou, B. (2010). Stiffness and strength evaluations of a shear connection system for frp bridge decks to steel girders. *Journal of Composites for Construction*, 15(3), 441–450.
- Davalos, J. F., Chen, A. & Zou, B. (2012). Performance of a scaled frp deck-on-steel girder bridge model with partial degree of composite action. *Engineering Structures*, 40, 51–63.
- Dreaves, A. (2018). Potential use of fibre-steel laminates in hybrid deck systems. TU Delft.
- Eom, J. & Nowak, A. S. (2001). Live load distribution for steel girder bridges. *Journal of Bridge Engineering*, 6(6), 489–497.
- Eurocode-1991-1-5. (2003). Brussels: European Committee for Standardization.
- Eurocode-1991-2. (2003). Brussels: European Committee for Standardization.
- Eurocode-1993-1-9. (2006). Brussels: European Committee for Standardization.
- Eurocode-1994-1-1. (2004). Brussels: European Committee for Standardization.
- Eurocode-1995-1-1. (2005). Brussels: European Committee for Standardization.
- Gürtler, H. W. (2004). Composite actions of frp bridge decks adhesively bonded to steel main girders (Unpublished doctoral dissertation). EPFL Lausanne.
- Keller, T. & Gürtler, H. (2005a). Composite action and adhesive bond between fiber-reinforced polymer bridge decks and main girders. *Journal of Composites for Construction*, 9(4), 360–368.

- Keller, T. & Gürtler, H. (2005b). Quasi-static and fatigue performance of a cellular frp bridge deck adhesively bonded to steel girders. *Composite Structures*, 70(4), 484–496.
- Keller, T. & Schollmayer, M. (2006). In-plane tensile performance of a cellular frp bridge deck acting as top chord of continuous bridge girders. *Composite structures*, 72(1), 130–140.
- Kwon, S.-C., Dutta, P. K., Kim, Y.-H. & Lopez-Anido, R. (2003). Comparison of the fatigue behaviors of frp bridge decks and reinforced concrete conventional decks under extreme environmental conditions. *KSME international journal*, 17(1), 1–10.
- Lambregts, S. (2019). Implementation of a ply inclination in the classical laminate theory. TU Delft.
- Mabsout, M. E., Tarhini, K. M., Frederick, G. R. & Kesserwan, A. (1999). Effect of multilanes on wheel load distribution in steel girder bridges. *Journal of Bridge Engineering*, 4(2), 99–106.
- Olivier, G. & Csillag, F. (2020). Bolted joints for frp decks (Tech. Rep.). Delft: TU Delft, Arup, Rijkswaterstaat.
- Park, K.-T., Kim, S.-H., Lee, Y.-H. & Hwang, Y.-K. (2006). Degree of composite action verification of bolted gfrp bridge deck-to-girder connection system. *Composite structures*, 72(3), 393–400.
- Reising, R. M., Shahrooz, B. M., Hunt, V. J., Neumann, A. R., Helmicki, A. J. & Hastak, M. (2004). Close look at construction issues and performance of four fiber-reinforced polymer composite bridge decks. *Journal of Composites for Construction*, 8(1), 33–42.
- Rijkswaterstaat. (2019). Vervanging en renovatie opgave van bruggen en viaducten.
- Satasivam, S., Feng, P., Bai, Y. & Caprani, C. (2017). Composite actions within steel-frp composite beam systems with novel blind bolt shear connections. *Engineering Structures*, 138, 63–73.
- Schreiner, J. & Barker, M. G. (2005). Lateral distribution in kansas dot steel girder bridge with frp deck.
- Swinnen, J. (2020). Modelling the mechanical performance of bolted deck-to-girder connections in frp-steel hybrid bridges. TU Delft.
- Tabsh, S. W. & Tabatabai, M. (2001). Live load distribution in girder bridges subject to oversized trucks. *Journal of Bridge Engineering*, 6(1), 9–16.
- Tarhini, K. M. & Frederick, G. R. (1992). Wheel load distribution in i-girder highway bridges. *Journal of Structural Engineering*, 118(5), 1285–1294.
- Tromp, L. (2018). Kansen voor vvk in de infrastructuur (Tech. Rep.). Rotterdam: Royal HaskoningDHV.
- Vassilopoulos, A. P. & Keller, T. (2011). *Fatigue of fiber-reinforced composites*. Springer.
- Waldron, C. J. (2001). Determination of the design parameters for the route 601 bridge: A bridge containing the strongwell 36 inch hybrid composite double web beam (Unpublished master's thesis). Virginia Tech.
- Zarifis, G. (2018). Application of bio-based frp on a road traffic bridge (Unpublished master's thesis). TU Delft.
- Zhang, Y. & Cai, C. (2007). Load distribution and dynamic response of multi-girder bridges with frp decks. *Engineering structures*, 29(8), 1676–1689.
- Zokaie, T. (2000). Aashto-lrfd live load distribution specifications. *Journal of bridge engineering*, 5(2), 131–138.
- Zou, B., Davalos, J. F., Chen, A. & Ray, I. (2010). Evaluation of load distribution factor by series solution for orthotropic bridge decks. *Journal of Aerospace Engineering*, 24(2), 240–248.

A

Benchmark study

At the start of the research, a SOFiSTiK model has been created to find out how to make a model for investigating the shear forces in connectors. This benchmark bridge will be loaded with different kind of loads to see which loads are relevant. Beside variations in bridge layout will be compared in a sensitivity analyses.

A.1. Layout

The benchmark bridge is 30 m long, 10 m wide simply supported bridge. At one end the movements of the supports in the x, y and z directions are constrained and at the other end the movement in y and z direction is constrained. The two main girders 1.8 m high, 0.4 wide and are made from S355 steel. The fibre reinforced polymers (FRP) deck consists out of two facings connected by webs. The webs are located perpendicular to the driving direction. Both the facings and the webs are 2 cm thick. The spacing between the webs is 12.5 cm and the center-to-center distance of the facings is 17 cm. For the facings symmetric anisotropic laminate is used. The webs use quasi isotropic laminate. The properties of both laminates can be seen in table A.1. The FRP and the girders are connected by bolts. The connectors are placed every 0.5 m between FRP webs. The connectors are placed 12.5 cm eccentric from the girder, so two connectors per half meter girder. The transverse stiffness of the connectors is equal to 100 kN/mm. Different types of loading will be applied.

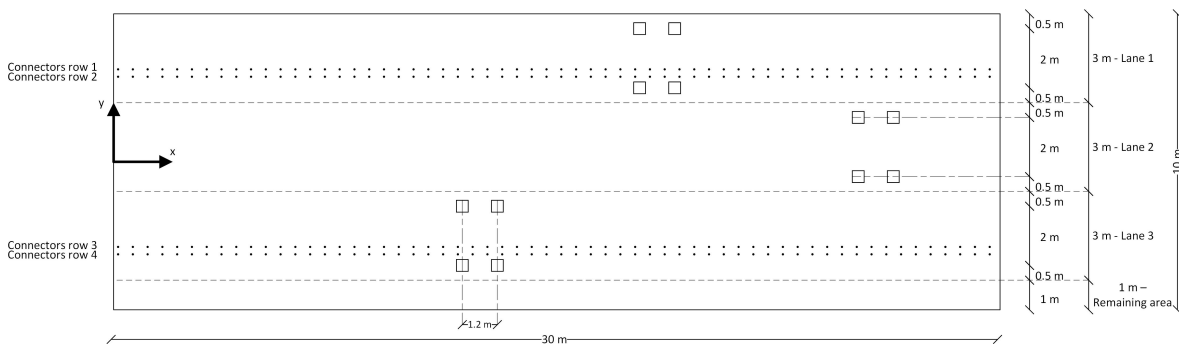


Figure A.1: A top view of the benchmark bridge.

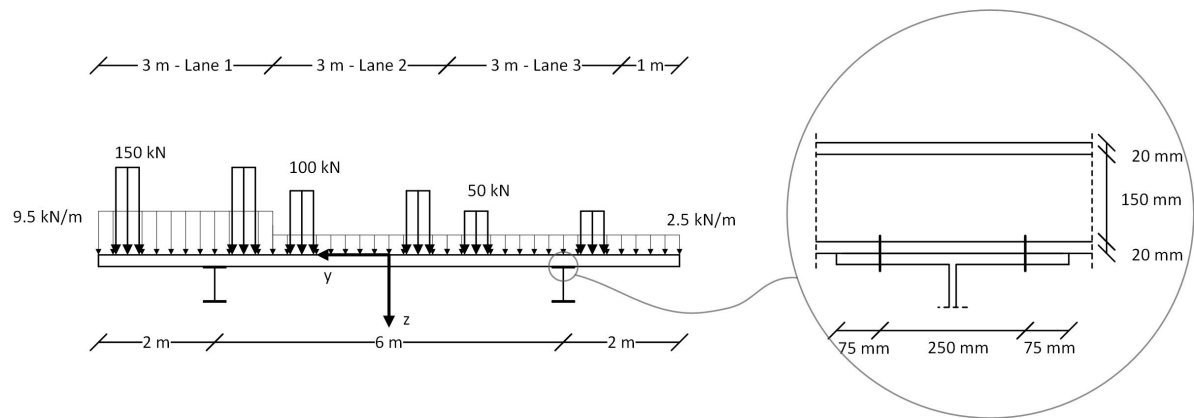


Figure A.2: A side view of the benchmark bridge load with load model 1 (LM1).

	0° [%]	±45° [%]	90° [%]	σ_1 [MPa]	σ_2 [MPa]	$\tau_{1,2}$ [MPa]
Facing	55	15	15	315	196	89.3
Web	25	25	25	227	227	113.6

Table A.1: The properties of the facings and webs that are used for the benchmark study.

A.2. Loading

Different loads are applied to analyse the shear force in the connectors. The loads are induced by traffic, temperature or time.

Eurocode 1991-2 (2003) presents the traffic load that must be taken into account for the static analysis of road bridges. Vertical forces are represented by 4 load models. Load model 1 consists out of a tandem system load and a distributed load, the value of the load depends on the lane. Load model 2 is a single axle load. Load model 3 is for special vehicles and load model 4 covers crowd loading. Load model 3 and 4 will be skipped. Beside the vertical forces also horizontal forces due to braking and acceleration of vehicles must be taken into account. Beside traffic load also temperature loads and creep will be investigated.

Self-weight of the bridge is not included in the analysis. Before the deck is connected with the support structure, the deck is already placed on the support structure. So when the deck and support structure are connected, there are no movements of the structure due to the self-weight and therefore also no shear forces in the connections.

Traffic load model 1

LM1 is a static traffic load which is used to analyse global effects. It consists of a tandem system with two axles in the first three lanes and a distributed load. The axles in lane 1, 2 and 3 is equal to 300, 200 and 100 kN respectively. The exact definition of the load is explained in section 6.1.1.

The benchmark bridge is modelled with SOFiSTiK. Instead of the full tandem system, only axle loads are applied. In the post-processing process, the axles are combined with a python script. The script searches for the worst combination of the load and calculates the maximum shear force for each connector. The results are presented per row of connectors, see figure A.1 for the definition of the connector rows for the benchmark bridge. Each dot represents the minimum or maximum shear force in a connector. A more elaborated explanation how the envelopes are created can be found in section 6.2.

The shear force in the connectors is in SOFiSTiK presented as the shear force in connectors in longitudinal direction (PX) and the shear force in connectors in transverse direction (PY). In the benchmark study both loading direction will be presented and discussed.

The envelope of shear forces in longitudinal direction due to LM1 for each row of connectors can be seen in figure A.3. The shape of all graphs looks like the shear diagram for a beam with a distributed load. This makes sense because the maximum values are found when the load is located close to the connections. The moving tandem system preforms as distributed load which results in the shear diagram. The magnitude of the shear forces is the largest for the connector rows close to the slow lane where the heaviest axles are located. The magnitude of the shear force in the connectors decreases for the connector rows further from the slow lane. The maximum shear forces can be found close to the supports. The magnitude of the shear force in the connectors close to the beginning and end of the bridge does not follow the linear straight line the connectors do follow. More about this phenomenon is explained later in this section.

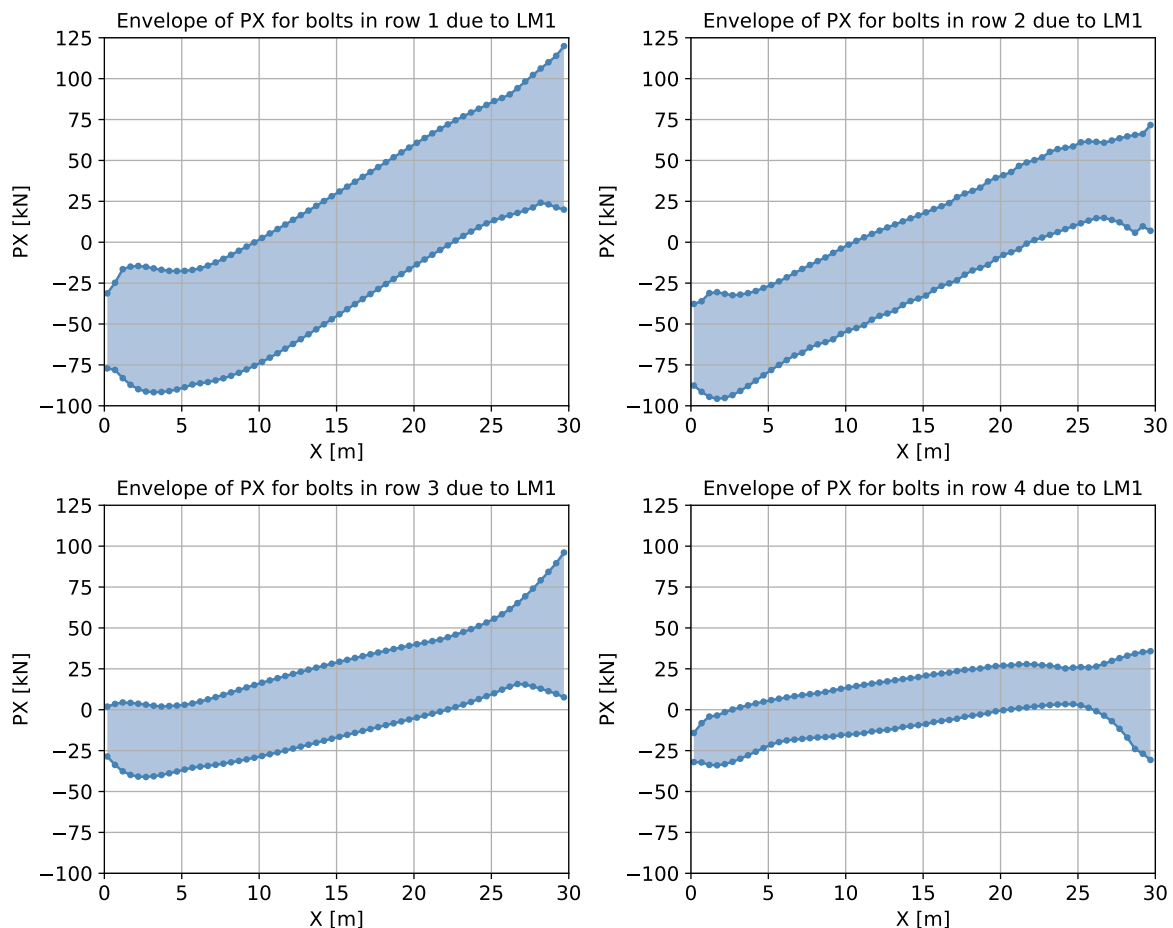


Figure A.3: Shear force in longitudinal direction per row due to LM1.

The envelope of shear force in transverse direction due to LM1 for each row of connectors can be seen in figure A.4. Almost all connectors in each row of connector have the same minimum and maximum shear force. The magnitude of shear force is the largest for the connector rows close to largest axle loads. The connectors close to the beginning and end of the bridge have a wider range of possible shear forces. The absolute minimum and maximum shear force in those connectors is larger than for the other, peaks are visible.

The connectors close to the beginning and end of the bridge do not follow the patterns that would be expected when following the other connectors. In the longitudinal direction the shear force range decreases at the side of the pinned support and increases at the side with the roller support. In the transverse direction, at both sides of the bridge increases of the shear force range are visible. In the last case the magnitude can increase significant.

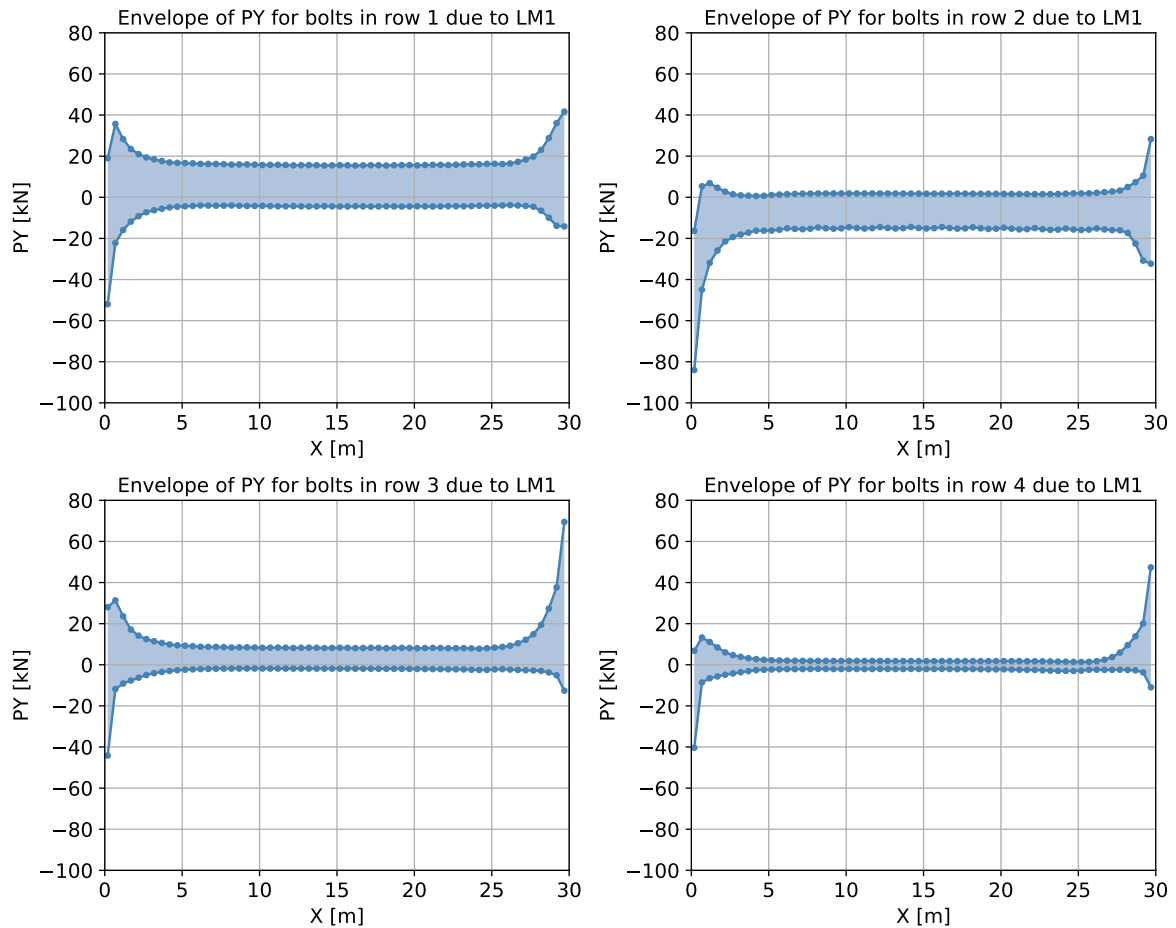


Figure A.4: Shear force in transverse direction per row due to LM1.

Axle loads result in deflections of the deck and girders. The axles load the bridge eccentric. The deflections are introduced on one side of the bridge, as a result the bridge wants to deform asymmetric. At the supports, there is no movement allowed. Exception is the roller support where movement in the longitudinal direction is allowed. The model uses 2D beam elements for the girders which are connected with the supports. So at the location of the supports, also the girders are not allowed to move. When the axle load is a few meters from the begin or end of the bridge, there is enough space to move back to the original situation with the fixed boundary conditions. However when the axle is close to the supports, the bridge wants to deform but the boundary conditions prevent part of this movement. Prevention of these deformations result in high shear forces in the connectors. So due to the chosen constrains at the supports, the shear forces in the connectors close to the support increases. Especially for the shear force in transverse direction this result in wrong values.

Traffic load model 2

load model 2 (LM2) is just like LM1 a static traffic load. LM2 is a single axle load of 400 kN. The wheel contact area is 0.6 by 0.35 m. This load model is used to analyse local effects. The layout of the axle can be seen in figure A.5. It should be applied at any location of the carriageway.

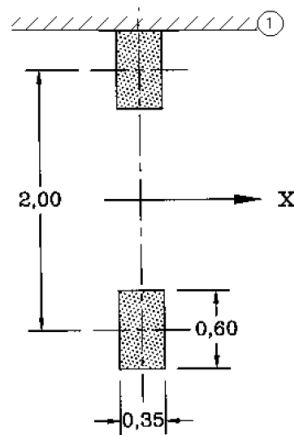


Figure A.5: Definition of the wheels and axles for traffic load model 2.

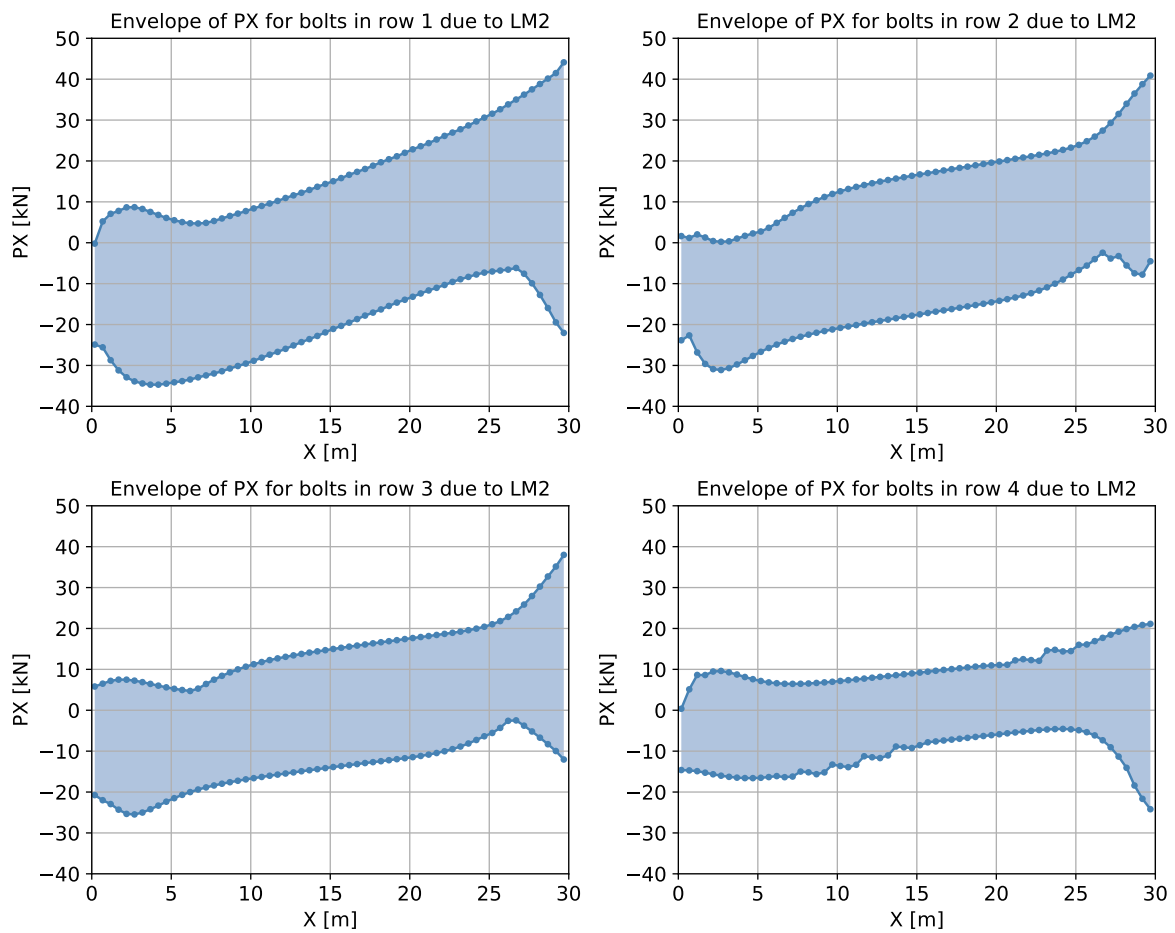


Figure A.6: Shear force in longitudinal direction per row due to LM2.

The shear force in the connections due to LM2 can be seen in figure A.6 and A.7. The results are comparable with the shear forces due to LM1. A difference is the magnitude. The maximum shear force is lower compared to LM1. The difference between the maximum shear force in the different connector rows is smaller than for LM1. This is because the axle load in each lane, also the faster lanes, has the same magnitude. Row 3 and 4 have slightly smaller values than row 1 and 2 due to the location of the lanes on the bridge.

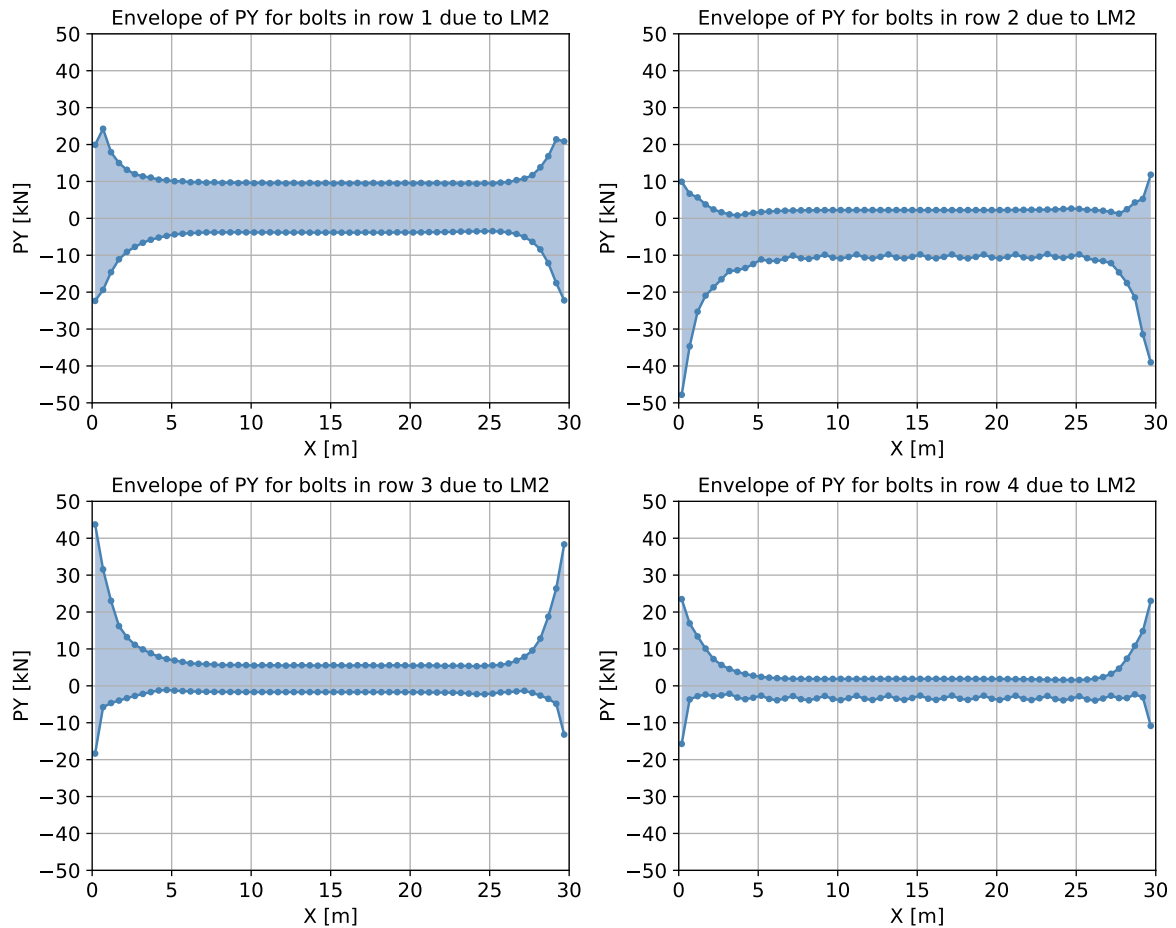


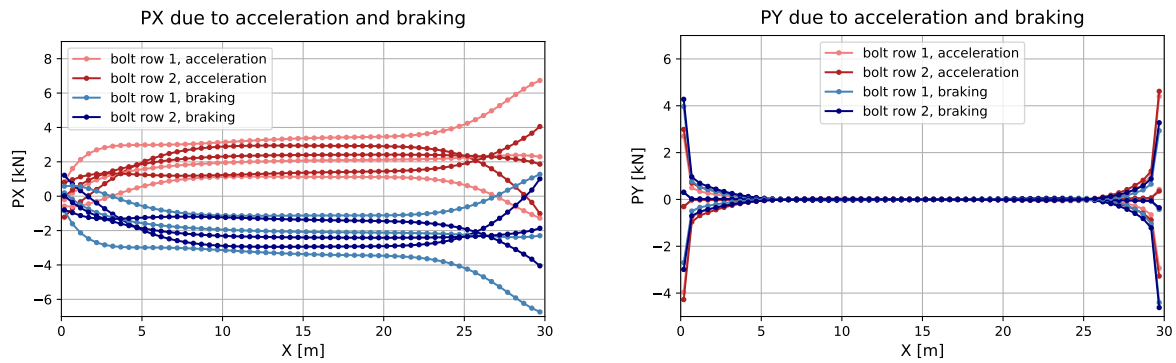
Figure A.7: Shear force in transverse direction per row due to LM2.

Acceleration and braking

Braking and acceleration of lorries results in horizontal loads on the bridge. The horizontal force shall be taken as a longitudinal force acting at the surfacing level of the carriageway. The value of the horizontal loads corresponds to the maximum vertical load and must be calculated with formula A.1. It can be simplified as shown in the second line of the formula with the reduction factors α equal to 1, the axle load in lane 1 (Q_{1k}) equal to 300 kN, the distributed load in lane 1 (q_{1k}) equal to 9 kN/m² and the lane width (w_1) equal to 3 m. The only variable left is the bridge deck length L.

$$\begin{aligned} Q_{1k} &= 0.6\alpha_{Q1}(2Q_{1k}) + 0.10\alpha_{q1}q_{1k}w_1L \\ Q_{1k} &= 360 + 2.7L \end{aligned} \tag{A.1}$$

The horizontal loads due to acceleration and braking are calculated as can be seen in A.8a and A.8b. Only the values for connector rows 1 and 2 are shown because these rows will be governing. The other rows have comparable results. Compared to the vertical loads the results are negligible. At the supports there are peaks visible in both loading directions, although the peaks are larger in the transverse direction. The changing values are due to boundary conditions at the supports where no movement is allowed.



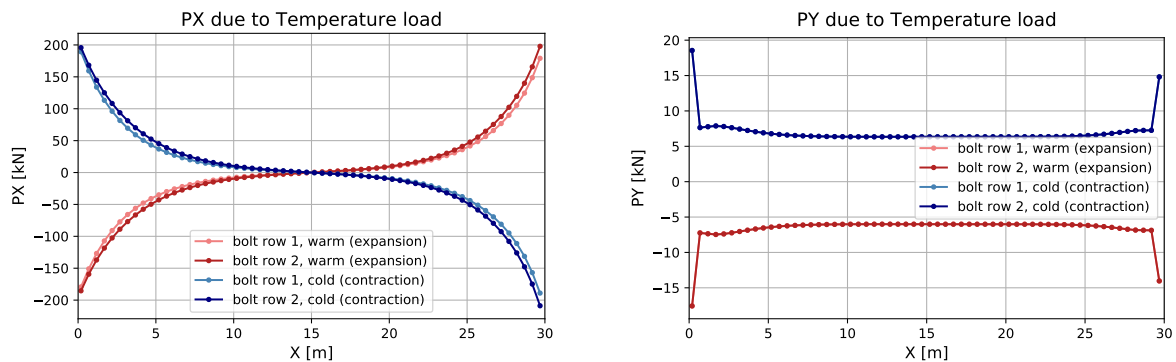
(a) Shear force in longitudinal direction.

(b) Shear force in transverse direction.

Figure A.8: Shear force due to horizontal traffic loads.

Temperature

Temperature load results in expansion or contraction of the bridge. Steel and FRP do not have the same expansion coefficient. The connectors force the girders and deck to keep the same expansion or contraction. This results in shear forces in the connectors. Two cases are investigated, contraction of -38°C and expansion of $+36^{\circ}\text{C}$. See section 6.1.2 for a more extensive explanation why these temperature loads are used.



(a) Shear force in longitudinal direction.

(b) Shear force in transverse direction.

Figure A.9: Shear force due to temperature loading.

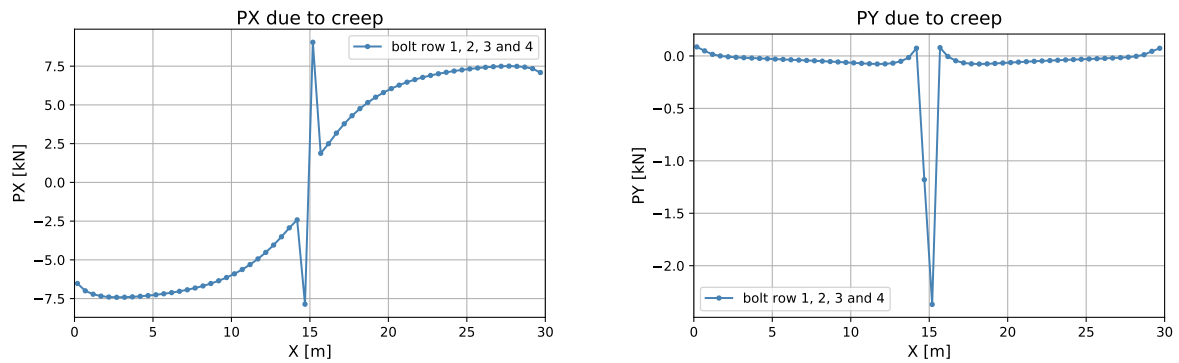
Extreme temperatures cause large shear forces in the connectors in longitudinal direction as can be seen in figure A.9a. In transverse direction the shear forces are much lower A.9b. Because the fibres in the facings are directed in the transverse direction the expansion and contraction is low compared to the steel girders. The expansion and contraction of the FRP in longitudinal direction, perpendicular to the fibres, is more than four times as large as the expansion and contraction of the steel. This results in large forces in the connectors, especially at the beginning and end of the bridge as the forces increase parabolic. Contraction or expansion has no influence on the results, only the sign changes, so the highest temperature difference is governing.

The connectors at the beginning and end of the bridge show a peak for the shear force in transverse direction. This peak is the result of boundary conditions for the supports. There is no movement allowed in transverse direction at the supports but due to the temperature loads the bridge wants to expand in this direction. This results in a peak load for the connectors close to the supports.

Changing the amount of fibres in each direction, or changing the expansion coefficient of the resin, changes the expansion coefficient of the FRP deck in both directions. So it is possible to reduce the shear forces in the connectors by changing the layout of the FRP deck.

Creep

Creep, caused by long term loading, will result in permanent stresses. When during construction piers are used as extra supports, the bridge is a continuous bridge during construction. Some of the self-weight is taken by the piers. When the deck is installed and connected to the girders the piers will be removed. The load which was taken by the piers must now be transported to the supports. This creep that is caused due to this construction method can be modelled with a point load in the middle of the bridge equal to the support reaction of the piers during construction. This method is governing over a distributed quasi-permanent load as the creep is higher.



(a) Shear force in longitudinal direction.

(b) Shear force in transverse direction.

Figure A.10: Shear force due to creep.

The shear force in the connections due to creep can be seen in figure A.10. In the middle a peak is visible. This is at the location where the point load is located. Towards the edges it gradually consolidated. Compared with traffic and temperature loads the values are low.

Discussion

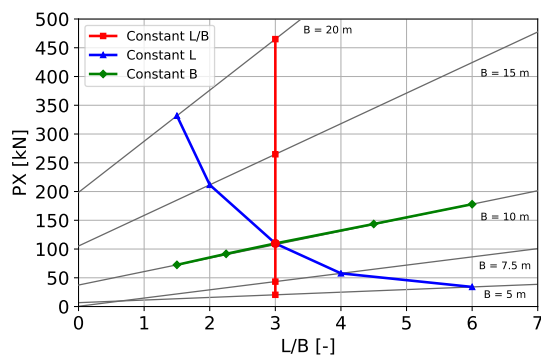
Regarding the results presented in this section, multiple conclusions can be drawn. First of all, there is a big difference between the magnitude of the shear forces in the connectors due to the different loads. LM1 which is used for global effects results in higher shear forces in the connectors than LM2 which is used for local effects. So LM1 is the governing traffic load model that should be used. In addition is the shear force in the connectors due to acceleration and braking negligible. The same can be said for the shear force in the connectors due to creep. The temperature load on the other hand can have a significant influence on the results and must always be taken into account.

The maximum PX is for all type of loads larger the maximum PY and so the PX is the governing load direction. Close to the supports there are deviations from the expected values due to the way the supports are modelled. Especially for the PY this is clearly visible. Also for the PX there are deviations but for LM1 the error of the maximum shear forces is permissible.

A.3. Sensitivity analyses

The influence of the bridge layouts is investigated by changing a single parameter in the layout of the bridge. The maximum shear force in the longitudinal direction of the connectors is compared for the different variations. Some connector results ended up with not realistic high values because only linear finite element analyses is used and the connectors will never fail in these type of analyses. However this still supports the goal of showing the influence of the changed bridge layout on the shear force in the connectors. The magnitude of the shear force is less important in this section.

Bridge dimensions



(a) The results of changed bridge dimensions.



(b) An example with marked in red the changed bridge dimensions.

Figure A.11: Sensitivity analysis of the bridge dimensions on the maximum shear force in the connectors.

Compared to the original layout, which has been discussed earlier in the chapter with dimensions of 30 by 10 m, several other dimensions has been calculated. They can be divided in three groups, the first group has the same Length(L)/Width(B) ratio as the basic model. The second group has a constant L but the B changes, an example can be seen in figure A.11b where the changed parameters are shown with red. The girder distance is kept in the same ratio as with the basic model so 1:3:1. A narrower bridge also influences the the number of lanes and thus the loads on the bridge. The third group has a constant B and here the L changes. The spacing between connectors is kept the same, so an increasing length increases the number of connectors. The basic model is marked with a red circular dot and is also the location where the lines intersect.

For the first group it can be seen that the shear force in the connectors increases when the bridge dimensions become larger. A larger span results in a larger shear force as the shear force is depending on the span. The increased width adds more load on the bridge and the eccentricity of the loads increases also. Especially in the transverse direction there is a large increase of the shear force in the connectors due to the eccentricity but also in the longitudinal direction there is some increase in the shear force due to the more eccentric load. The combined increase of length and width makes the increase in shear force considerably large.

In case the length of the bridge is constant, the shear force will increase when the bridge becomes wider. The same arguments can be used as before for a wider bridge. The influence of the changing width is about quadratic. Also for a constant width of the bridge, so a changed bridge length, the same arguments can be used as before why an increasing length increases the shear force. This time the influence is about linear.

Number of supports

The variations in layout applied over here regard the number of supports. The length of the bridge is kept constant with 30 m. An increasing number of intermediate supports decreases the shear force in the connectors for the same span. This makes sense because as shown in the section before, a smaller span decreases the maximum shear force. The effect is almost linear. The nearly straight line is in agreement with figure A.11a where the length of the bridge was changed with a constant width (green line). When comparing bridges with a single span with length L against bridge with multiple spans with a length L, this is not shown in the figure, the difference in maximum shear force is within a few percent.

When there are multiple spans, often the span in the middle of the bridge is longer than the spans at the edges of the bridge. As a second case the ratio between the different spans is changed. Instead of three equal spans of 10 m (span ratio of 1:1:1), the span ratio is changed so the span in the middle is 15 m long and the other spans are 7.5 m (span ratio of 1:2:1). This results in a small decrease in the maximum shear force from 60 to 50 kN. Changing the ratio even further to 1:3:1 reduced the maximum shear force to 45 kN. Because the largest value is found close to the beginning and ending of the bridge, and the span next to those supports decreases, the shear force also decreases. The reason the maximum shear force at the end support is a bit higher than maximum shear force at the other supports is probably due to the constrains that are used in the model.

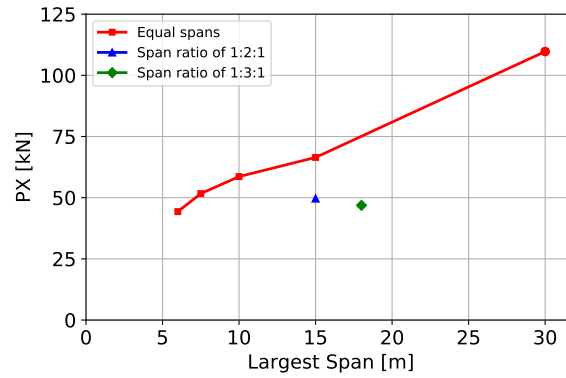
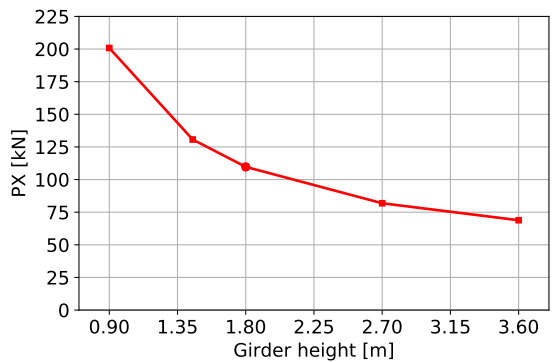


Figure A.12: Sensitivity analysis of intermediate supports on the maximum shear force in the connectors.

Girder height



(a) The results of a changing girder height.

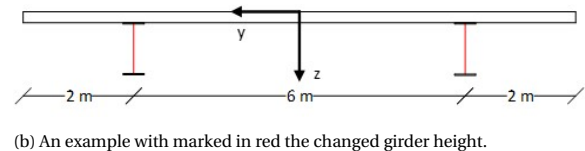


Figure A.13: Sensitivity analysis of the girder height on the maximum shear force in the connectors.

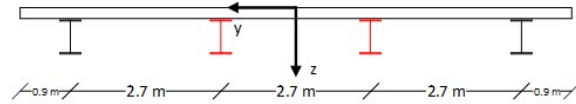
The shear stress (τ) of a beam can be calculated with formula A.2. As can be seen the formula is beside the thickness of the section (t) and the shear force (V) depending on both the first moment of inertia (S) and the second moment of inertia (I). The order of the height in the first moment of inertia is h^2 and in the second moment of inertia is h^3 . So the shear stress is theoretically depending on $\frac{1}{h}$. When the girder height is doubled, the shear force is nearly halved. The result is not exactly halved because the model is 3D and also takes into account other effects as can be seen in figure A.13a.

$$\tau = \frac{V * S}{t * I} \quad (\text{A.2})$$

Number of main girders



(a) The results of a changed number of girder.

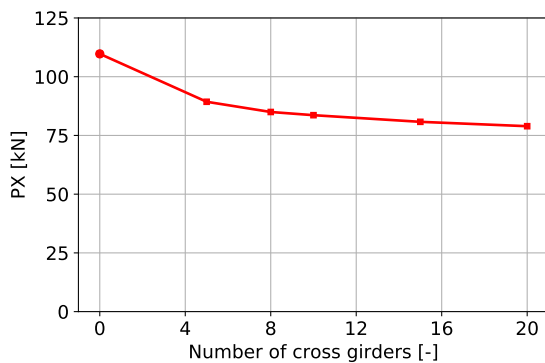


(b) An example with marked in red the changed number of girders.

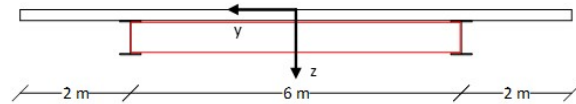
Figure A.14: Sensitivity analysis of the number of girders on the maximum shear force in the connectors.

More main girders means more support for the deck and more bolted connections. The distance between the girder is kept on $1:3_{n-2}:1$ so for four girders the distance is $1:3:3:1$. More girders also means less eccentricity of the forces. This all decreases the shear force in the connections.

Number of cross girders



(a) The results of a changed number of cross girders.

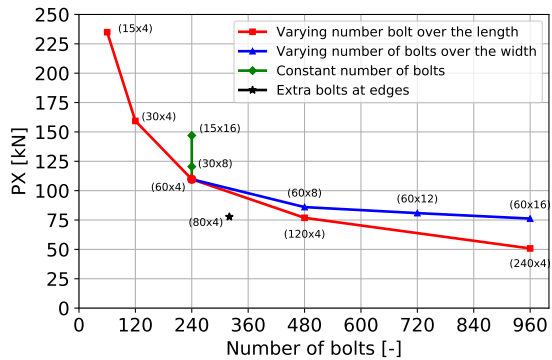


(b) An example with marked in red the added cross girders.

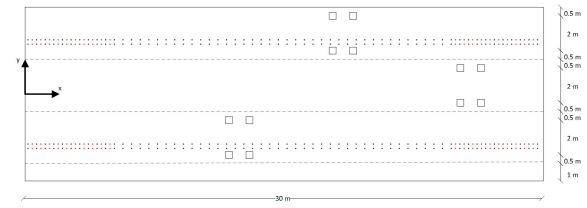
Figure A.15: Sensitivity analysis of the number of cross girders on the maximum shear force in the connectors.

The cross girders do not help in carrying the load. In this case the cross girders are even not connected to the deck. But cross girders help to ensure that the main girders act together. So it would be expected that the addition of cross girders decreases the shear force as the load is spread more equal over the connectors. And as can be seen this is the case. More cross girders decrease the shear force in the connectors, although especially the addition of a few cross girders make a significant difference compared to no cross girders.

Number of connectors



(a) The results of a changed number of connectors.



(b) An example with marked in red the extra connectors.

Figure A.16: Sensitivity analysis of the number of connectors on the maximum shear force in the connectors.

The number of connectors influences the shear force in the connectors. Different layout are compared. First the connector spacing over the length is changed, second the number of connectors in width direction of the girder and third both cases are changed in such a way that the number of connectors is the same. A special case is investigated as well where the number of connectors at the first and last five meters is doubled. The number of connectors is mentioned in the graph between brackets. The first number is the number of connectors in longitudinal direction and the second in transverse direction. Increasing the number of connectors in the transverse direction means there are more connectors on each half of the girder. Because of the minimum spacing between the connectors, the feasibility of the designs with multiple connectors per half girder will depend on the width of the flanges of the girders. For example, four connectors on each half of the girder will require an extremely width girder and will therefore not be feasible for most girders.

Increasing the number of connectors in the longitudinal direction reduces the shear force quadratic. The same can be said when increasing the number of connectors in the transverse direction although the reduction is smaller. When the number of connectors is kept the same it is again visible that more connectors in longitudinal direction decrease the shear force in the connectors more than having more connectors in transverse direction. However when extra girders where added, the number of connectors in the transverse direction increased as well. This was much more effective to reduce the maximum shear force in the connectors with the same amount of connectors.

Figure A.17 shows the influence of adding extra connectors at the edges. As can be seen the minimum and maximum shear force is reduced. Placing the connectors in the position where they are needed is probably a cost effective solution to decrease the shear force in the connectors.

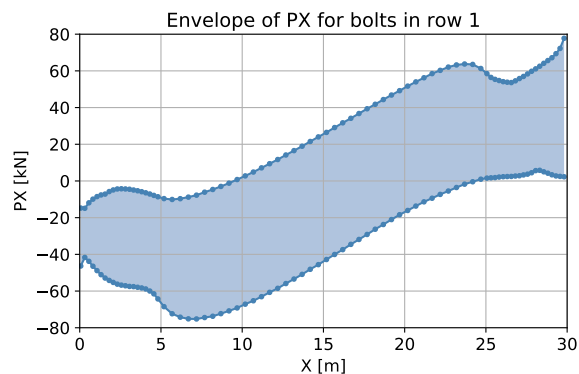


Figure A.17: Envelope of shear forces in the connectors in longitudinal direction for row 1 with extra connectors at the first and last 5 m.

Transverse stiffness of connectors

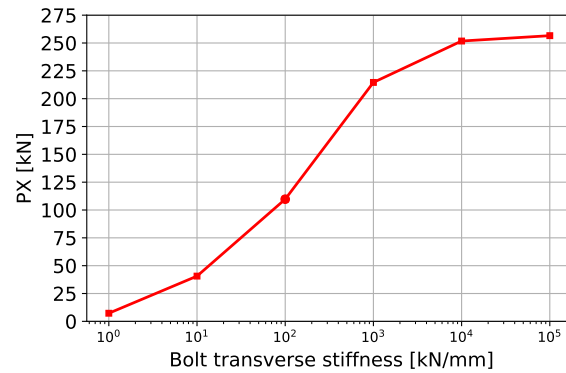


Figure A.18: Sensitivity analysis of the transverse connector stiffness on the maximum shear force in the connectors.

An increase in the transverse stiffness of the connectors results in an increasing shear force in the connectors. When a connector is stiffer, it attracts more force. The load is spread over less connectors. The opposite happens when the transverse stiffness decreases. The connectors can transfer less force so it is spread over more connectors. It seems the graphs flattens at extremely high and low transverse stiffness. For extremely low stiffness it goes to 0 kN, for extreme high stiffness it goes to about 260 kN.

(This page is intentionally left blank)

B

Classical laminate theory

The fibre direction affects the elastic behaviour of fibre reinforced polymers (FRP) plies and laminates. The fibre in an unidirectional ply are all parallel to the 1-axis, as can be seen in figure B.1. Because it is a 3 dimensional structure there is also a 3-axis which corresponds to the direction perpendicular to the plane of the ply. The relation between stress and strain can be expressed with the compliance matrix. In equation B.1 the stress strain relation is showed for any orthotropic material. A unidirectional ply is an transversely isotropic material. The elastic modulus is the same in all directions perpendicular to the fibre. The compliance matrix can be adjusted as shown in equation B.2.

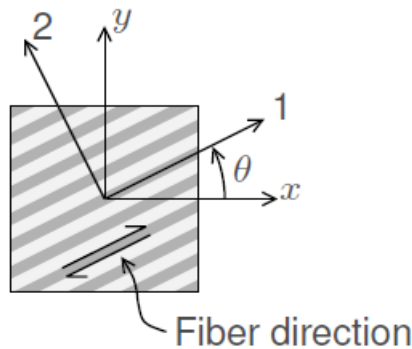


Figure B.1: The fibre directions in an uniformly distributed ply.

$$\begin{bmatrix} \epsilon_{11} \\ \epsilon_{22} \\ \epsilon_{33} \\ \gamma_{23} \\ \gamma_{31} \\ \gamma_{12} \end{bmatrix} = \begin{bmatrix} \frac{1}{E_1} & -\frac{\nu_{12}}{E_2} & -\frac{\nu_{13}}{E_3} & 0 & 0 & 0 \\ -\frac{\nu_{21}}{E_1} & \frac{1}{E_2} & -\frac{\nu_{23}}{E_3} & 0 & 0 & 0 \\ -\frac{\nu_{31}}{E_1} & -\frac{\nu_{32}}{E_2} & \frac{1}{E_3} & 0 & 0 & 0 \\ 0 & 0 & 0 & \frac{1}{G_{23}} & 0 & 0 \\ 0 & 0 & 0 & 0 & \frac{1}{G_{31}} & 0 \\ 0 & 0 & 0 & 0 & 0 & \frac{1}{G_{12}} \end{bmatrix} \begin{bmatrix} \sigma_{11} \\ \sigma_{22} \\ \sigma_{33} \\ \sigma_{23} \\ \sigma_{31} \\ \sigma_{12} \end{bmatrix} \quad (\text{B.1})$$

$$\begin{bmatrix} \epsilon_{11} \\ \epsilon_{22} \\ \epsilon_{33} \\ \gamma_{23} \\ \gamma_{31} \\ \gamma_{12} \end{bmatrix} = \begin{bmatrix} \frac{1}{E_1} & -\frac{\nu_{12}}{E_1} & -\frac{\nu_{12}}{E_1} & 0 & 0 & 0 \\ -\frac{\nu_{12}}{E_1} & \frac{1}{E_2} & -\frac{\nu_{23}}{E_2} & 0 & 0 & 0 \\ -\frac{\nu_{12}}{E_1} & -\frac{\nu_{23}}{E_2} & \frac{1}{E_2} & 0 & 0 & 0 \\ 0 & 0 & 0 & \frac{2(1+\nu_{23})}{E_2} & 0 & 0 \\ 0 & 0 & 0 & 0 & \frac{1}{G_{12}} & 0 \\ 0 & 0 & 0 & 0 & 0 & \frac{1}{G_{12}} \end{bmatrix} \begin{bmatrix} \sigma_{11} \\ \sigma_{22} \\ \sigma_{33} \\ \sigma_{23} \\ \sigma_{31} \\ \sigma_{12} \end{bmatrix} \quad (\text{B.2})$$

B.1. ABD matrix

A laminate consists out of multiple plies with the fibres in different directions. The classical laminate theory can be used to calculate the properties of a laminate. The classical laminate theory assumes thin FRP plates with all fibres parallel to the plane of the laminate. Due to this assumptions the compliance matrix can be reduced to a 3x3 matrix. The reduced stiffness matrix \bar{Q} , see equation B.4, is used to express the relation between the stress and strain in the local coordinate system. Notice that the inverse matrix must be used as the stress and strain have swapped places The reduced stiffness matrix must be calculated for each ply. In case the same composite material is used in each ply, the values of the matrices will be equal.

$$\bar{\sigma} = \bar{Q}\bar{\epsilon} \quad (\text{B.3})$$

$$\bar{Q} = \begin{bmatrix} \bar{Q}_{11} & \bar{Q}_{12} & 0 \\ \bar{Q}_{12} & \bar{Q}_{22} & 0 \\ 0 & 0 & \bar{Q}_{66} \end{bmatrix} = \begin{bmatrix} \frac{1}{E_1} & -\frac{\nu_{12}}{E_1} & 0 \\ -\frac{\nu_{12}}{E_1} & \frac{1}{E_2} & 0 \\ 0 & 0 & \bar{Q}_{66} \end{bmatrix}^{-1} = \begin{bmatrix} \frac{E_1^2}{E_1 - \nu_{12}^2 E_2} & \frac{\nu_{12} E_1 E_2}{E_1 - \nu_{12}^2 E_2} & 0 \\ \frac{\nu_{12} E_1 E_2}{E_1 - \nu_{12}^2 E_2} & \frac{E_1 E_2}{E_2 - \nu_{12}^2 E_1} & 0 \\ 0 & 0 & G_{12} \end{bmatrix} \quad (\text{B.4})$$

The transformation matrix T can be applied under the assumption that plane stress conditions are applicable. The reduced stiffness matrix in the global coordinate system can be calculated as shown below in equation B.5.

$$Q = T\bar{Q}T^T \quad (\text{B.5})$$

$$T = \begin{bmatrix} \cos^2 \theta & \sin^2 \theta & -2 \cos \theta \sin \theta \\ \sin^2 \theta & \cos^2 \theta & 2 \cos \theta \sin \theta \\ \cos \theta \sin \theta & -\cos \theta \sin \theta & \cos^2 \theta - \sin^2 \theta \end{bmatrix} \quad (\text{B.6})$$

The A, B and D matrix can be calculated according to equation B.7. The matrices have the same dimensions as the global reduced stiffness matrix and will be used to form the ABD matrix.

$$\begin{aligned} A &= \sum_{j=1}^n (z_j - z_{j-1}) Q_j \\ B &= \frac{1}{2} \sum_{j=1}^n (z_j^2 - z_{j-1}^2) Q_j \\ D &= \frac{1}{3} \sum_{j=1}^n (z_j^3 - z_{j-1}^3) Q_j \end{aligned} \quad (\text{B.7})$$

The stiffness relation between the stress resultant N (membrane stress) and M (bending moment) and the deformations ϵ (mid plane strain) and κ (curvature) can now be introduced.

$$\begin{bmatrix} N_x \\ N_y \\ N_{xy} \\ M_x \\ M_y \\ M_{xy} \end{bmatrix} = \begin{bmatrix} A_{11} & A_{12} & A_{16} & B_{11} & B_{12} & B_{16} \\ A_{12} & A_{22} & A_{26} & B_{12} & B_{22} & B_{26} \\ A_{16} & A_{26} & A_{66} & B_{16} & B_{26} & B_{66} \\ B_{11} & B_{12} & B_{16} & D_{11} & D_{12} & D_{16} \\ B_{12} & B_{22} & B_{26} & D_{12} & D_{22} & D_{26} \\ B_{16} & B_{26} & B_{66} & D_{16} & D_{26} & D_{66} \end{bmatrix} \begin{bmatrix} \epsilon_x \\ \epsilon_y \\ \epsilon_{xy} \\ \kappa_x \\ \kappa_y \\ \kappa_{xy} \end{bmatrix} \quad (\text{B.8})$$

With the numbers from the ABD matrix it is possible to calculate the laminate properties as shown in equation 4.2.

B.2. Thermal expansion

The thermal expansion coefficient is also a property that can be calculated for the laminate. The required input are is expansion coefficient in the principal directions of the plies. The first thing that must be done is calculate the expansion coefficient of the plies in the global directions. This can be done with equation B.9.

$$\begin{aligned}\alpha_{x,ply} &= \cos^2 \theta \alpha_1 + \sin^2 \theta \alpha_2 \\ \alpha_{y,ply} &= \sin^2 \theta \alpha_1 + \cos^2 \theta \alpha_2 \\ \alpha_{xy,ply} &= 2 * \cos \theta \sin \theta (\alpha_1 - \alpha_2)\end{aligned}\tag{B.9}$$

Now the thermal resultats must be calculated for each ply and added together.

$$\begin{aligned}N_x^t &= \sum_{j=1}^n (\alpha_{x,ply} * Q_{11} + \alpha_{y,ply} * Q_{12} + \alpha_{xy,ply} * Q_{16})(z_j - z_{j-1}) \\ N_y^t &= \sum_{j=1}^n (\alpha_{x,ply} * Q_{12} + \alpha_{y,ply} * Q_{22} + \alpha_{xy,ply} * Q_{26})(z_j - z_{j-1}) \\ N_{xy}^t &= \sum_{j=1}^n (\alpha_{x,ply} * Q_{16} + \alpha_{y,ply} * Q_{26} + \alpha_{xy,ply} * Q_{66})(z_j - z_{j-1}) \\ M_x^t &= \frac{1}{2} \sum_{j=1}^n (\alpha_{x,ply} * Q_{11} + \alpha_{y,ply} * Q_{12} + \alpha_{xy,ply} * Q_{16})(z_j^2 - z_{j-1}^2) \\ M_y^t &= \frac{1}{2} \sum_{j=1}^n (\alpha_{x,ply} * Q_{12} + \alpha_{y,ply} * Q_{22} + \alpha_{xy,ply} * Q_{26})(z_j^2 - z_{j-1}^2) \\ M_{xy}^t &= \frac{1}{2} \sum_{j=1}^n (\alpha_{x,ply} * Q_{16} + \alpha_{y,ply} * Q_{26} + \alpha_{xy,ply} * Q_{66})(z_j^2 - z_{j-1}^2)\end{aligned}\tag{B.10}$$

The last step is to calculate the expansion coefficient of the entire laminate.

$$\begin{bmatrix} \alpha_x \\ \alpha_y \\ \alpha_{xy} \\ \kappa_x \\ \kappa_y \\ \kappa_{xy} \end{bmatrix} = \begin{bmatrix} A_{11} & A_{12} & A_{16} & B_{11} & B_{12} & B_{16} \\ A_{12} & A_{22} & A_{26} & B_{12} & B_{22} & B_{26} \\ A_{16} & A_{26} & A_{66} & B_{16} & B_{26} & B_{66} \\ B_{11} & B_{12} & B_{16} & D_{11} & D_{12} & D_{16} \\ B_{12} & B_{22} & B_{26} & D_{12} & D_{22} & D_{26} \\ B_{16} & B_{26} & B_{66} & D_{16} & D_{26} & D_{66} \end{bmatrix}^{-1} \begin{bmatrix} N_x^t \\ N_y^t \\ N_{xy}^t \end{bmatrix}\tag{B.11}$$

By midplane strains caused due to temperature difference can be expressed by multiplying α values by the temperature difference. The midplane strain represents the load that is applied on the structure.

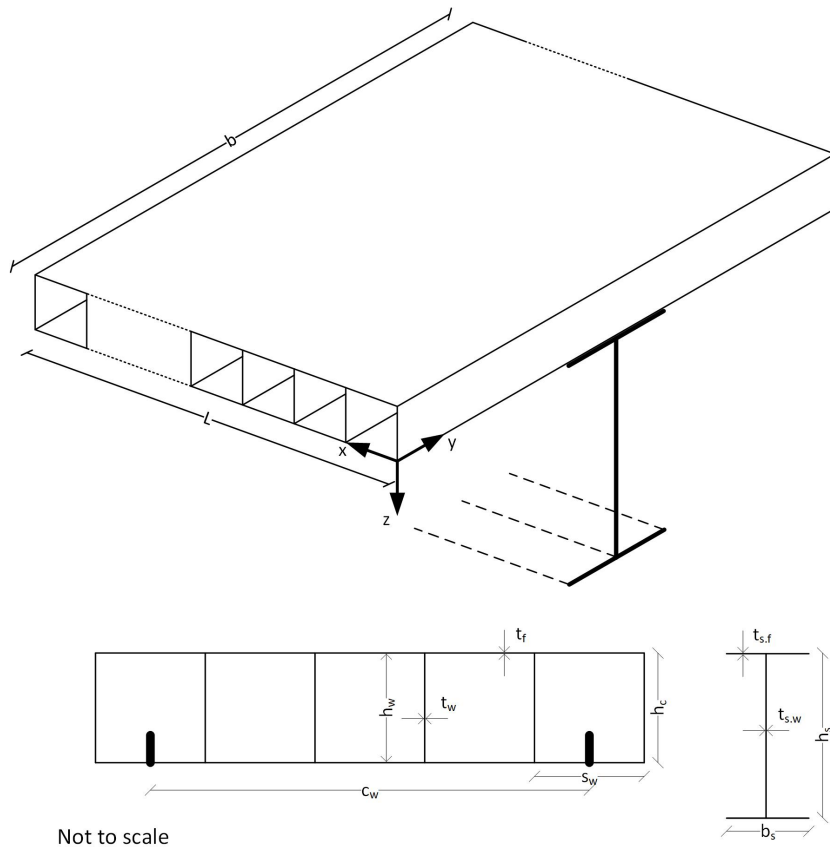
(This page is intentionally left blank)

C

Verification model

Properties and dimensions of the deck

For the verification the layout of the generic bridge is used. The facings and deck have different compositions. Laminate 3 is used for the facings and laminate 4 is used for the webs. The properties and dimensions of the FRP deck and steel girder are presented in the tables below. For the verification only a third of the bridge width is used as the verification is done per main girder. An overview of the bridge and its dimensions can also be seen in figure C.1. The length of the bridge, L , is 14400 mm. The width of the bridge, b , is 2400 mm.



Not to scale

Figure C.1: The geometry of the verification model.

FRP deck

The geometry of the FRP deck can be seen in table C.2. c_w is the distance between the bolted connectors. The properties of the facing and web can be seen in table C.1.

	$E_1 [MPa]$	$E_2 [MPa]$	$G_{12} [MPa]$	ν_{12}
Facing (laminate 3)	18,750	25,023	5,244	0.198
Webs (laminate 4)	15,309	15,309	8,931	0.46

Table C.1: The properties of the FRP deck used for the verification.

t_f [mm]	h_w [mm]	t_w [mm]	h_c [mm]	s_w [mm]	c_w [mm]
20	160	10	200	120	480

Table C.2: The dimensions of the FRP deck used for the verification, the dimensions can also be seen in figure 3.8a.

Steel girder

The geometry of the steel girder can be seen in table C.4. The properties of the steel girder can be seen in table C.3. A_{girder} is the cross sectional area of the girder where A_a is the cross sectional area of the web only.

	$E_{steel} [MPa]$	$G_a [MPa]$	$A_{girder} [mm^2]$	$A_a [mm^2]$	$I_{girder} [mm^4]$
Steel girder	210,000	80,769	18,750	12500	2.489×10^9

Table C.3: The properties of the steel girder used for the verification.

h_s [mm]	b_s [mm]	$t_{s,w}$ [mm]	$t_{s,f}$ [mm]
1000	250	12.5	12.5

Table C.4: The dimensions of the steel girder used for the verification.

Stiffness coefficients

The out-of-plane shear stiffness of the deck K_1 is obtained by multiplying the normalised out-of-plane shear stiffness with the effective width b_e . The normalised out-of-plane shear stiffness of the deck is equivalent to a shear stress τ_{xz} caused by a unit displacement of 1 mm between the upper and lower flat panels Satasivam et al. (2017). The shear stiffness is taken from experiments of Gurtler (2004), where $G_{xz} = 3.3$ MPa.

$$k_1 = \tau_{xz} = G_{xz} \times \frac{1}{h_c}$$

$$k_1 = 0.0165 \text{ N/mm}^3$$

$$K_1 = \hat{k} \times b_e$$

$$k_3 = 100,000 \text{ N/mm}$$

$$K_3 = 2 \times k_3$$

$$K_a = \frac{A_a}{A_{girder}}$$

$$K_a = 0.667$$

k_3 is the transverse stiffness of the connectors, which is equal to 100,000 N/mm. This must be multiplied by 2 because there are two connectors per cross section. K_a is the Timoshenko shear coefficient.

Effective bending stiffness

The effective bending stiffness is determined with the method according to Eurocode-1995-1-1 (2005). The cross section has been divided into three regions, see figure 3.12. For each region the properties are determined as well as a reduction factor. The reduction factors are adjusted by Satasivam et al. (2017) for fibre reinforced polymers (FRP) decks and steel superstructure connected by bolted connectors. It takes into account that only partial hybrid interaction will occur.

Region 1 - top facing

The properties and reduction factor for region 1, the FRP top facing are determined here. The effective width is determined with Eurocode-1994-1-1 (2004). b_0 is the distance between the shear connectors and b_{ei} is the effective width of the FRP flange on each side of the girder:

$$\begin{aligned}
 h_1 &= t_f = 20 \text{ mm} \\
 E_1 &= E_{2.f} = 25,023 \text{ MPa} \\
 b_0 &= 200 \text{ mm} \\
 b_{ei} &= \frac{L}{8} = 1,800 \text{ mm} \\
 b_{1.eff} &= b_0 + 2 \cdot b_{ei} = 3,800 \text{ mm} \\
 A_1 &= b_{1.eff} \cdot h_1 = 76,000 \text{ mm}^2 \\
 I_1 &= \frac{b_{1.eff} \cdot h_1^3}{12} = 2.533 \times 10^6 \text{ mm}^4 \\
 K_1 &= b_{1.eff} \cdot k_1 = 62.7 \text{ N/mm}^2 \\
 \gamma_1 &= \frac{1}{1 + \frac{\pi^2 E_1 A_1}{K_1 L^2}} \\
 \gamma_1 &= 0.409
 \end{aligned}$$

Region 2 - bottom facing

The properties and reduction factor for region 2, the FRP bottom facing are determined here. The reduction factor γ_2 is 1 by definition:

$$\begin{aligned}
 h_2 &= t_f = 20 \text{ mm} \\
 E_2 &= E_{2.f} = 25,023 \text{ MPa} \\
 b_{2.eff} &= b_{1.eff} = 3800 \text{ mm} \\
 A_2 &= b_{2.eff} \cdot h_2 = 76,000 \text{ mm}^2 \\
 I_2 &= \frac{b_{2.eff} \cdot h_2^3}{12} = 2.533 \times 10^6 \text{ mm}^4 \\
 \gamma_2 &= 1
 \end{aligned}$$

Region 3 - steel girder

The properties and reduction factor for region 3, the steel girder are determined here:

$$\begin{aligned}
 h_3 &= h_{girder} = 1000 \text{ mm} \\
 E_3 &= E_{steel} = 210,000 \text{ MPa} \\
 A_3 &= A_{girder} = 18,750 \text{ mm}^2 \\
 I_3 &= I_{girder} = 2.489 \times 10^9 \text{ mm}^4 \\
 K_3 &= 2 * k_3 = 200000 \text{ Nmm} \\
 \gamma_3 &= \frac{1}{1 + \frac{\pi^2 E_3 A_3 c_w}{K_3 L^2}} \\
 \gamma_3 &= 0.690
 \end{aligned}$$

Distances from the regions to the neutral axis

For each of the three regions the distance to the neutral axis must be calculated. The distances can be seen in figure 3.12. The calculation is done with the following formulas:

$$\begin{aligned}
 a_2 &= \frac{\gamma_1 E_1 A_1 (h_1 + h_2) - \gamma_3 E_3 A_3 (h_2 + h_3)}{2 \cdot (\gamma_1 E_1 A_1 + \gamma_2 E_2 A_2 + \gamma_3 E_3 A_3)} \\
 a_2 &= -253.813 \text{ mm} \\
 a_1 &= -\left(h_c - \frac{h_1}{2} - \frac{h_2}{2} - a_2 \right) \\
 a_1 &= -433.813 \text{ mm} \\
 a_3 &= \frac{h_2}{2} + \frac{h_3}{2} + a_2 \\
 a_3 &= 256.187 \text{ mm}
 \end{aligned}$$

Effective bending stiffness

All information needed to calculate the effective bending stiffness is now known. The effective bending stiffness is calculated with the follow formula:

$$\begin{aligned}
 EI_{eff} &= \sum_{i=1}^n (E_i I_i + \gamma_i E_i A_i a_i^2) \\
 EI_{eff} &= E_1 I_1 + \gamma_1 E_1 A_1 a_1^2 + E_2 I_2 + \gamma_2 E_2 A_2 a_2^2 + E_3 I_3 + \gamma_3 E_3 A_3 a_3^2 \\
 EI_{eff} &= 9.701 \times 10^{14} \text{ Nmm}^2
 \end{aligned}$$

Mid-span displacement

The mid-span displacement is calculated with the following formula. The distributed load q is equal to 10 kN/m^2 :

$$\begin{aligned}
 u_z &= \frac{5}{384} \frac{q b L^4}{EI_{eff}} + \frac{1}{8} \frac{q b L^2}{k_a G_a A_a} \\
 u_z &= 14.775 \text{ mm}
 \end{aligned}$$

D

Bridge layout

The dimensions of the girder bridges can be seen in the table below. The parameters can be found in figure 4.3

Name	L [m]	$n_{support}$	W [m]	n_b	n_λ	Traffic lanes	B [m]	λ [m]	Facing laminate
Avenhornerbrug oost	97.85	5	14.93	5	5	2	3	24.48	2
Avenhornerbrug west	97.85	5	14.93	5	5	2	3	24.48	2
Brug elsloo	77.4	2	4.72	2	11	1	2.36	7.68	2
Brug Hedel (aanbrug noord)	218.79	6	16.42	6	31	2	2.34	7.2	2
Brug Hedel (aanbrug zuid)	88.29	3	16.42	3	13	2	2.34	7.2	2
Brug Rhenen	532.4	10	14.5	10	301	2	4.8	1.8	1
Brug spannenburg (aanbrug oost)	52.35	3	9	3	5	2	1.5	12.96	2
Brug spannenburg (aanbrug west)	13	2	9	2	2	2	1.5	12.96	2
Brug verkeersbrug Venlo	225.28	5	22.5	5	21	4	3.75	11.28	3
Dochterensebrug	69	2	4.43	2	58	1	2.16	1.2	1
Dorrebrug	60.04	4	4.37	4	39	1	2.16	1.56	1
Grensbrug	60.04	4	4.37	4	39	1	2.16	1.56	1
Hagesteinbrug (noord oost)	64.64	2	14.7	2	2	3	2.94	64.64	2
Hagesteinbrug (noord west)	64.64	2	14.7	2	2	3	2.94	64.64	2
Hagesteinbrug (zuid oost)	316.14	7	14.7	7	7	3	2.94	52.64	2
Hagesteinbrug (zuid west)	316.14	7	14.7	7	7	3	2.94	52.64	2
Ijsselbrug A12 oost	300.55	6	9.25	6	31	2	4.6	9.96	3
Ijsselbrug A12 oost aanbrug	240.46	7	9.25	7	25	2	4.6	9.96	3
Ijsselbrug A12 west	300.55	6	9.25	6	31	2	4.6	9.96	3
Ijsselbrug A12 west aanbrug	240.46	7	9.25	7	25	2	4.6	9.96	3
John Frostbrug (aanbrug)	251.92	7	22	7	35	4	2.75	7.44	2
Moggezompsebrug	69	2	4.43	2	58	1	2.16	1.2	1
Molenbrug (zijoverspanning oost)	203.26	5	19.4	5	14	3	2.77	15.6	2
Molenbrug (zijoverspanning west)	53.23	2	19.4	2	4	3	2.77	17.76	2
Nieuw Vossemeer (zijoverspanning oost)	212.56	7	12.5	7	31	2	4.15	7.08	3
Nieuw Vossemeer (zijoverspanning west)	212.56	7	12.5	7	31	2	4.15	7.08	3
Oude schouw brug (aanbrug oost)	52.35	3	11.76	3	3	3	1.96	26.16	2
Uitwellingerga brug	26.72	2	10	2	13	2	5.04	2.04	1
Vossenbrinkbrug	60.04	4	4.37	4	39	1	2.16	1.56	1

The dimensions of the arch bridges can be seen in the table below. The parameters can be found in figure 4.4

Name	L [m]	W [m]	W_{arch} [m]	H [m]	n_v	n_b	n_λ	Traffic lanes	B [m]	λ [m]	Facing laminate
Amsterdamsebrug	89.32	18.5	9.4	15	10	7	11	2	1.57	8.93	2
Bathsebrug	140.4	16.43	16.43	17	12	2	54	2	16.43	2.65	1
Brug Berg	76.6	6.6	6.6	6.9	12	8	14	2	0.93	5.75	2
Brug Bunde	58.6	6.54	6.54	6	9	8	11	1	0.93	5.86	2
Brug Geulle	58.6	6.54	6.54	6	9	8	11	1	0.93	5.86	2
Brug Hedel	126.51	16.48	16.48	18	11	9	13	2	2.06	10.54	2
Brug Itteren	58.6	6.54	6.54	6	9	8	11	1	0.93	5.86	2
Brug Obbicht	76.6	6.54	6.54	6.9	12	8	14	2	0.93	5.75	2
Brug oude maasje	42	4.37	4.37	6.4	8	2	-	1	4.37	42	2
Brug Salesdreef	42	4.37	4.37	6.4	8	2	-	1	4.37	42	2
Brug stein	76.6	9.06	6.54	6.9	12	8	14	2	0.93	5.75	2
Brug urmond	76.6	12.43	6.54	6.9	12	8	14	2	0.93	5.75	2
De Meernbrug	119.25	17.6	14.1	16	14	10	16	4	1.76	7.95	2
Diepenheimsebrug	88.38	4.37	4.37	10	9	2	-	1	4.37	88.38	2
Hoeselderbrug	41.05	4.37	4.37	6.4	8	2	-	1	4.37	41.05	2
John Frostbrug	120	23.02	14.1	17	15	9	17	4	1.76	7.5	2
Jutphasebrug	89.32	14.61	7.75	12.3	10	6	12	2	1.55	8.12	2
Leemslagenbrug	41.05	4.37	4.37	6.4	8	2	-	1	4.37	41.05	2
Maarsserbrug	88.88	15.64	8.5	13.5	10	6	12	2	1.7	8.08	2
Nieuw Vossemeer	140.4	12.5	12.5	13	12	2	54	3	12.5	2.65	1
Schalkwijksebrug	172.8	16.81	11.4	15	12	4	33	2	3.8	5.4	3
Slaakbrug	140.85	19.87	19.87	16	11	2	67	4	19.87	2.14	1
Tankinkbrug	41.05	4.37	4.37	6.4	8	2	-	1	4.37	41.05	2
Thoolsebrug	140.4	17.54	17.54	15	12	2	54	3	17.54	2.65	1
Verkeersbrug Doesburg	88	15.35	12.55	12	10	7	12	2	2.09	8	2
Warmtinkbrug	41.05	4.37	4.37	6.4	8	2	-	1	4.37	41.05	2
Wilhelminabrug	121.2	18.4	10.7	17	14	8	16	2	1.78	8.08	2